

AD-A103 026

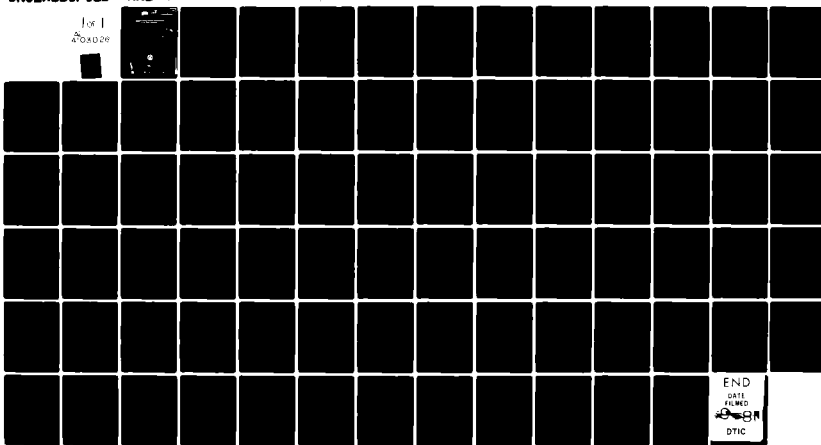
NAVAL RESEARCH LAB WASHINGTON DC  
MAGNETIC ENERGY STORAGE AND CONVERSION IN THE SOLAR ATMOSPHERE. (U)  
JUL 81 D S SPICER  
NRL-MR-4550

F/6 3/2

UNCLASSIFIED

NL

For 1  
47040-28



END  
DATE FILMED  
DTIC

AD 1970 00026

| REPORT DOCUMENTATION PAGE   |                                     | READ INSTRUCTIONS BEFORE COMPLETING FORM                    |              |                               |                          |               |                |                       |              |                                     |
|---|-------------------------------------|---|--------------|-------------------------------|--------------------------|---------------|----------------|-----------------------|--------------|-------------------------------------|
| 1. REPORT NUMBER  | 2. GOVT ACCESSION NO.               | 3. RECIPIENT'S CATALOG NUMBER                               |              |                               |                          |               |                |                       |              |                                     |
| NRL Memorandum Report 4550  | AD-A103 026                         |   |              |                               |                          |               |                |                       |              |                                     |
| 4. TITLE (and Subtitle)   |                                     | 5. TYPE OF REPORT & PERIOD COVERED                          |              |                               |                          |               |                |                       |              |                                     |
| MAGNETIC ENERGY STORAGE AND CONVERSION IN THE SOLAR ATMOSPHERE  |                                     | Interim report on a continuing NRL problem                  |              |                               |                          |               |                |                       |              |                                     |
| 7. AUTHOR(s)  |                                     | 6. PERFORMING ORG. REPORT NUMBER                            |              |                               |                          |               |                |                       |              |                                     |
| Daniel S. Spicer  |                                     |   |              |                               |                          |               |                |                       |              |                                     |
| 9. PERFORMING ORGANIZATION NAME AND ADDRESS   |                                     | 10. PROGRAM ELEMENT, PROJECT, TASK AREA & WORK UNIT NUMBERS |              |                               |                          |               |                |                       |              |                                     |
| Naval Research Laboratory<br>Washington, D.C. 20375   |                                     | W14709<br>41-0982-0-1                                       |              |                               |                          |               |                |                       |              |                                     |
| 11. CONTROLLING OFFICE NAME AND ADDRESS   |                                     | 12. REPORT DATE   |              |                               |                          |               |                |                       |              |                                     |
| National Aeronautics and Space Administration<br>Washington, D.C. 20546   |                                     | July 1, 1981  |              |                               |                          |               |                |                       |              |                                     |
| 14. MONITORING AGENCY NAME & ADDRESS (if different from Controlling Office)   |                                     | 13. NUMBER OF PAGES   |              |                               |                          |               |                |                       |              |                                     |
|   |                                     | 79  |              |                               |                          |               |                |                       |              |                                     |
| 16. DISTRIBUTION STATEMENT (of this Report)   |                                     | 15. SECURITY CLASS. (of this report)                        |              |                               |                          |               |                |                       |              |                                     |
| Approved for public release; distribution unlimited.  |                                     | UNCLASSIFIED  |              |                               |                          |               |                |                       |              |                                     |
| 17. DISTRIBUTION STATEMENT (of the abstract entered in Block 20, if different from Report)  |                                     | 15a. DECLASSIFICATION/DOWNGRADING SCHEDULE                  |              |                               |                          |               |                |                       |              |                                     |
| 18. SUPPLEMENTARY NOTES   |                                     |   |              |                               |                          |               |                |                       |              |                                     |
| Prepared for the PHYSICS OF THE SUN (MONOGRAPH) CHAPTER 10 (ed. P. A. Sturrock)   |                                     |   |              |                               |                          |               |                |                       |              |                                     |
| 19. KEY WORDS (Continue on reverse side if necessary and identify by block number)  |                                     |   |              |                               |                          |               |                |                       |              |                                     |
| <table> <tr> <td>Solar Flares</td> <td>Magnetohydrodynamic Stability</td> </tr> <tr> <td>Pre-Flare Energy Storage</td> <td>Double Layers</td> </tr> <tr> <td>Flare Triggers</td> <td>Anomalous Resistivity</td> </tr> <tr> <td>Reconnection</td> <td>Atmospheric Electrodynamic Coupling</td> </tr> </table>  |                                     |   | Solar Flares | Magnetohydrodynamic Stability | Pre-Flare Energy Storage | Double Layers | Flare Triggers | Anomalous Resistivity | Reconnection | Atmospheric Electrodynamic Coupling |
| Solar Flares  | Magnetohydrodynamic Stability       |   |              |                               |                          |               |                |                       |              |                                     |
| Pre-Flare Energy Storage  | Double Layers                       |   |              |                               |                          |               |                |                       |              |                                     |
| Flare Triggers  | Anomalous Resistivity               |   |              |                               |                          |               |                |                       |              |                                     |
| Reconnection  | Atmospheric Electrodynamic Coupling |   |              |                               |                          |               |                |                       |              |                                     |
| 20. ABSTRACT (Continue on reverse side if necessary and identify by block number)   |                                     |   |              |                               |                          |               |                |                       |              |                                     |
| <p>A review of the theoretical problems associated with preflare magnetic energy storage and conversion is presented. The review consists of three parts; preflare magnetic energy storage, magnetic energy conversion mechanisms, and preflare triggers. In section 2, the relationship between magnetic energy storage and the electrodynamic coupling of the solar atmosphere is developed. By accounting for the electrodynamic coupling of the solar atmosphere, we are able to examine the fundamental problems associated with the concept of <i>in situ</i> versus remote</p> |                                     |   |              |                               |                          |               |                |                       |              |                                     |

(Continued)

*C*  
SECURITY CLASSIFICATION OF THIS PAGE (When Data Entered)

20. ABSTRACT (Continued)

magnetic-energy storage. Furthermore, this approach permits us to distinguish between the roles of local and global parameters in the storage process.

Section 3 is focused on the conversion mechanisms that can explain, in principle, the rapid energy release of a flare. In addition, we discuss how electrodynamic coupling eventually dictates which mechanism(s) is responsible for releasing the stored magnetic energy, and how the global coupling dictates the final evolution of the relevant mechanism. Section 4 examines preflare triggers and section 5, we examine the most promising directions for future research into the problem of magnetic-energy storage and conversion of the Sun.

*B*  
SECURITY CLASSIFICATION OF THIS PAGE (When Data Entered)

*TR*

## CONTENTS

|   |    |
|---|----|
| 10.1 INTRODUCTION .....   | 1  |
| 10.2 GLOBAL ELECTRODYNAMIC COUPLING AND MAGNETIC ENERGY STORAGE .....               | 1  |
| 10.2.1 The Importance of Global Electrodynamic Coupling .....                       | 1  |
| 10.2.2 In Situ Storage of Magnetic Energy .....                                     | 19 |
| 10.3 MAGNETIC FREE ENERGY DISSIPATION MECHANISMS .....                              | 29 |
| 10.3.1 The Magnetic Dissipation Times and $\beta$ .....                             | 30 |
| 10.3.2 Double Layers .....  | 31 |
| 10.3.3 Anomalous Joule Heating Due to D.C. Anomalous Resistivity .....              | 34 |
| 10.3.4 Double Layers and Anomalous Resistivity .....                                | 42 |
| 10.3.5 Ideal Magnetohydrodynamics (MHD) and Reconnection Mechanisms in Flares ..... | 43 |
| 10.3.6 Which Dissipation Mechanism Will Prevail? .....                              | 66 |
| 10.4 THE PREFLARE STATE AND FLARE TRIGGERS .....                                    | 67 |
| 10.5 MAGNETIC ENERGY STORAGE AND CONVERSION<br>FUTURE RESEARCH .....                | 70 |
| ACKNOWLEDGMENTS .....   | 71 |
| REFERENCES .....  | 71 |

|  |  |
|--|--|
| Accession For                                  |  |
| NTIS SPA&I <input checked="" type="checkbox"/> |  |
| DTIC TAB <input type="checkbox"/>              |  |
| Unannounced <input type="checkbox"/>           |  |
| Justification                                  |  |
| By   |  |
| Distribution/                                  |  |
| Availability Codes                             |  |
| A-1 and or                                     |  |
| Dist Special                                   |  |

*AP*

## MAGNETIC ENERGY STORAGE AND CONVERSION IN THE SOLAR ATMOSPHERE

### 10.1 INTRODUCTION

In the past, the problem of storage and conversion of magnetic energy on the Sun has been investigated primarily in the context of solar flares, although increasing evidence has appeared, in recent years, that this problem is relevant to other forms of solar activity, such as atmospheric heating (Kuperus *et al.*, 1981.) Hence, due to the relevance of magnetic-energy storage and conversion to diverse aspects of solar activity, the present review while emphasizing the physics of flares, is applicable to other solar phenomena as well. In §10.2, the relationship between magnetic energy storage and the electrodynamic coupling of the solar atmosphere is developed. This approach, which originates in the ionospheric-magnetospheric literature (e.g., Roederer, 1979), is both comprehensive and lucid, while including the standard view of magnetic energy storage (*cf.* Van Hoven *et al.*, 1980). By accounting for the electrodynamic coupling of the solar atmosphere, we are able to examine the fundamental problems associated with the concept of *in situ* versus remote magnetic-energy storage. Furthermore, this approach permits us to distinguish between the roles of local and global parameters in the storage process.

Section 10.3 is focussed on the conversion mechanisms that can explain, in principle, the rapid energy release of a flare. We emphasize physical understanding of these mechanisms, as opposed to mathematical rigor. In addition, we discuss how electrodynamic coupling eventually dictates which mechanism(s) is responsible for releasing the stored magnetic energy, and how the global coupling dictates the final evolution of the relevant mechanism. No attempt is made to review the flare models in which these processes are utilized, since a comprehensive and objective review of this controversial topic already exists (Sturrock, 1980). Section 10.4 examines preflare triggers and in §10.5, we examine the most promising directions for future research into the problem of magnetic-energy storage and conversion on the Sun.

### 10.2 GLOBAL ELECTRODYNAMIC COUPLING AND MAGNETIC ENERGY STORAGE

#### 10.2.1 The Importance of Global Electrodynamic Coupling

In this section, we introduce the concept of global electrodynamic coupling in the solar atmosphere, and examine how electrodynamic coupling affects both the magnetic-energy storage process and the macroscopic stability of those plasma-magnetic field configurations in which this storage might occur. We first review how currents are generated and transported and what conditions need to be satisfied for storage of magnetic energy. Next we introduce equivalent circuit analogs, to facilitate discussion of the electrodynamic concepts relevant to solar conditions. The primary advantage of this approach is that it allows us to greatly simplify complex magnetic field-current systems, while still incorporating the appropriate physics. We conclude this section by discussing the fundamental problems of *in situ* versus remote magnetic-energy storage with a critical examination of present-day understanding of MHD loop stability.

10.2.1.1 Magnetic fields arise as a result of electric charges in motion, that is, currents. Magnetic energy storage arises when a current system, driven by external sources of electromotive force, emf, does work against the induced emf's induced by the build-up of the current

system itself. This work is stored in the magnetic field associated with the currents, and can be regained by allowing the currents to decay. Thus, to maintain the stored magnetic energy, the preflare state must have the ability to generate new magnetic energy and permit its transport at a rate which is faster than dissipation can cause its conversion to other forms of energy. To store magnetic energy in the solar atmosphere, therefore, we must address the question of how currents are generated and subsequently transported to the storage volume. In the case of a flare the photosphere generates currents which are subsequently transported into the higher atmosphere. However, these currents do not simply stop somewhere in the atmosphere, but must flow in such a way as to satisfy the requirement of current continuity  $\nabla \cdot \mathbf{J} = 0$ ,\* where  $\mathbf{J}$  is the current density. If  $\mathbf{J}$  is resolved into a field aligned current,  $\mathbf{J}_{\parallel}$ , and a current perpendicular to the magnetic field,  $\mathbf{J}_{\perp}$ , we can relate  $\mathbf{J}_{\parallel}$  to  $\mathbf{J}_{\perp}$  by  $\nabla \cdot \mathbf{J}_{\parallel} = -\nabla \cdot \mathbf{J}_{\perp}$ ; that is,  $-\nabla \cdot \mathbf{J}_{\perp}$  acts as a source for the field aligned currents. Hence,  $\mathbf{J}_{\parallel}$  communicates between adjacent regions of the solar atmosphere: the hot fully-ionized coronal plasma is coupled electrodynamically with the colder partially-ionized photospheric plasma.  $\mathbf{J}_{\parallel}$ , therefore represents the means by which magnetic energy is transported from the "generator" ( $-\nabla \cdot \mathbf{J}_{\perp}$ ) to its "storage" site.

The origins of  $\mathbf{J}_{\perp}$  and, hence  $\mathbf{J}_{\parallel}$  can be understood as follows. Using the single-fluid momentum equation (and neglecting gravity),

$$\rho \frac{d\mathbf{v}}{dt} = -\nabla p + \frac{\mathbf{J} \times \mathbf{B}}{c}, \quad (10.2.1)$$

and taking the vector cross product of (2.1) with  $\mathbf{B}$  yields

$$\mathbf{J}_{\perp} = \frac{c\mathbf{B} \times \nabla p}{B^2} - \frac{c\rho}{B^2} \frac{d\mathbf{v}}{dt} \times \mathbf{B}, \quad (10.2.2)$$

where  $p$  is the total gas pressure,  $\rho$  the mass density, and  $\mathbf{v}$  the bulk velocity of the plasma. Note that (10.2.1) reveals nothing about  $\mathbf{J}_{\parallel}$ . Equation (10.2.2) demonstrates that  $\mathbf{J}_{\perp}$  arises in regions with pressure gradients and convective flow fields. Using  $\nabla \cdot \mathbf{J}_{\parallel} = -\nabla \cdot \mathbf{J}_{\perp}$  and (10.2.2), we find (Sato and Iijima, 1979)

$$\mathbf{J}_{\parallel} = B_0 \int_0^s \left\{ \frac{c\rho}{B} \frac{d}{dt} \left( \frac{\mathbf{B} \cdot \nabla \times \mathbf{v}}{B^2} \right) + \frac{\mathbf{J}_{\perp} \cdot \nabla \mathbf{B}}{B^2} - \frac{1}{\rho B} \left[ \mathbf{B} \times \left( \frac{\rho}{B^2} \frac{d\mathbf{v}}{dt} \right) \cdot \nabla p \right] \right\} ds, \quad (10.2.3)$$

where the integration is performed over the field aligned coordinate  $s$  and incompressible flow was assumed. Equation (10.2.3) illustrates the various means by which  $-\nabla \cdot \mathbf{J}_{\perp}$  gives rise to a  $\mathbf{J}_{\parallel}$  in a fluid theory. The vorticity term (the left most term in the curly brackets) is the source usually believed to generate the currents believed to cause flares (e.g., Stenflo, 1969; Heyvaerts, 1974b). Note that if the integrand in (10.2.3) were zero,  $\mathbf{J}_{\parallel} = \alpha B_0$  would result, where  $\alpha$  is the constant of integration for a specific field line. Thus, force free currents must communicate between regions producing  $-\nabla \cdot \mathbf{J}_{\perp}$  (cf. §10.2.2).

The physical processes that lead to the generation of  $\mathbf{J}$  have their origins in the different motions electrons and ions experience in the direction perpendicular to the magnetic field, which result from either the small electron to ion mass ratio (the first and third terms in (10.2.3)) or from the difference in the sign of the charge (the second term in (10.2.3)).

From a physical point of view, electrodynamic coupling arises when the resistivity *tensor*,  $\eta$ , varies from some finite value to effectively zero along a given field line in the presence of an external force. This can be understood in the solar context as follows. Consider two domains connected by a magnetic field (Figure 10.1). The first domain, denoted by PC (perfectly conducting), satisfies Ohm's law in the ideal MHD approximation,

\*We are justified in assuming  $\nabla \cdot \mathbf{J} = 0$  if we only consider phenomena for which the displacement current can be neglected, as is the case here.

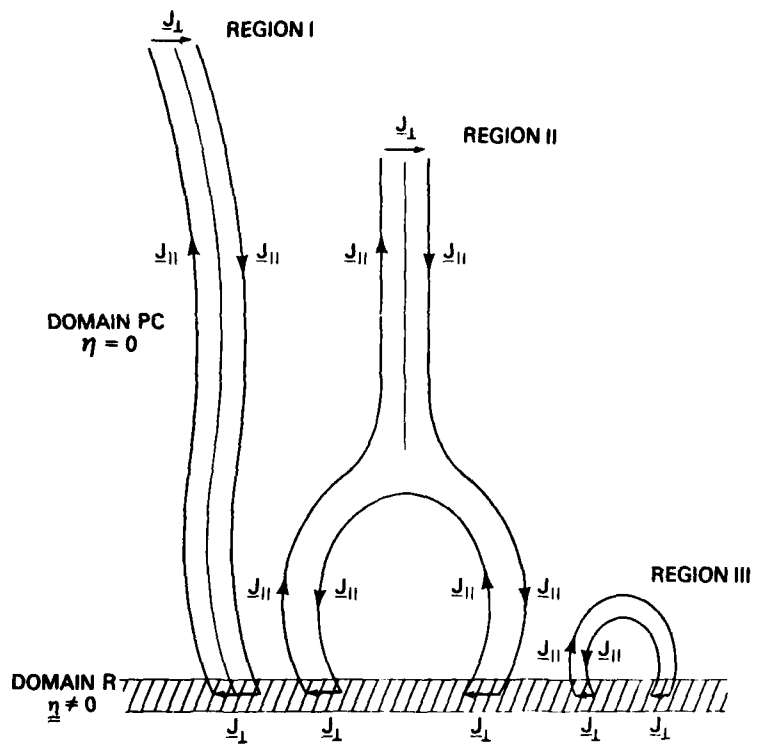


Figure 10.1 — Schematic of three simple current paths embedded in a plasma with two resistivity domains: perfectly conducting (PC) and resistive (R). Each path illustrates the typical magnetic configuration found in the solar atmosphere: Region I, open; Region II, partially open and closed; and Region III, closed.

$$\mathbf{E} + \frac{\mathbf{v} \times \mathbf{B}}{c} = 0, \quad (10.2.4)$$

which implies that region PC is flux preserving.\* The second domain, denoted by  $R$  (resistive), is characterized by an Ohm's Law

$$\mathbf{E} + \frac{\mathbf{v} \times \mathbf{B}}{c} = \eta \cdot \mathbf{J}. \quad (10.2.5)$$

Contained in  $\eta$  are components that connect neighboring fields lines (Pedersen conductivity), and thus allow the discharge of excess charges produced in domain PC or the flow of currents perpendicular to  $\mathbf{B}$ . In Figure 10.1, we have split domain PC into three separate regions following Roederer (1979): Region I, corresponding to field lines starting at the photosphere and ending in the solar wind, as in coronal holes; Region II, corresponding to field lines which comprise a helmet streamer; and Region III, corresponding to field lines entering domain PC and then closing back into domain  $R$ , such as occurs in loops. Note that some loop field lines may exist entirely in domain  $R$ . Assuming that some external force exists in  $R$  such that  $\nabla \cdot \mathbf{J}_\perp \neq 0$ , then the field-aligned currents  $\mathbf{J}_{\parallel}$  will link domains  $R$  and PC. If  $\nabla \cdot \mathbf{J} = 0$  is to be satisfied in the MHD domain, then a  $\mathbf{J}_\perp$  must exist in both regions I and II. Since  $\mathbf{J}_\perp$  is non-zero in regions I and II of domain PC, a Lorentz force ( $\mathbf{J} \times \mathbf{B}$ ) in domain PC attempts to force the plasma in domain PC into co-motion. Thus, a plasma in domain PC of regions I and II, which is initially free of external forces, will become co-moving with the resistive plasma in domain  $R$ , if the resistive plasma is under the influence of an external force.

Region III presents a special case in that the symmetry of  $\mathbf{J}_{\parallel}$ , with respect to the two possible sources of  $\mathbf{J}_\perp$  in domain  $R$ , will dictate whether current continuity is satisfied by a  $\mathbf{J}_\perp$  existing in domain PC or in  $R$ . Figure 10.2 illustrates four possible loop current systems. In general, symmetric current systems with  $\mathbf{J}_{\parallel} \neq 0$  in PC imply that a  $\mathbf{J}_\perp$  exists in PC. Asymmetric current systems allow  $\mathbf{J}_{\parallel}$  to close in PC or in  $R$  depending on the degree of asymmetry in  $\mathbf{J}_{\parallel}$ .

Because energy storage involves both local and global quantities, e.g., current density  $\mathbf{J}$  and total current  $I$ , and because we will use global equivalent circuits to illustrate several concepts about energy storage, it is pertinent to investigate the relationship between *global quantities*, such as total inductance  $L$ , total resistance  $R_0$  and total current  $I$ , and *local quantities*, such as resistivity and current density. Consider first the equation of motion for the electron component of the plasma

$$n_e m_e \frac{d\mathbf{v}_e}{dt} = -n_e e (\mathbf{E} + \frac{\mathbf{v}_e \times \mathbf{B}}{c}) - \nabla P_e + n_e e \eta \cdot \mathbf{J}, \quad (10.2.6)$$

where  $P_e$  is the electron pressure,  $n_e$  the electron density, and  $\mathbf{v}_e$  the electron drift velocity. Neglecting the electron inertia (LHS of (10.2.6)), setting  $\mathbf{E} = -\nabla \phi - \frac{1}{c} \frac{\partial \mathbf{A}}{\partial t}$ , and integrating (10.2.6) yields

$$\int_1^2 \mathbf{E}_0 \cdot d\mathbf{l} = \int_1^2 (\eta \cdot \mathbf{J}) \cdot d\mathbf{l} + \int_1^2 \nabla \phi \cdot d\mathbf{l} + \frac{1}{c} \int_1^2 \frac{\partial \mathbf{A}}{\partial t} \cdot d\mathbf{l}, \quad (10.2.7)$$

where

$$\mathbf{E}_0 = \frac{1}{n_e e} \nabla P_e + \frac{\mathbf{v}_e \times \mathbf{B}}{c}; \quad (10.2.8)$$

the integrations in (10.2.7) are performed over the current path between points 1 and 2 in the plasma. The LHS of (10.2.7) is the applied voltage  $V$ , and the terms on the RHS of (10.2.7)

\*Here we ignore for now regions within PC where the ideal MHD approximation can break down, such as in neutral sheets or in tearing layers (cf. Vasiliunas, 1976).

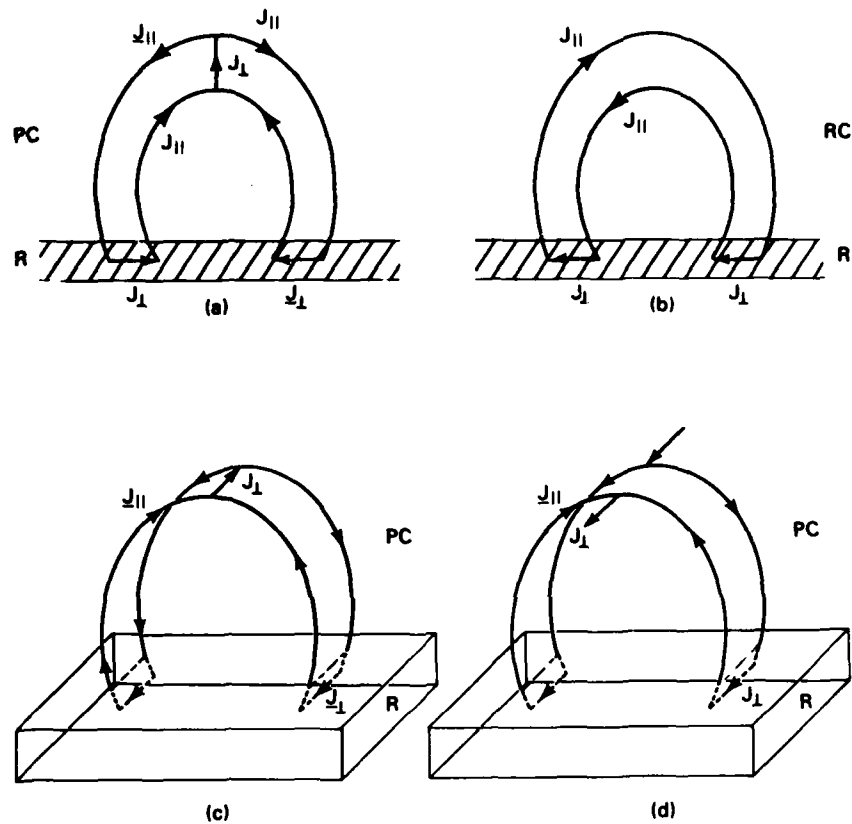


Figure 10.2 -- Schematic of four possible current paths that can occur in a closed loop

are, respectively, the resistive, capacitive, and inductive voltage drops.  $\mathbf{E}_0$  contains both a rotational and an electrostatic term. A relatively small displacement of electrons (with negligible currents) will cause the capacitive term to cancel the electrostatic part of  $\mathbf{E}_0$ ,  $\nabla P_e$ . However, a much larger current is driven continuously through the plasma by the solenoidal part of  $\mathbf{E}_0$ ,  $\mathbf{v}_e \times \mathbf{B}_0$ , and its attendant  $\mathbf{B}$  fields. If the capacitive term in (10.2.7) is neglected, for the moment, and the integration path is assumed to be that of a simple loop circuit, as is depicted in Figure (10.3), Equation (10.2.7) yields:

$$V = IR_0 + \frac{d}{dt}(IL), \quad (10.2.8)$$

where

$$V = \int_L \mathbf{E} \cdot d\mathbf{l}, \quad (10.2.9)$$

$$IR_0 = \int_L (\eta \cdot \mathbf{J}) \cdot d\mathbf{l}, \quad (10.2.10)$$

and

$$\frac{d}{dt}(IL) = \frac{1}{c} \int_L \frac{\partial \mathbf{A}}{\partial t} \cdot d\mathbf{l}. \quad (10.2.11)$$

Equations (10.2.9), (10.2.10), and (10.2.11) straight forwardly demonstrate that the contribution of local quantities along the current path determines  $R_0$ ,  $L$  and  $I$ . A more subtle conclusion is that the evolution of the relevant circuit depends not only on the local parameters but also on the global aspects of the entire circuit (see below). In addition, the current path may be very complicated and not amenable to analytic treatment.

The standard approach for both laboratory (e.g., Book *et al.*, 1978) and space plasma (e.g., Boström, 1974; Alfvén, 1977) situations is to develop a representative global circuit analog of the electrodynamic phenomenon of interest, and to couple this circuit analog to equations which specify the evolution of the local parameters (e.g., Book *et al.*, 1978).

Regardless of which type of region in PC we consider, resistive dissipation in  $R$  is expected to dominate resistive dissipation in PC (ignoring for now the possibility of instabilities occurring in PC that both limit and dissipate currents) so that magnetic energy storage is strongly dependent on domain  $R$ . This latter point can be clarified further by considering a simple lumped circuit (Figure 10.3) with a battery at potential  $V$ , an inductor with self-inductance  $L$ , and a resistor with total resistance  $R_0$ . At  $t=0$  switch  $A$  is closed. At this instant, there is no current in the circuit and the voltage drop across the resistor is zero. However, there is a voltage drop across the inductor given by  $Ldl/dt$  and equal to  $V$ , where  $I$  is the net current. As soon as the current begins to flow, a voltage begins to appear across the resistor, resulting in a decreased voltage drop across the inductor and a decrease in  $dl/dt$ . The final steady-state value of the current,  $I_0$ , is determined by  $R_0$  and the battery emf. In steady-state the complete emf is across the resistor, since  $dl/dt$  is zero. Hence, the maximum magnetic energy stored,  $1/2 LI_0^2$ , is strongly dependent on  $R_0$ , since  $I_0 = V/R_0$ . This simply reflects the fact that a current will not flow without a load. In addition because the net current grows and decays in time as  $L/R_0$ , we see that not only is the total energy stored dependent on the resistivity of domain  $R$ , but also the rate at which it is stored.

Although  $I_0$  always is determined by  $V/R_0$ , the total energy stored and the rate at which it is stored or dissipated can be enhanced greatly by allowing the inductance to vary with time. Consider the circuit in Figure 10.4. The inductance of the generator is denoted by  $L_g(t)$ , which is an explicit function of time; similarly, the total resistance, neglecting Joule heating, is represented by  $R_0(t)$ . The load inductance is represented by  $L_L$  which is constant in time, and any resistance associated with the load circuit is included as a constant term in  $R_0(t)$ . The circuit depicted in Figure 10.4 is described mathematically by

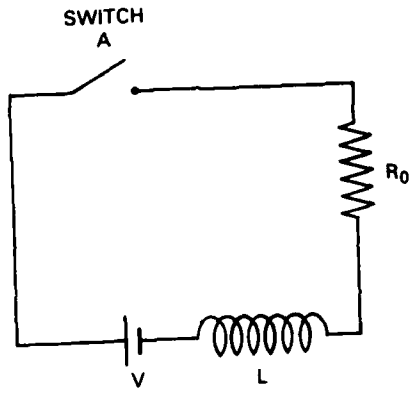


Figure 10.3 — A simple LR circuit with an inductor,  $L$ , a resistance,  $R_0$ , and an applied voltage,  $V$

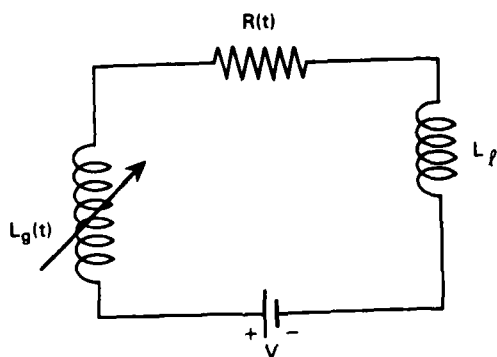


Figure 10.4 — An LR circuit illustrating how allowing for a time dependent inductance can greatly enhance either the magnetic energy storage rate or conversion rate (see text)

$$(L_t + L_k) \dot{I} + \dot{L}_k I + I R_0 = 0. \quad (10.2.12)$$

the solution of which is

$$I(t) = I_0 \left( \frac{L_{k_0} + L_t}{L_k + L_t} \right) \exp \left[ - \int_0^t \frac{R_0(t') dt'}{L_k(t') + L_t} \right], \quad (10.2.13)$$

where  $I_0$  and  $L_{k_0}$  are the values of the current and generator inductance, respectively, at  $t = 0$ . From (10.2.13) it can be shown that, if  $\dot{L}_k > 1$  and the condition

$$\left( \frac{L_k + L_t}{L_t} \right) \alpha_1^2(t) > 1 \quad (10.2.14)$$

is satisfied, and  $L_k(\tau) = 0$ , the circuit will contain more stored magnetic energy than it contained initially, where

$$\alpha_1 = \exp \left\{ - \int_0^\tau \frac{R_0(t) dt}{L_k(t) + L_t} \right\}. \quad (10.2.15)$$

Note that  $R_0$  still affects the rate of energy storage and the total energy stored.

The electrodynamic coupling of the solar atmosphere also plays a fundamental role in stabilizing potential instabilities that can occur in domain PC and thereby alter the ability of the current system to store magnetic energy. Consider a plasma in PC which is disconnected from domain  $R$ . If an external force  $\mathbf{F}$  is applied, the plasma will undergo a force drift  $\mathbf{V}_F = c \mathbf{F} \times \mathbf{B}/B^2 e$ , which in turn causes a force current density  $\mathbf{J}_F = cn \mathbf{F} \times \mathbf{B}/B^2$ . The plasma then will become polarized in such a way as to generate an electric field which results in an acceleration exactly equal to  $\mathbf{F}/\rho_0$ . However, if this plasma is now connected to domain  $R$ , the polarization charges will drain into or draw neutralizing charges from domain  $R$  in the form of parallel currents,  $\mathbf{J}_{\parallel}$ , so that the effect of  $\mathbf{F}$  on the plasma will be altered. For example, if an ideal MHD interchange instability were to occur in region III driven by the external force of gravity, the resultant perpendicular polarization electric fields then can be shortcircuited by neutralizing parallel currents drawn from domain  $R$ . This is sometimes referred to as line tying (cf. §10.2.2.2 for the relationship between this picture of line tying and the MHD picture).

Returning to regions I and II of Figure 10.1, the following question naturally arises: Where does the current path close, in these two regions, if the current generator is in domain  $R$ ? In the case of region I, the current path can close at infinity and still satisfy the condition  $\nabla \cdot \mathbf{J} = 0$ . Current closure in region II could easily result from the presence of a neutral sheet in the helmet streamer. Even if there is no current generator in region  $R$ , currents still can exist in regions I and II; since a solar-wind dynamo could induce a  $\mathbf{J}_L$ , the polarization charges generated then can drain into or draw neutralizing charges from domain  $R$  in the form of  $\mathbf{J}_{\parallel}$ . Thus, domain  $R$  will act as a resistive load dissipating the electrodynamic energy generated by the solar wind. A similar phenomenon could occur in region II due to the flow fields around the helmet streamer. This implies that the solar wind can act like a dynamo and feed electrodynamic energy back into the solar atmosphere.

The current path obviously plays an important role in magnetic energy storage. Referring again to Figure 10.1 only those paths taken by currents in regions II and III of domain PC can result in energy storage, because the stresses resulting from the current closure condition can be balanced by reactive inertial stresses in the photosphere. If the currents followed those paths allowed in region I, any electrodynamic energy generated by a photospheric dynamo simply would propagate out into the solar wind, with no storage. Even a current path such as that indicated in region II is, to some degree, susceptible to loss of electrodynamic energy, for reasons similar to those associated with region I. Those current paths which could occur in region

III (Figure 1) are least likely to allow energy to propagate out to the exosphere of the sun. However, anyone of these paths can lead to problems of energy storage. In particular, an asymmetric path in which the dynamo-generated  $J_{\parallel}$  and the closure  $J_{\perp}$  both close in region R can result in minimal energy storage in PC, if Joule dissipation is too large in R. Hence, while the current paths characteristic of loops are the most likely for generating the stresses necessary for energy storage in PC, they can still present theoretical problems.

### 10.2.1.2 Examples of Circuit Models

To illustrate the quantitative application of equivalent circuits to magnetic energy storage and conversion and, at the same time, to demonstrate some important effects associated with the flare-related transport and storage of new magnetic energy in the solar atmosphere we consider two flare model geometries: a loop (or loops), Figure (10.5a), and an inverted Y geometry, Figure (10.7a). Consider, first, a circuit analog of a loop. Within the magnetized portion of the photosphere and convection zone (domain R) the resistivity is highly anisotropic and, therefore, a tensor quantity<sup>†</sup>. Because of this high anisotropy in the resistivity, large currents can flow perpendicular to the magnetic field if an external force exists in the photosphere and/or convection zone that can force the partially ionized gas across magnetic-field lines. According to (10.2.2), either a pressure gradient or a flow field can drive  $J_{\perp}$ . In the following discussion we assume that a flow field  $u = u \hat{e}_x$ , switched on at  $t = 0$ , is responsible for driving a current in the  $-y$  direction, perpendicular to a magnetic field in the  $z$  direction, that ends in another part of domain R after passing through domain PC (Figure 10.6). In addition, we assume that  $\Omega_{ce}/\nu_e \gg 1$ , where  $\Omega_{ce}$  and  $\nu_e$  represent the electron gyro frequency and effective collision frequency respectively, so that the ions are responsible for electrical power generation. At  $t = 0^+$ , each field line which connects the foot of the loop containing the generator to its magnetically conjugate foot containing the load is nearly equipotential, due to the high conductivity parallel to  $\mathbf{B}$  in domain PC. At  $t = 0^+$ , however, the flow field results in an emf, given by  $u B_z/c$ , that will drive a current in the  $-y$  direction. Hence, a potential difference will exist perpendicular to the magnetic field, since the current produced need not satisfy  $\nabla \cdot \mathbf{J} = 0$ . At points where  $\nabla \cdot \mathbf{J} \neq 0$ , charge accumulates and, in a sense, anodes exist with a separation  $d$  and at potentials  $\Phi(0)$  and  $\Phi(d)$ . Since the electrons are line-tied ( $\Omega_{ce}/\nu_e \gg 1$ ), they cannot move perpendicular to  $\mathbf{B}$  to neutralize the charge accumulation. However, this charge accumulation causes a potential difference to exist between the magnetically conjugate feet of the loop, so that a flow of electrons is induced along the field lines linking the points of potential difference in an attempt to remove this charge imbalance. Since the potential at each "anode" of the "generator" is of different polarity, antiparallel currents develop between the conjugate feet of the loop. Hence, there exists a current loop made up of both  $J_{\parallel}$  and  $J_{\perp}$  components between the conjugate feet, with the current being driven by the flow field.

To estimate the magnitude of the flow-field velocity as well as the time required to build up and store an amount of magnetic energy  $E_F = 1/2 L I_0^2$ , we refer to Figure (10.6) and note that the maximum available electrical power is the kinetic energy density of the flow field delivered through the surface area  $S_{\perp}$  between the anodes; that is

$$P_{\max} = \frac{1}{2} nm_{\perp} u^3 S_{\perp} \quad (10.2.16)$$

To store  $E_F$  in a time  $\Delta t_{\perp}$  requires

$$\frac{\epsilon}{2} nm_{\perp} u^3 S_{\perp} \Delta t_{\perp} \approx E_F, \quad (10.2.17)$$

where the factor  $\epsilon$  represents the efficiency of flow to electrical-energy conversion. Since  $\Delta t_{\perp} \approx L/R_F$  (cf. Figure 10.8), we find  $u$  must satisfy the inequality

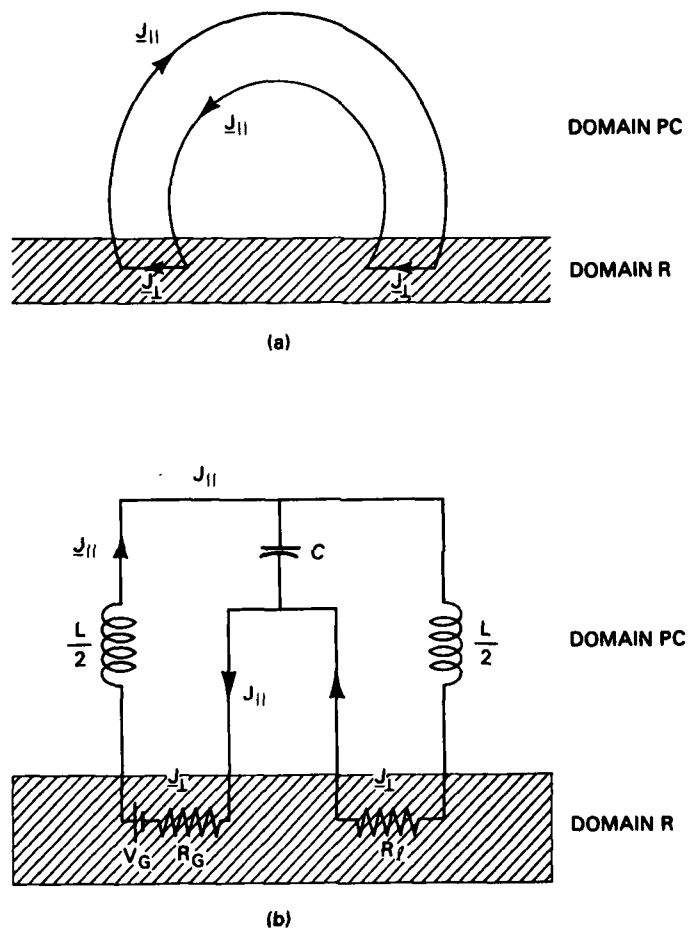


Figure 10.5 — Illustrates an equivalent circuit for a closed loop.  $V_G$  and  $R_G$  represent the current generator voltage and resistive load, respectively,  $R_I$  the resistive load in the other foot of the loop,  $C$  the capacitance associated with the polarizability of a magnetized plasma, and  $L$  the total inductance of a loop.

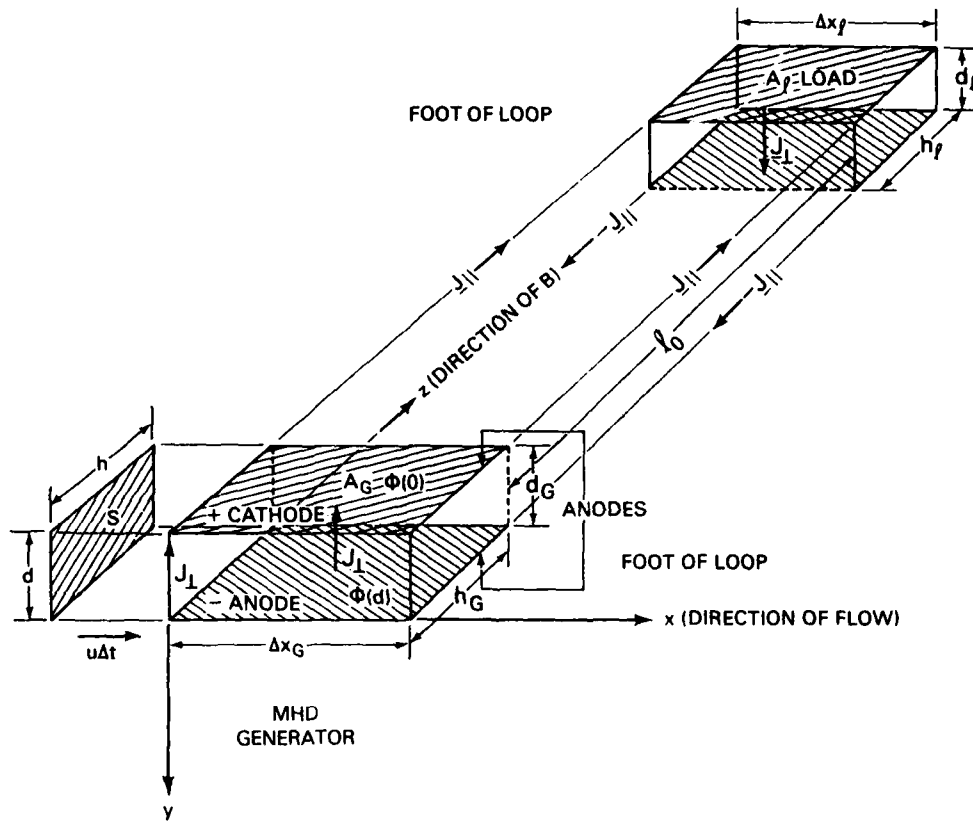


Figure 10.6 — Schematic of the current system set up in a loop by a flow field directed perpendicular to one foot of the loop (see text)

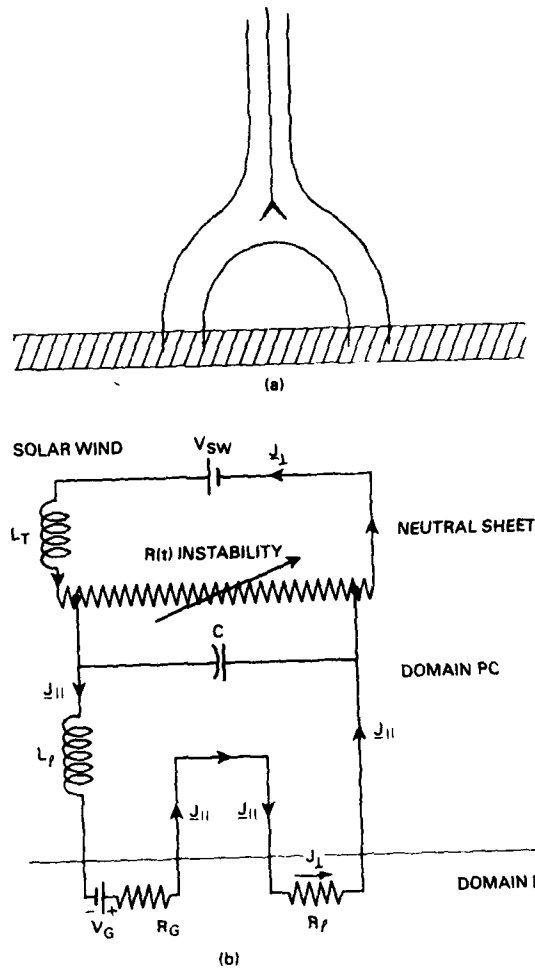


Figure 10.7 — Schematic of an equivalent circuit for an inverted-Y type flare model (see text)

$$u \geq \left( \frac{I_0^2 \eta_1^e}{10 \epsilon (1 - \alpha_e) m_e n \Delta x_e h_e^2} \right)^{1/3}, \quad (10.2.18)$$

where  $R_T = R_L + R_e = R_e/(1 - \alpha_e)$ ,  $\alpha_e = (1 + R_e/R_L)^{-1}$ , which is a measure of the impedance matching between generator and load and  $R_e = \eta_1^e d_e / \Delta x_e h_e$ . The quantity  $\alpha_e$  reflects the well-known fact that the power conversion efficiency of a generator increases as the ratio of the external to internal load increases, up to a maximum  $\alpha_e = 1/2$  for the present case. Equation (10.2.18) clearly requires  $1 - \alpha_e \leq 1$  since otherwise  $u$  will become intolerably large although the energy storage time will shorten since  $\Delta t_e = L (1 - \alpha_e) / R_e$ . To estimate the required  $u$  and  $\Delta t_e$  for a large flare, e.g., with  $E_F \approx 10^{32}$  ergs output, we note that  $L \approx l_0/c^2$  (Figure 10.6) and that  $\Delta x_e \approx 10^{10}$  cm and  $l_0 \approx 10^9$  cm are typical for such a flare. Using  $\eta_1^e \approx 10^{-10}$  sec,  $h_e \approx 5 \times 10^8$  cm,  $d_e \approx 10^9$  cm and  $n \approx 10^{17}$  cm<sup>-3</sup> as typical temperature minimum values, we find  $\Delta t_e \approx 5 \times 10^6 (1 - \alpha_e)$  secs and  $u > 3.4 \times 10^5 (\epsilon (1 - \alpha_e))^{-1/3}$ , and a total current  $I_0 \approx 10^{22}$  sta-amps (from  $E_F = L I_0^2 / 2$ ). If  $\epsilon \approx 0.1$  and  $\alpha_e = 1/2$  then  $\Delta t_e \approx 2.5 \times 10^6$  secs and  $u \geq 10^5$  cm/s. Both of these values, while rough estimates, appear reasonable for the preflare state.

We can use the simple-loop equivalent circuit to understand the preflare storage process both, qualitatively and quantitatively, by solving the equivalent circuit equation corresponding to Figure 10.5b:

$$L \frac{dI}{dt} + I R_T = V_g, \quad (10.2.19)$$

which yields the trivial solution\*

$$I = \frac{V_g}{R_T} (1 - e^{-R_T t / L}), \quad (10.2.20)$$

where we have assumed that  $V_g$ ,  $R_T$ , and  $L$  are independent of time and spatially integrated to include their maximum contributions from both domains R and PC.

The total magnetic energy stored, the rate of magnetic energy storage, and the rate of Ohmic heating are, respectively

$$\frac{LI^2}{2} = \frac{L}{2} \frac{V_g^2}{R_T^2} (1 - e^{-R_T t / L})^2, \quad (10.2.21a)$$

$$\frac{d}{dt} \left( \frac{LI^2}{2} \right) = \frac{V_g^2}{R_T} e^{-R_T t / L} (1 - e^{-R_T t / L}), \quad (10.2.21b)$$

and

$$I^2 R_T = \frac{V_g^2}{R_T} (1 - e^{-R_T t / L})^2. \quad (10.2.21c)$$

Figure (10.8) illustrates the well-known time dependence of (10.2.21a-c) in dimensionless units. Note that all of the generated electrical power is stored magnetically until  $t \approx 0.69L/R_T$ , after which the Ohmic heating term dominates and the rate of magnetic energy storage drops precipitously. Since the Ohmic heating varies as  $I^2 R_T$ , the plasma in the temperature minimum is being Ohmically heated by a power input level of  $\geq 10^{26}$  erg/s in a volume  $\approx 10^{26}$  cm<sup>3</sup>.

\*We have neglected the capacitive term since it only gives rise to LRC ringing and does not appreciably effect the energy storage process. The frequency of the ringing is  $\sqrt{1/LC}$  and, depending on the frequency region, corresponds to various normal modes of a magnetized plasma, such as Alfvén waves.

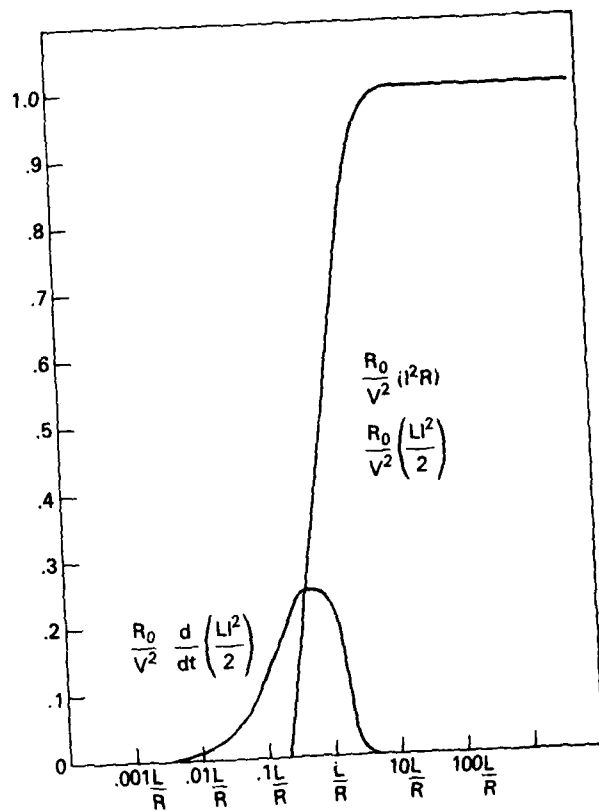


Figure 10.8 — Schematic of the rate of magnetic energy storage,  $(R_0 d/dt (L^2/2)/V_0^2)$ , the rate of Joule heating  $(R_0 I^2 R/V^2)$ , and the magnitude of the magnetic energy stored globally,  $L^2 R_0/V_0^2$ , in a simple circuit model such as in Figure 10.3

Since we have assumed the current is distributed uniformly throughout the generating or load volume, the Ohmic heating does not exceed the global radiation losses from the volume ( $\approx 10-50 \text{ erg/cm}^3/\text{s}$ , Machado and Emslie, 1979). However, there can be regions within either the generator or load volumes where the local Joule heating rates equal or exceed the local radiation losses. Under these circumstances, preflare heating of the temperature minimum should occur. In addition, if the heating should exceed the local radiation losses plasma expansion into the loop should occur. This expansion may be gradual or rapid, depending on the Joule heating rate, and can be dominant in one foot of the loop as opposed to the other due to impedance mismatch ( $\alpha_c \neq 1/2$ ). Since any increase in mass density can alter the energy balance and pressure equilibrium in the remainder of the loop, by increasing the radiation losses and absorbing more heat flux from the corona, highly turbulent mass flows should exist within loops prior to flares. These mass flows are expected particularly in the transition-zone volumes of loops, due to the precarious energy balance there (Kuperus and Athay, 1967). Hence, we conclude that preheating of the temperature minimum, density enhancements within loops, and turbulent processes within loops all may occur as natural by-products of preflare magnetic-energy storage.

A multiple-loop equivalent circuit is illustrated in Figure (10.9). This circuit demonstrates several important concepts, that to the authors' knowledge, have never been discussed in the literature. In our earlier discussions we have emphasized circuits that are coupled *conductively* by flowing currents. However, two or more loops can couple strongly with one another *inductively* if they are sufficiently close together. Under these circumstances a mutual inductance exists between these two loops. This concept is easily extended to multiple-loop systems. An alternative situation is for a loop to be coupled inductively to an open magnetic configuration, such as an inverted-Y configuration. This concept of inductively coupling distinct magnetic configurations in the solar atmosphere has *radically* new implications for flare theory and needs further theoretical study. Consider the following examples:

- (1) The magnetic-flux variation resulting from a one-loop flare induces large emfs and, thus, currents in a neighboring loop, thereby triggering a flare in the neighboring loop, if sufficient magnetic energy is stored therein;
- (2) Emerging magnetic flux induces temporal variations of the global field configuration in which magnetic energy already is stored. These inductive field changes produce large emfs and currents, thus causing the global field configuration to release its energy in the form of a flare. *No mechanical coupling* of the two configurations is required, as is generally required in emerging flux flare models (e.g., Heyvaerts *et al.*, 1977); and
- (3) A time-varying magnetic field due to, e.g., emerging flux or a flare loop, couples inductively with an inverted-Y field configuration. The induced emf produces accelerated streams of electrons and protons that move into the photosphere or out into the solar wind along that portion of the inverted-Y configuration with open field lines, depending on the direction of the emf, producing radio bursts such as Type III, U and type V bursts. *No transport of particles across field lines is required.*

We should note that, because of the high electrical conductivity in the solar atmosphere, the skin depth,  $\Delta x_s \approx c/\omega_{pe} \sqrt{\nu_{ei} \Delta t}$ , where  $\nu_{ei}$  is the electron-ion collision time and  $\omega_{pe}$  the plasma frequency, can be very small if the timescale of flux variation,  $\Delta t$ , is small. Hence, very large current densities can be produced as well as high-energy particle streams (Spicer, 1981b).

The equivalent circuit model also yields a potential explanation of "homologous" sequences of flares, which are regularly spaced in time, appear to come from the same volume

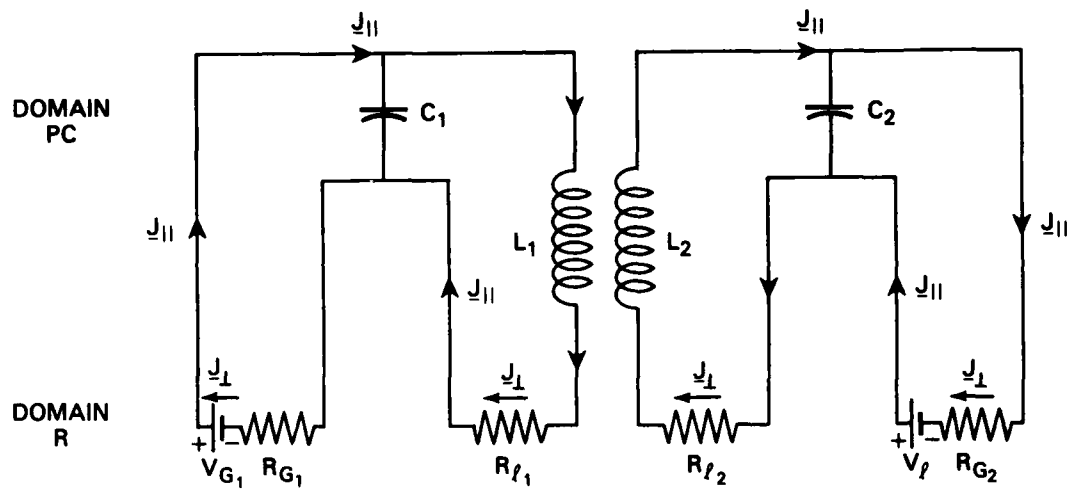


Figure 10.9 — The equivalent circuits of two juxtaposed loops interfacing inductively, as opposed to mechanically conductively

in the solar atmosphere and are quite similar in form (Ellison, 1963; Svestka, 1976). The interval between such flares is observed to increase with importance, to as much as  $> 10^6$ s for events of Importance 3. According to the single loop circuit model presented earlier in this section, the largest flare requires  $\Delta t_s > 5 \times 10^6$ s for energy storage to occur, while for small flares this time certainly is shorter. For a sequence of flares to occur, spaced roughly by  $\Delta t_s$ , the basic current system and thus the original magnetic field configuration must remain intact. However, if the fields vent out the top of the atmosphere the current system is changed, and the value of the inductance will depend on how the current closes in the new field configuration. If the current closes at infinity the new current-field configuration cannot repeat the flare in a time  $\Delta t_s$ , because the circuit time constant becomes infinite as the inductance becomes infinite; to restate, the rate at which magnetic energy is stored goes to zero because an infinite time is required to transport energy to infinity. From these arguments, we conclude that the phenomenon of "homologous" flares demands that the current system close at a distance above the photosphere not greater than  $10^{10}$ cm, to ensure that the time between sequences of flares is sufficiently short.

The question of "homologous" flares and open magnetic fields leads naturally to the helmet streamer or Y type flare model, depicted in Figure (10.7a) (Carmichael, 1964; Sturrock, 1966, 1967, 1972, 1974; Kopp and Pneuman, 1976; Pneuman 1978, 1979, 1980, 1981). Much of the present discussion of currents in closed loops (or multiple loop) field configurations also is true for Y-type field configurations. However, there is one important difference: part of the current must close not only in domain R, at both feet of the streamer, but also in domain PC. An external force must therefore exist in the tail of the helmet streamer which produces an emf capable of driving a perpendicular current of sufficient magnitude, and through a large enough area, to close the circuit. This applied emf must be of the right sign as not to oppose the photospheric emf. If it does oppose the photospheric emf, its magnitude must be less than that of the photospheric emf; otherwise, the external force - presumably the solar wind - will be the source of generator energy. Most versions of helmet-streamer flare models, as presently proposed, in fact rely on the solar wind instead of the photosphere as the source of flare energy. Barnes and Sturrock (1972) have investigated numerically a modified form of the helmet-streamer model, in which they assume a photospheric generator: field-line twisting at the feet of a loop that opens up after the field becomes too greatly stressed by the twisting. A model such as Barnes' and Sturrocks' would yield similar magnitudes for the photospheric flow velocity and energy storage time as the simple loop model discussed earlier. However, it remains to be demonstrated that, once the loop opens the current still can close low in the atmosphere; since otherwise, the configuration would cease to be of use for storing magnetic energy and could not explain "homologous" flares.

Models that do use the solar wind as a power source of the flare, either in the pre-flare or in the post-flare period (Kopp and Pneuman, 1976; Pneuman, 1978, 1979, 1980, 1981), encounter difficulties because the flow velocities that give rise to the  $J_\perp$  which closes the current in the helmet must be at least as large as the flow velocities we estimated in §10.2.1.2 for the photospheric generator; the currents must still go through the photospheric load, since without a load currents do not flow. Because the number density of the coronal plasma is  $\gtrsim 10^6$  less than the photospheric plasma, the flow velocities perpendicular to the field of the streamer required of a coronal-wind generator will be  $\gtrsim 10^2$  larger ( $\gtrsim 10^8$ cm/s) than those required of the photospheric generator unless the area of the coronal generator is increased by  $\gtrsim 10^6$  (up to  $\gtrsim \times 10^{21}$ cm<sup>2</sup>). However, even increasing the area by a factor of  $\gtrsim 10^6$  will not improve a model that attempts to power the post-flare phase with the solar wind, for the following reasons. The maximum power available is  $P_{\max} \approx nm\mu_\perp^3 S/2$ , where S denotes the area perpendicular to the magnetic field through which the plasma flows and  $\mu_\perp$  is the magnitude of the flow speed perpendicular to the magnetic field and *not* the radial coronal wind velocity. Taking  $n \approx 10^8$ cm<sup>-3</sup>,  $\mu_\perp \approx 10^6$  cm/sec and  $S \approx 10^{21}$ cm<sup>2</sup>, we find  $P_{\max} \approx 10^{23}$  erg/s, which is barely

enough to heat a coronal loop. The Kopp-Pneuman model is even more extreme, physically, because the model requires potential magnetic fields between the photosphere and coronal heights of  $\geq 1.2R_{\odot}$ , and non-potential fields above that height. In other words, their model implies that the current system closes completely in domain PC. We find such a current system unphysical since their model contains no electrodynamic coupling to the photosphere, yet includes electron beams propagating into the photosphere which are, by definition, currents and part of the current system. Kopp and Pneuman argue that part of the source of free energy in their model is the energy expended by an erupting prominence while distorting the overlying magnetic fields. This distortion causes an increase in the energy of the magnetic field, which then is utilized to explain other aspects of the flare phenomenon. However, these authors fail to point out that the  $J \times B$  forces which initially distorted the fields also produce perpendicular currents, *e.g.*, polarization currents, thus causing large potential differences along field lines which are normally equipotential. This causes the excess charge to drain into or draw neutralizing charges from the photosphere to remove the potential differences, thereby dissipating much of the energy that went into distorting the fields (Spicer, 1976).

An equivalent circuit of a helmet-streamer model, shown in Figure (10.7b) is based on the model proposed by Bostrom (1974) for the magnetotail. We have added a photospheric voltage source to model the photospheric current generator, which can be removed for a model which is completely solar-wind driven.

Equivalent circuits for more complicated magnetic configurations, such as prominences, are more difficult to specify. However, attempts have been made to satisfy the current closure condition for prominences (Kuperus and Raadu, 1974; Van Tend and Kuperus, 1978; Kuperus and Van Tend, 1979) who model a prominence with a line current that closes via a mirror current in the photosphere. Their equivalent circuit is similar to that discussed for a simple loop, but the total resistance must be modified to account for the long photospheric current path. Their work has been extended further with diffuse current profiles by Lerche and Low (1980a,b,c), who have developed a prescription for constructing equilibrium fields for any horizontal prominence and with an arbitrary magnetic field. However, the stability of these solutions has yet to be addressed (*cf.* of §10.2.2.2).

#### 10.2.1.3 The Rate of Magnetic Energy Transport and the Energy Storage Location

It is commonly, albeit incorrectly, stated in the literature that magnetic energy only can be transported at the Alfvén speed (*e.g.*, Van Hoven *et al.* 1980; Brown and Smith, 1980). We need only consider an electron beam propagating at the speed of light, which constitutes a current with a drift speed of  $c$ , to illustrate that magnetic energy can be transported at any velocity up to that of light. The Alfvén velocity is but one speed associated with the dielectric properties of a magnetized plasma, and is important only for transmitting low frequency signals of voltage, current, and inductance changes. For example, when a voltage source is switched on suddenly in a circuit made up of a magnetized plasma and a load, the current surge propagates through the circuit with a dispersion of speeds determined by the frequency spectrum excited and the wave modes which can be supported by the dielectric properties of the magnetized plasma. The specific mode which will transport the bulk of the power associated with the current surge depends on the power spectrum associated with the switching voltage. One of these modes may be the Alfvén-wave mode or a mode that propagates at the speed of light. In fact, it is well-known that switching operations or short circuits in transmission lines used in utilities, which cause a change from steady state, result in current surges (*i.e.*, beams), accompanied by a self-consistent voltage surge that propagate at light speeds. However, such utility circuits cannot support Alfvén waves because they are not normal modes of such circuits whereas a magnetized plasma can support Alfvén waves as well as higher velocity waves.

The above discussion leads to the question, "can an energy release by some dissipation mechanism occurring in the corona be driven *directly* from the photosphere?" The answer to this question is a "qualified no," if we mean that a voltage source in the photosphere directly drives a flare, because the maximum power available from a generator (cf. §10.2.1.2, Equation (10.2.16)) would be  $\approx 10^{26}$  erg/s unless the flow velocity in domain  $R$  is roughly an order of magnitude larger than that obtained previously. However, it is possible for the bulk of the magnetic energy required for a flare to be stored slowly remote (as opposed to local, i.e., *in situ* storage) from the site of energy release, and be brought to the site at speeds up to that of light; this remote storage site may well be the photosphere. An example to be discussed in more detail in §10.3 concerns the results of a sudden local increase in the distributed circuit impedance of a loop. Because the inductance of a loop is so large, the circuit attempts to keep constant the product of the inductance and *net* current, that is, the magnetic flux ( $LI$ ). The circuit accomplishes this by generating a large-amplitude voltage wave with an accompanying current wave (surge) which will propagate at whatever speed is necessary, up to the speed of light, to keep the flux constant. This behavior of high-inductance circuits is, in particular, the essence of double-layer and anomalous resistivity flare models (cf. §10.3.2). Also note that accounting for the global aspects of the entire electrodynamic circuit demonstrates that it is not only the local properties of the plasma, but also the global properties, that are important (Alfvén, 1977).

#### 10.2.1.4 The Magnitudes of Magnetic Fields Required by Magnetically Driven Flare Models

One puzzling aspect of magnetically driven flare models is the large currents, and thus large magnetic fields required to drive the flare. These fields typically range from a few hundred gauss to 1000 gauss or more. In fact, the observed energy densities of flare plasmas require fields of 500 gauss or more to contain them (Widing and Spicer, 1981). Part of the solution to this problem is obtained by noting that  $\nabla \cdot \mathbf{J} = 0$  implies that the net current must vanish globally. From Ampere's equation in integral form,

$$\oint \mathbf{B} \cdot d\mathbf{l} = \frac{4\pi}{c} \int \mathbf{J} \cdot d\mathbf{S},$$

we note that a surface integral taken outside the volume containing anti-parallel currents must vanish and, as is shown in §10.2.2,  $\nabla \cdot \mathbf{J} = 0$  is required for MHD equilibrium. Hence, large currents and fields can, in principle, exist in such solar magnetic configurations. In addition, if these currents are locally force free\* (cf. §10.2.2.1), the mutual repulsion that arises from anti-parallel currents will be locally suppressed.

#### 10.2.2 In situ Storage of Magnetic Energy

The prevalent view of the preflare state maintains that the flare free energy must be stored in coronal magnetic fields because it appears to be released there (Svestka, 1976; Van Hoven *et al.* 1980) as opposed to in a remote photospheric site; hence the term "*in situ* storage." There are two principal arguments for this view. The first argument is based on the *observational* fact that no large changes in the photospheric structure have been detected to date throughout the duration of most flares (cf. Svestka, 1976 for a review). The second argument is essentially theoretical: the free energy required to drive a large flare is  $\approx 10^{32}$  ergs and the only source of this energy that can be identified observationally is the atmospheric magnetic field (Parker, 1957). To release  $\approx 10^{32}$  ergs of atmospheric magnetic field requires relaxing  $\approx 500$  gauss to 400 gauss within a volume of  $\approx 6 \times 10^{28} \text{ cm}^3$ . Note that the magnetic pressure associated with such fields is two to three orders of magnitude greater than the ambient gas pressure, as is discussed later. While both arguments suffer from observational and theoretical difficulties (cf. §10.2.2.4), the proposition of *in situ* storage of magnetic energy has motivated a majority of the theoretical studies related to flare physics. The

\*It seems to be a general trait of force free field solutions to have anti-parallel currents.

preponderance of these studies have utilized the concept of force free fields (§10.2.2.1), that is, fields for which the Lorentz force vanishes. The utilization of force-free fields is motivated by the need to slowly build up magnetic energy *in situ* by stressing the magnetic fields ( $\mathbf{J}_\parallel \times \mathbf{B} \neq 0$ ) while maintaining a relatively stable (*cf.* §10.2.2.1) large-scale magnetic configuration in a low pressure atmosphere. Under these conditions, large-scale equilibrium magnetic configurations only can be either potential with no free energy (current sources are external to the atmosphere, that is, below the photosphere) or force-free, because the plasma pressure gradients in the atmosphere are smaller than the magnetic pressure by up to four orders of magnitude and therefore cannot support  $\mathbf{J} \times \mathbf{B}$  forces (*e.g.*, Van Hoven *et al.* 1980). This form of *in situ* magnetic energy storage has resulted in basically two classes of flare models: those models which utilize magnetic dissipation mechanisms driven by  $\mathbf{J}_\parallel$  and those driven by  $\mathbf{J}_\perp$  (Spicer and Brown, 1980; 1981). The  $\mathbf{J}_\perp$  class of models are of the current sheet or field reversal variety (§10.3.5), and accordingly draw energy from the photosphere via  $\mathbf{J}_\perp$ , since  $\mathbf{J}_\perp$  is the means by which the upper and lower portions of solar atmosphere are electrostatically coupled (*cf.* §10.2.1), or mechanical energy in the form of *in situ* flows must exist to drive the  $\mathbf{J}_\perp$  current (Spicer and Brown, 1980; 1981). The helmet-streamer circuit model (Figure 10.7b) illustrates the essentials of the applicable energy sources.

Because of the commonly held view that preflare magnetic energy storage involves *in situ* force-free fields, and because there are still unanswered theoretical questions associated with the view, the following section comprises a brief but thorough review of the concept of force-free fields and the physical constraints associated with them.

### 10.2.2.1 Theoretical Aspects of Force Free Fields

Force free fields are equilibrium solutions to a *reduced* set of magnetostatic equations based on the assumption that the pressure gradient either vanishes or is negligibly small; thus corresponding to a low  $\beta$  plasma magnetic-field configuration, where  $\beta = 8\pi P/B^2$  (*e.g.*, Longmire, 1963).\* The relevant force-free equations are

$$\nabla \times \mathbf{B} = \alpha_0(\mathbf{r})\mathbf{B}, \quad (10.2.22)$$

where  $\alpha_0$  is a scalar function defined by

$$\mathbf{B} \cdot \nabla \alpha_0 = 0, \quad (10.2.23)$$

so that  $\alpha_0$  is a surface function. The use of magnetostatic equilibria solutions in a clearly time varying problem (energy storage requires time) is justified only if the magnetic field evolves in a time much longer than a MHD transit time, the time it takes a MHD wave to propagate the shortest magnetically determined spatial scale of the plasma-magnetic field configuration, PMFC; the system thus appears to evolve through successive stages of quasi-static force-free equilibria each being in a higher energy state if energy storage is to occur. Since magnetic storage takes  $\sim 10^6$  sec, this assumption is reasonable.

From the virial theorem it can be shown that no plasma-magnetic field configuration can be globally force free, only locally (*e.g.*, Longmire, 1963; Shafranov, 1966; Schmidt, 1979). Indeed, a fundamental result of the virial theorem is that the total pressure outside the region occupied by the force-free magnetic field must be greater than the mean pressure inside the force-free region. In laboratory magnetic confinement experiments where force free fields are involved, such as reverse field pinches (RFP), this external pressure is represented by a highly conducting immovable wall. Such a wall does not exist in the solar atmosphere, however, implying that a force-free field must be surrounded either by a high-pressure gas blanket, which could only occur in the low atmosphere, or by a potential field whose normal component matches that of the force free field across their common boundary. This implies that the

\*We emphasize that  $\alpha_0$  is a local quantity and varies by orders of magnitude within a given solar plasma-magnetic field configuration.

magnitude of the potential field is comparable to that of the force-free field. Thus, if the release of  $10^{32}$  ergs by a large flare is to be explained with force free fields, we require  $\geq 500$  gauss potential fields distributed over volumes much greater than  $10^{29} \text{ cm}^3$ . An alternative is to assume that the principal field is potential with parallel currents (Syrovatskii, 1966; Barnes and Sturrock, 1972; Sakurai and Uchida, 1977; Uchida and Sakurai, 1977).

If  $\alpha_0$  is constant then the curl of (10.2.22) yields

$$\nabla^2 \mathbf{B} + \alpha_0^2 \mathbf{B} = 0. \quad (10.2.24)$$

the vector Helmholtz equation. This equation is linear and has a general solution in terms of poloidal and toroidal components (Ferraro and Plumpton, 1966). Various authors have utilized (10.2.24) to compute, in various coordinate systems, the structure of force-free fields and thus the magnetic energy stored in the atmosphere using magnetograph line of sight field measurements and adjusting  $\alpha_0$  independently to achieve at least gross agreement with observations (Raadu and Nakagawa, 1971; Nakagawa and Raadu, 1972; Nakagawa, 1973; Tanka and Nakagawa, 1973; Nakagawa, 1974; Levine, 1975, 1976; Chiu and Hilton, 1977; Barbosa, 1978; Nakagawa, 1978; Nakagawa *et al.*, 1978). It is expected that this kind of calculation will be greatly improved by using vector magnetograph measurements to determine  $\alpha_0 = (\nabla \times \mathbf{B}) \cdot \mathbf{B} / B^2$  with higher precision.

Sakurai (1979) has developed a numerical approach in which the set of equations (10.2.22-10.2.23) are expressed in terms of curvilinear coordinates, using Euler potentials, based on the observed magnetic-field configuration. By assuming a very coarse mesh and a simple representation of the field variation along field lines, Sakurai was able to compute approximate forms of quite general field configurations.

A more general approach to the problem of relating force-free fields to energy storage involves relaxing the  $\alpha_0 = \text{constant}$  assumption. However, this approach results in highly complex, non-linear differential equations with solutions that are not necessarily unique and are difficult to interpret physically (Low and Nakagawa, 1975; Jockers, 1976; Low, 1977a,b; Anzer, 1978; Birn *et al.* 1978; Heyvaerts *et al.*, 1979; Hood and Priest, 1980). This lack of uniqueness in the solutions, as well as their interpretation, is undoubtedly related to the fact that (10.2.22) is arrived at by imposing *a priori* the condition that  $\mathbf{J} \times \mathbf{B} = 0$  everywhere without regard to boundary conditions *e.g.*,  $\nabla \cdot \mathbf{J}_\parallel = -\nabla \cdot \mathbf{J}_\perp$ , solving the resulting equations, and then attempting to match the solutions to boundary conditions not arrived at from a physically consistent treatment of the whole set of relevant equations. A self-consistent approach would follow, for example that given by Pereversev *et al.* (1978).

### 10.2.2.2 Preflare Stability of Magnetic Configurations

Associated with the question of *in situ* energy storage and force free fields is the stability of such fields. That is, what kinds of force free fields can exist in quasi-equilibrium before the equilibrium becomes unstable? Before reviewing the published literature on force-free field stability it is worthwhile to examine the relationship between electrodynamic coupling of the solar atmosphere,  $\nabla \cdot \mathbf{J} = 0$ , and stability.

In order to solve the magnetostatic equilibrium equations (neglecting gravity),

$$\nabla p = \frac{\mathbf{J} \times \mathbf{B}}{c}. \quad (10.2.25)$$

$$\nabla \times \mathbf{B} = \frac{4\pi}{c} \mathbf{J}. \quad (10.2.26)$$

and

$$\nabla \cdot \mathbf{B} = 0. \quad (10.2.27)$$

we proceed by seeking low  $\beta$  solutions. At  $\beta = 0$  the global magnetic field must be a vacuum field and due to external currents.

The first-order perturbation to the vacuum field, due to a plasma pressure  $p$ , is

$$\nabla p = \frac{\mathbf{J}_1 \times \mathbf{B}_0}{c} . \quad (10.2.28)$$

$$\nabla \times \mathbf{B}_1 = \frac{4\pi}{c} \mathbf{J}_1 . \quad (10.2.29)$$

and

$$\nabla \cdot \mathbf{B}_1 = 0 . \quad (10.2.30)$$

where  $\mathbf{J}_1$  is the plasma current density,  $\mathbf{B}_0$  the vacuum field and  $\mathbf{B}_1$ , the perturbation in  $\mathbf{B}_0$  due to finite gas pressure. Following Taylor (1963) we note that (10.2.28)-(10.2.30) do not, in general, possess a solution for any given  $p$  (this is also true of (10.2.25)-(10.2.27)). We therefore need to determine the conditions which  $p$  must satisfy in order for a solution to exist. The first condition arises from taking the scalar product of (10.2.28) with  $\mathbf{B}_0$  to obtain

$$\mathbf{B}_0 \cdot \nabla p = 0 \text{ or } \frac{\partial p}{\partial s} = 0, \quad (10.2.31)$$

where  $s$  is measured along a field line. Equation (10.2.31) implies that  $p$  is constant on a field line, so that isobaric (magnetic) surfaces exist. Next we take the vector product of (10.2.28) with  $\mathbf{B}_0$  to obtain

$$\mathbf{J}_{11} = c \frac{\mathbf{B}_0 \times \nabla p}{B^2} \quad (10.2.32)$$

so that

$$\mathbf{J}_1 = c \frac{\mathbf{B}_0 \times \nabla p}{B^2} + \lambda \mathbf{B}_0. \quad (10.2.33)$$

where  $\lambda$  is an arbitrary scalar function.

The requirement that  $\nabla \cdot \mathbf{J}_1 = 0$  yields

$$\mathbf{B}_0 \cdot \nabla \lambda = -2 \nabla \mathbf{B}_0 \cdot (\nabla p \times \mathbf{B}_0) / B_0^3. \quad (10.2.34)$$

or

$$\frac{d\lambda}{ds} = -2 \nabla \mathbf{B}_0 \cdot (\nabla p \times \mathbf{B}_0) / B_0^4. \quad (10.2.35)$$

A sufficient condition for this equation to possess a unique single-valued solution for  $\lambda$  along a given field line is (Newcomb, 1959)

$$\int_1^2 \nabla \mathbf{B}_0 \cdot \frac{(\nabla p \times \mathbf{B}_0)}{B^4} ds = 0, \quad (10.2.36)$$

where the integration is performed from the point where the field line enters to the point where it first leaves the volume of interest (Taylor, 1963). If (10.2.36) is satisfied, a unique  $\lambda$  always can be constructed from (10.2.33). The condition (10.2.36) is therefore both necessary and sufficient.

Physically, (10.2.36) expresses the fact that a perpendicular current cannot be divergence free, except in cases of high symmetry (Longmire, 1963), so that parallel currents must exist to carry off excess charge. Thus, *equilibrium* requires there be no accumulation of charge on a field line. In fact (10.2.36) represents a boundary condition that the *local* force-free fields must satisfy if they are to match on to the global magnetic configuration. Hence, the electrodynamic coupling of the solar atmosphere plays an important role in understanding equilibrium configurations. We emphasize that the concept of equilibrium as opposed to steady state is, strictly speaking, incompatible with magnetic energy storage: since equilibrium implies no flows, by definition, electrical power generation would occur only through pressure gradients. However, we can use the concept of equilibrium if the time scales of energy storage and instability are sufficiently different, as already noted.

The investigation of magnetohydrodynamic (MHD) stability, in particular of coronal loops and prominences, is a problem first examined by Anzer (1968) and Raadu (1972). More recent studies (Van Hoven *et al.* 1977; Chiuderi *et al.* 1977; Giachetti *et al.* 1977; Hood and Priest, 1979; Silleen and Kattenberg, 1979; Hasan, 1979) were precipitated by the Skylab observations which suggest that the so-called compact flares originate in loops (*cf. e.g.*, Sturrock, 1980 and Brown *et al.* 1981 for reviews) and by the loop flare model developed by Spicer (1975, 1976, 1977a,b, 1981a,b) and Colgate (1978). The essence of the majority of these papers is the following. In a series of papers, Van Hoven *et al.* (1977), Chiuderi *et al.* (1977), and Giachetti *et al.* (1977) present a MHD marginal stability analysis of a loop using as a model a cylindrically symmetric loop in which they investigate the role of a positive transverse (to the magnetic field) gas-pressure gradient in the MHD stability of a loop made up of a Bessel function force-free field (Lundquist, 1950). Their loop model is essentially a weakly non-force-free field embedded in a high- $\beta$  force-free environment. On the other hand, Silleen and Kattenberg (1979) determined the growth rates for kink instabilities driven by a Bessel function force-free field which was assumed to be embedded in a potential low- $\beta$  potential field, which is in agreement with requirements imposed by the virial theorem. Hasan (1979), who also determined growth rates, investigated the stability of a cylindrically symmetric force-free field with constant pitch and found it always unstable, consistent with the results of Anzer (1968). Hasan also included the effect of a small positive transverse pressure gradient which he found to be stabilizing, as did Chiuderi, Giachetti, and Van Hoven in their series of papers. Hood and Priest (1979) also examined the stability of a constant-pitch field, as well as a variable pitch field (uniform axial field). The results of Hood and Priest differ from Hasan's for the constant pitch case because Hasan did not include the effects of line tying of the field lines in the photosphere. Most of these papers in one way or the other attempted to include line tying of the loop's ends in their stability analyses, some more rigorously than others. Hood and Priest (1979), in particular, make the strong claim that line tying, as opposed to shear stabilization, is the dominant MHD stabilizing feature of coronal loops. However, Spicer (1976) and Spicer and Brown (1981) point out that this is only part of the picture, since the three-dimensional aspects of the loop (see below) have not been accounted for in loop stability analyses to date. Their argument is based on the physical fact that line tying and magnetic shear stabilization are very closely related physically to one another. To illustrate, consider a magnetic system that is shearless (*i.e.*, §10.3.5 and below), so that the pitch of the lines of force are independent of position. This permits the free interchange of any two field lines, separated by any distance of that magnetic-field configuration. This interchange occurs simply because the field lines are identical, *i.e.*, the system is degenerate. As is well known, such an interchange is highly unstable (Kadomtsev, 1966): it causes a minimal distortion of the magnetic field, thereby minimizing the  $v \times B$  restoring forces the distortion of the magnetic field might produce, which would tend to cause the equilibrium state to be restored. The perturbation then would tend to grow. Hence, by inducing shear, the field lines form an angle with respect to one another, which effectively *limits* the length over which interchange of the field lines can occur.

Line tying, which imposes the condition that the field lines have a finite *length* and are embedded in a plasma with high conductivity at each end, has an effect similar to shearing the field lines. This occurs for two reasons: line tying limits the maximum wavelength of a perturbation to the length of the system, and inhibits the long-wavelength interchange of field lines. This can be seen as follows: suppose two field lines are frozen to conducting endplates. To obtain instability, the change in the potential energy must be negative. The only way to interchange two field lines frozen at different points on an endplate is to twist the field lines which excites shear Alfvén waves: this, however, requires energy. Hence, the potential energy of the system will increase, not decrease, due to this form of interchange. Tying the field lines thus tends to increase the stability of the system.

From the electrodynamic coupling viewpoint, line tying and shear stabilization are equivalent in their nature. Consider a shearless field that is line tied. If a low frequency perturbation that generates an electric field perpendicular to the magnetic field is excited, a polarization current that is also perpendicular to  $\mathbf{B}$  is likewise excited. These polarization currents will result in Alfvén waves that propagate to the endplates. Since the magnetic-field lines are normal to the endplates and the electric field carried by the Alfvén wave is perpendicular to the magnetic field, the electric field will be tangential to the perfectly conducting endplates and must vanish there (Gibbons and Spicer, 1981). Alternately, and more generally since the photosphere is not perfectly conducting, the polarization charges will drain in or draw neutralizing charges from the photosphere in form of anti-parallel currents transported by Alfvén waves (cf. §10.3.5).

Next, consider a sheared magnetic field which results when a *net* parallel current is added to the shearless plasma magnetic field just considered. This causes the field lines to twist about the plasma. Field lines will then run part of their course on one side of the plasma and part on the other side. If now excess positive charges are added to one part of the plasma and excess negative charges to another by a polarization current, caused by a perturbation, these excess positive and negative charges can communicate with one another as the field twists from one side to the other side of the plasma. If the field lines were straight, communication between different parts of the plasma only could occur parallel to the field. In the MHD picture, shear stabilization (cf. §10.3.5) is provided by imposing an equilibrium variation of the magnetic field with direction due to a net current. This forces any perturbed quantity to vary parallel to  $\mathbf{B}$  unless the perturbation is constant over a magnetic flux surface. This forced variation parallel to  $\mathbf{B}$  will tend to couple to shear Alfvén waves that stabilize the system (cf. §10.3.5).

What is perhaps most surprising about the problem of line tying is that a general sufficient condition for stability due to line tying in three dimensions already exists (Solov'ev, 1975), as was pointed out by Spicer (1976), which was derived using Hamada coordinates (Hamada, 1962). The stability condition, in cylindrically symmetric geometry, is

$$\frac{\pi c B_z^2}{L^2} > 2 J_z B_\theta / r \quad (10.2.37)$$

where  $B_z$  and  $B_\theta$  are the axial and azimuthal components of the magnetic field respectively,  $L$  the loop length and  $J_z$  the axial current. It is trivial to show that a Bessel function model violates (10.2.37) at the zeroes of the zeroth order Bessel function: since  $J_z = \alpha_0 B_z / (\alpha_0 r)$ ,  $B_z > 2\alpha_0 L^2 B_\theta / (\pi r c)$  must always be satisfied by  $B_z = \alpha_0 J_0(\alpha_0 r)$ ,  $J_0$  being the zeroth order Bessel function. For  $J_z = \text{const}$ ,  $B_z = \text{const}$ , the sufficient condition (10.2.37) leads to

$$J_z L / \pi c B_z < 1. \quad (10.2.38)$$

which is roughly four times more stringent than the stability criterion for an analogous configuration bent into a torus of radius  $R$ , for which  $L = 2\pi R$ .

There are many other problems associated with the stability of magnetic loops that most authors chose to ignore. For this reason, it is worth discussing these problems in more detail to really appreciate what we are faced with if we really want to understand the problem of the MHD stability of any plasma-magnetic field configuration that exists in the solar atmosphere, and how it affects magnetic energy storage.

To store *in situ* magnetic energy sufficient to explain a flare in an exponential atmosphere requires that the energy be stored within a rather large volume ( $> 10^{28} \text{ cm}^3$ ) in the solar atmosphere, since storage in a small volume would cause the energy density of the magnetic field to be so large that the field would simply expand at roughly the Alfvén speed until it achieved global pressure balance with the ambient pressure. Thus, to build-up and store magnetic energy requires that the magnetic configuration not develop any internal instabilities that might lower its stored energy before a sufficient amount is accumulated to explain a flare. MHD expansion of a magnetic field is the most likely way a magnetic configuration will take to lower its energy density. This can be seen by using the conservation of magnetic flux  $\Phi = \int \mathbf{B} \cdot d\mathbf{A} \approx B \cdot A$  so that the total magnetic energy varies as

$$E_m \approx \Phi^2 \int \frac{ds}{A}. \quad (10.2.39)$$

where  $s$  is measured along a field line and  $A$  is the cross-sectional area of the flux tube. To lower  $E_m$  by expansion requires the field line to shorten, *e.g.*, the field line can untwist if it is twisted and for the flux tube area to increase. In terms of lumped circuit parameters,  $E_m = \Phi I/2$  since  $\Phi = LI$ , so that  $I$  must decrease in the MHD approximation and therefore the current density since  $I = \int \mathbf{J} \cdot d\mathbf{A}$ . Thus storage of *in situ* magnetic energy requires very special conditions to be satisfied to prevent expansion, conditions which must be understood if *in situ* storage is to be a valid concept.

MHD stability investigative techniques must be applied very carefully to solar magnetic configurations since it is not clear, at least from the literature, what constitutes an unstable magnetic configuration. Most of the papers discussed above treat, *e.g.*, loop stability as if they were treating tokamak or RFP stability (some even used the same boundary conditions), even though these are confined plasma-magnetic field configurations (enclosed by conducting immovable walls) whose reasons for existence are totally alien to the solar atmosphere. Thus, it is critical to define what constitutes an unstable plasma-magnetic field configuration in the context of an exponential atmosphere and of our ability to observe these configurations. That is, we are not really interested in whether a plasma-magnetic field configuration is stable for all times, but rather in whether or not the configuration exists long enough for sufficient energy to be stored in it. This concept of stability differs from the standard definition, which requires stability with respect to all growing perturbations, including those that take an infinitely long time. Thus, what is really needed is stability with respect to perturbations which grow in times shorter than the time it takes to store the magnetic energy required to explain the flare. In addition we need to ask whether a given type of unstable mode will significantly affect the energy storage process. For example, "does it really matter if local pressure-driven interchange (Suydam) modes are unstable within a loop if they do not strongly affect the global stability and thus the energy storage process?" In laboratory plasmas, Suydam modes apparently saturate at low amplitudes and continuously re-adjust the plasma pressure profile, presumably by enhanced convective transport (*e.g.*, Bodin and Newton, 1980). If this is the case, then a stability analysis of *e.g.*, a loop, which demonstrates that a given plasma-magnetic field configuration is stable to Suydam modes would discard a mechanism for enhanced matter and energy transport across field lines, processes whose occurrence is strongly indicated by observations. Alternately, a stability analysis might show, *e.g.*, that a given plasma magnetic field configuration of a loop is unstable to Suydam modes, thus leading to the dismissal of this configuration as inappropriate for coronal loops. Unfortunately, this erroneous line of thinking predominates in the papers

discussed above. In view of these arguments, we feel that a more useful approach than that of marginal stability, as applied to loop stability, is what is known as " $\sigma$  stability" (Groedbloed and Sakanaka, 1974), in which perturbations growing more slowly than  $\exp(\sigma t)$ , where  $1/\sigma$  is some characteristic time (e.g., the L/R magnetic energy storage time) are ignored because these modes grow too slowly to be important or alternatively the complete eigenvalue problem needs to be solved to determine growth times. Regardless of the chosen approach, an understanding of those saturation mechanisms which govern the growth of various modes in an open system, such as the exponential atmosphere, must be achieved before an understanding of global stability of a loop, for example, becomes a reality.

Another question which must be answered is, "what do we mean by global stability and what does local stability tell us about global stability?" The answer to the latter part of the question is that local stability tells us nothing about global stability (cf. e.g., Kadomtsev, 1966). On the other hand, global stability requires a knowledge of the appropriate boundary conditions and the *three*-dimensional structure of the plasma-magnetic field configuration. If the configuration is, e.g., cylindrical with axial and azimuthal homogeneity we can ignore the  $\theta$ ,  $z$  coordinates and concentrate on the stability of the configuration in the inhomogeneous radial direction. This constitutes a global stability analysis because the configuration is the same everywhere as a function of  $\theta$  and  $z$ . If e.g., the  $r$  and  $z$  coordinates are not ignorable then a stability analysis of some slice of that configuration taken at some  $z = z_0$  constitutes a local stability analysis and is equivalent to studying the stability of particle motion in a two-dimensional potential well while ignoring one of the degrees of freedom of the particle. Presently, all the MHD stability analyses of solar structures are local in nature and tell us nothing about global stability, despite claims to the contrary. In general, inhomogeneity parallel to the field of a given configuration has been ignored, even though such inhomogeneity can radically alter the global stability of the configuration and thus affect the amount of magnetic energy that can be stored therein (Spicer and Brown, 1981). In addition, the one-dimensional configurations that have been studied were chosen because of mathematical convenience without being justified on physical grounds.

Two other problems with stability studies of loops are, "what are the appropriate boundary conditions and what are the appropriate geometries?" The standard approach is to straighten, e.g., a loop into a cylinder and demand the field lines to be tied to perfectly conducting plates. This approach has two unfortunate drawbacks. First, line tying isolates the configuration from disturbances propagating into the volume between the plates, while helping to short circuit disturbances generated within the volume — i.e., hard wall boundary conditions. While it is understandable that the dense, highly conducting photosphere can damp disturbances propagating into it from the corona, it is hard to understand why disturbances generated in or below the photosphere should not be allowed to propagate into the corona to disturb the configurations in it — i.e., transmitting boundary conditions. After all, waves and shear flows are known to exist in the photosphere, and it appears very artificial to suppress their effect on the configurations in the corona. Indeed, Spicer (1976) has pointed out the possibility that kink or resistive kinks can be parametrically driven unstable by photospheric motions. A more appropriate treatment of the boundary conditions at the photosphere would be to treat the photosphere as a resistive boundary layer through which disturbances can propagate, be damped, and also communicate between neighboring field lines through  $J_i$ . However, this would require abandoning the energy-principle approach to MHD stability because the driving function would no longer be self-adjoint.

The second drawback to assuming cylindrical geometry for a loop is that, because curvilinear terms in the metric coefficients, as well as inhomogeneities in more than one spatial direction, can radically alter the stability of a system the choice of geometry is very important. This point does not seem to be appreciated in the MHD stability papers cited. They argue that

the curvilinear terms are small because the inverse aspect ratio ( $\epsilon = a/R$ ) of the loop is small, where  $a$  is the thickness of the loop and  $R$  the global radius, so that a cylindrically symmetric approximation is valid. This is true only when considering growth rates of certain well-recognized instabilities, such as  $m = 1$  kinks (Spicer, 1976). However, if a cylindrically symmetric loop were always assumed, then modes which occur only when a cylinder is bent, such as ballooning modes or tilting modes would never occur. Let us consider the ballooning mode further, to illustrate the salient points discussed above concerning inhomogeneity in more than one dimension, and the importance of including the curvilinear terms in MHD stability analyses. For a bent loop in which a current flows, there are three forces associated with geometrical effects that have no analog in slab geometry: two forces due to both local and global curvature (only the first occurs in cylindrical geometry), and an outward force that results from the fall off in field strength of the toroidal component (or principle field of, e.g., a loop) of the magnetic field that results from external currents. This last force clearly is a geometric effect, since it is not balanced directly by a change in plasma pressure. In addition, it varies along a field line from one foot of the loop to the other, and achieves maximum strength at the top of the loop for symmetric field strengths at the feet of the loop. The ballooning mode is an interchange mode that is *localized* to a region at the top of a loop where there exists unfavorable curvature (Schmidt, 1979) and is driven by this purely toroidal force. It is difficult for a mode to localize itself along a field line, since it will set up shear Alfvén waves which are stabilizing (cf. §10.3.5). We can model this mechanism by noting that an interchange instability has a growth rate  $\gamma_i^2 = k_1 g_{\text{eff}}$ , while the stabilizing effect of Alfvén waves is  $\gamma_i^2 = -V_{\text{th}}^2/L_0^2$  so that

$$\gamma^2 = k_1 g_{\text{eff}} - V_{\text{th}}^2/L_0^2. \quad (10.2.40)$$

where  $L_0$  is the characteristic length of a disturbance along a field line, approximately  $Rq/2$  ( $q = 2\pi r B_z/L_0 B_{\theta}$ , cf. §10.3.5),  $k_1$  the characteristic gradient scale length of the pressure, approximately  $r^{-1}$ ; and  $g_{\text{eff}}$  the effective gravity due to curvature effects, approximately  $2V_{\text{th}}^2/R$ , where  $V_{\text{th}}$  is the ion thermal velocity. This yields an approximate  $\beta$  necessary for

stability of the loop against ballooning modes (Spicer, 1976):  $\beta \approx \frac{V_{\text{th}}^2}{V_{\text{th}}^2} \leq \frac{2RB_{\theta}^2}{rB_z^2}$ . The reader

should take note of two points. First, (10.2.40) is identical to the result one obtains from line tying of interchange modes (Kulsrud, 1967). This is because line tying localizes the mode to a maximum wavelength corresponding to the length of a loop, while ballooning modes are localized because of the variation of the toroidal component of the field with position. The second point is that the ballooning mode would never appear in a cylindrically symmetric analysis of a loop, even though a loop is susceptible to such a mode (Spicer, 1976). These two points clearly illustrate the fundamental problems associated with treating loops in the cylindrically symmetric approximation with homogeneity in  $\theta$  and  $z$ : inhomogeneity and curvilinear terms tend to localize driving forces along field lines which drive unstable those processes preferred by some researchers, as the flare mechanism; this localization tends to make it harder to destabilize these mechanisms, thereby allowing more energy to be stored before an instability occurs. In addition, the greater the localization of these driving forces the more violent these mechanisms will be when they do occur (Spicer, 1976; Spicer and Brown, 1981).

### 10.2.2.3 The Taylor-Woltjer Theorem and Energy Storage

The stability of force-free magnetic field configurations and the storage of magnetic energy in such configurations is a very critical problem associated with solar flares as discussed in the previous section. A powerful and promising approach to understanding the stability of force-free configurations is to use the Taylor-Woltjer theorem (Woltjer, 1958; Taylor, 1974). The Taylor-Woltjer approach extremizes the magnetic energy  $W = 1/8\pi \int B^2 d^3x$  subject to the constraint that  $K = \int \mathbf{A} \cdot \mathbf{B} d^3x$  be held constant, where  $\mathbf{A}$  is the vector potential and  $K$  is an invariant of the motion called the magnetic helicity within the context of ideal HMD. By introducing a Lagrange multiplier  $\lambda_1$  for the constraint, the first variation,  $\delta W$ , of  $W - \lambda_1 K/2$  yields

$$\nabla \times \mathbf{B} = \lambda_1 \mathbf{B}, \quad (10.2.41)$$

where  $\lambda_1$  is a constant. For this special class of force-free equilibria we have  $\mathbf{B} = \lambda_1 \mathbf{A} + \nabla \chi$ , from which follows  $W = \lambda_1 K/2$ , where  $\chi$  is an arbitrary gauge scalar function. Thus, the solution to (10.2.41) with the smallest value of  $\lambda_1$  is the lowest energy state and is expected to be stable. We cannot extend this approach into the vacuum region which bounds the force-free region, where  $K$  is no longer conserved and  $\lambda_1 = 0$ .

The second variation of  $W - \lambda_1 K/2$  is just

$$\delta^2 W = \int (\delta^2 \mathbf{B} - \lambda_1 \delta \mathbf{A} \cdot \delta \mathbf{B}) d^3 \mathbf{x}, \quad (10.2.42)$$

which is just the usual potential energy  $\delta W$  of linearized ideal MHD for force-free equilibria and zero pressure, but with the addition constraint that  $\delta \mathbf{A}$  is related to the plasma displacement  $\xi$  via  $\delta \mathbf{A} = \xi \times \mathbf{B}$ . Thus, the ideal MHD energy principle can be expressed in terms of  $\delta^2 W$ , with the added constraint that  $\mathbf{B} \cdot \delta \mathbf{A} = 0$ . This result implies  $\delta W \geq \delta^2 W$ , which guarantees that  $\delta^2 W > 0$  is sufficient for ideal MHD stability. As shown by Finn *et al.* (1981) the condition  $\mathbf{B} \cdot \delta \mathbf{A} = 0$  can be satisfied everywhere except at a mode rational surface (*cf.* 10.3.5). The Finn *et al.* proof utilized a plasma-perfectly conducting rigid wall interface boundary condition. However, it is trivial to extend their proof to a plasma-plasma interface boundary condition, because  $\delta \mathbf{A} = \delta \mathbf{v} \times \mathbf{B}$ , where  $\delta \mathbf{v}$  is the plasma displacement velocity associated with the perturbation, is required at such boundaries; hence,  $\mathbf{B} \cdot \delta \mathbf{A} = 0$  there. If no mode rational surface occurs in the plasma-field configuration,  $\delta^2 W = \delta W$  and we have a necessary and sufficient condition for ideal MHD stability (Finn *et al.*, 1981).

Norman (1979) has utilized the Taylor-Woltjer Theorem to postulate that the post-flare field configuration is a force-free field with constant  $\lambda_1$ . He obtained this result by using a two timescale ( $t_0$  and  $t_1$ ) expansion of the invariant  $K$ , where  $t_0$  is the characteristic timescale of the flare release mechanism and  $t_1$  the characteristic timescale associated with energy storage. Clearly,  $t_0 \ll t_1$ , as discussed in §10.2.1.2, which justifies Norman's assumption that the photospheric boundary conditions will not change appreciably during the energy release phase. However, since the coronal boundary (*e.g.*, the plasma-vacuum interface) should change during the energy release, Norman's assumption needs further investigation.

We can conclude from the Taylor-Woltjer Theorem and Norman's results that a preflare force-free field should *have* mode rational surfaces if it is to become ideal MHD or resistance MHD unstable, and that  $\lambda_1$  cannot be the minimum eigenvalue if it is to become ideal MHD unstable.

#### 10.2.2.4 Strengths and Weaknesses of In Situ Versus Remote Energy Storage

While the concept of *in situ* energy storage is very appealing physically, there remains a great deal of theoretical work to be done before it becomes an unambiguously demonstrated concept. Many of the reasons for this state of affairs are discussed throughout §10.2.2. In summary, the theoretical weaknesses associated with *in situ* coronal storage are:

- (i) large coronal fields, distributed over large volumes, are required;
- (ii) expansion of the magnetic field must be prevented: the suggestion that potential fields will prevent expansion remains to be verified;
- (iii) all current theoretical studies ignore electrodynamic coupling of the solar atmosphere, which is an *absolute* prerequisite for understanding the nature of the current systems in

the solar atmosphere, as well as the magnetic-field structures and their global stability. There is simply no physical justification for assuming various one-dimensional magnetic field configurations and studying, e.g., their stability, particularly if these field configurations are manufactured solely for mathematical convenience without regard for physical constraints (such as the virial theorem); and

(iv) we must attempt to understand the effect on energy storage of photospheric disturbances propagating into the energy storage volume.

The principle strength of *in situ* storage is that the flare energy is stored exactly where it is needed to explain the flare. However, this is only an apparent strength because it rests on a possibly dubious interpretation of observations: that no large changes in the photospheric structure are observed throughout the duration of most flares (*cf.* Svestka, 1976). We have used the term dubious because sheared flow fields tangential to the solar surface, which are required for both *in situ* and remote storage as well as directly driving the flare, are difficult to detect observationally. In addition, because it is clearly possible to transport electromagnetic energy at speeds up to that of light in high inductive systems, there is no *a priori* justification for ignoring the possibility of remote inductive storage, particularly since no significant photospheric structure changes are expected from the transport of magnetic energy to a coronal site of dissipation. Nevertheless, a remote storage site still suffers the same theoretical difficulties as an *in situ* storage site, because an inductive current source requires the existence of large, essentially constant (as a function of time) net currents coupling various segments of the solar atmosphere. The primary advantage of a remote storage site is that the bulk of the inductive storage volume will be photospheric, as opposed to coronal, thus reducing the requirement that large fields must be distributed throughout a large coronal volume.

### 10.3 Magnetic Free Energy Dissipation Mechanisms

As demonstrated in §10.2 the preflare state can be *modelled* by identifying the appropriate magnetic geometry, the form of the power source, and the global closure of the current system. Hence from the equivalent circuit point of view, the preflare problem is reduced to identifying a power supply, an inductor for magnetic energy storage, and a load to draw the current. In the context of this analogy, the mechanism which converts stored magnetic energy to observable, flare associated forms of energy can be identified as an enhanced effective impedance, introduced at a specific location along the current path. This enhanced impedance would lead to a rapid decay of part or all of the stored inductive energy, in a time far shorter than the time required to store this energy. If this view is accepted, we must identify the physical origins of this enhanced effective impedance, and establish its proper role in the simple circuit analog used to model the flare phenomenon. The identification of the origins for this enhanced impedance has lead, on occasion, to heated debates amongst theoreticians in the solar physics community. Surprisingly, an examination of both the plasma physics and the solar flare literature shows that only three mechanisms exist that can cause irreversible dissipation of up to  $10^{32}$  erg of magnetic free energy in a time required by observations: *anomalous Joule heating*, *reconnection* (neutral sheets, current sheets, tearing modes, resistive kinks), and *double layers* (current interruption). In terms of lumped, or distributed, circuit parameters, anomalous Joule heating is modelled most simply by an anomalous resistance in parallel ( $J_{\perp}$ -driven) or in series ( $J_{\parallel}$ -driven) with the load resistance, reconnection by an  $L$  term and double layers by a leaky capacitor with an internal resistance in series with the inductor \*. In this section we present an overview of these mechanisms, including recent developments concerning their applicability to solar phenomena.

\* Normally, a plasma cannot store charge parallel to a magnetic field because of high electron and ion mobility along field lines. However, double layers violate this condition.

### 10.3.1 The Magnetic Dissipation Times and $\beta$

There are two physical quantities we need to examine, before proceeding, in order to clarify the importance of these flare mechanisms in dissipating stored magnetic free energy: the characteristic local and global magnetic-energy dissipation times,  $\tau_L$  and  $\tau_G$ , respectively. As magnetic field lines move through a plasma, the induced currents result in Joule heating; thus, energy is removed from the field and appears in the plasma as heat. The energy per unit volume lost from the field in a time  $\tau_L$  is  $\eta J^2 \tau_L$ , so that the magnetic energy dissipation time is expressed approximately by

$$\tau_L = \frac{B^2}{8\pi\eta J} \quad (10.3.1)$$

Using Ampere's equation, (10.3.1) is transformed to

$$\tau_L = \frac{2\pi(\delta l)^3}{\eta c^2}, \quad (10.3.2)$$

where  $\delta l$  is the characteristic scale length of the magnetic field,  $\mathbf{B}$ , associated with the induced plasma current,  $\mathbf{J}$ . Since  $\tau_L$  is a *local* quantity, it does not reveal anything about the characteristic *global* magnetic-energy dissipation time,  $\tau_G = L/R$ , unless we integrate  $\tau_L$  along the entire current path, where  $L$  is the total inductance and  $R$  the total resistance. For example, consider a current-carrying loop of length  $L_0$  with a load resistance  $R_T$  in its feet. If a sharp increase in resistivity, in series with the current, were introduced along some fraction of the loop length,  $\Delta s$ , the global time constant would be expressed approximately by:

$$\tau_G = \frac{L}{\left(R_T + \frac{\Delta s}{\tau_L c^2}\right)}. \quad (10.3.3)$$

Two categories of models for flare energy storage are thus suggested. If  $R_T \ll \Delta s / \tau_L c^2$ , then  $\tau_G = \frac{L_0 \tau_L}{\Delta s}$ , and all of the globally stored energy,  $LI^2/2$ , is dissipated across the enhanced impedance within  $\Delta s$ . To explain a flare that releases  $\approx 10^{32}$  erg in  $\approx 10^3$  s, this case requires  $LI^2/2 \approx 10^{32}$  ergs and  $\tau_G \approx 10^3$  s; thus the entire reservoir of stored magnetic energy is released at a rate determined by the global time constant. Conversely, if  $R_T \gg \Delta s / \tau_L c^2$ , only a small fraction of the globally stored energy is released expressed approximately by

$$\frac{\Delta s LI^2}{\tau_L c^2 R_T}.$$

To explain a flare energy release of  $\approx 10^{32}$  erg in  $\approx 10^3$  s, this case requires that  $LI^2/2 \gg 10^{32}$  ergs. Hence, only a small fraction of the stored energy is dissipated, and the global time constant plays no role because it remains relatively unchanged as does the total magnetic energy reservoir. This distinction between types of storage models is important for evaluating the feasibility of many flare energy release mechanisms proposed to date. To illustrate, two of the flare mechanisms reviewed here, double layers and anomalous resistivity, require essentially constant currents to operate throughout a flare, because they will switch off very quickly if the net current decays sufficiently. The distinction between classes of storage models also may help explain homologous flares, particularly if future observations show that homologous flares repeat in times much shorter than the storage times computed in §10.2.1.2.

Returning to Equation (10.3.2), we see that basically two mechanisms can decrease the local dissipation time: either the scale length of the spatial variation of  $\mathbf{B}$  is decreased, i.e., the field gradients are steepened; the resistivity is increased, or both occur. As shown in §10.3.5,

reconnection mechanisms decrease  $\tau_L$  by driving the scale lengths  $\delta_l$  to smaller values, while anomalous Joule heating mechanisms further decrease  $\tau_L$  by increasing the effective resistivity in addition. The reduction of  $\tau_L$  is the key to understanding reconnection and anomalous Joule heating flare mechanisms. However, the role of  $\tau_L$  in the double-layer mechanism is unclear, as is discussed in §10.3.4.

In §10.2.2.1, we introduced the local quantity  $\beta$  as a measure of the ratio of the internal energy density to the magnetic energy density; we also pointed out that, for low- $\beta$  equilibrium configurations, the magnetic field is essentially force free ( $J_{\parallel}$ -dominated) or potential. Note that  $\beta$  also plays an important role in determining the Joule heating rate of a plasma. If  $\beta^*$  represents the  $\beta$  associated with the free magnetic energy then the Joule heating time can be expressed as  $\tau_J \approx nkT/\eta J^2 \approx 2\beta^* \tau_L$ ; thus, for a fixed  $\tau_L$ , the Joule heating time is shorter for smaller values of  $\beta^*$ . Hence, plasma heating is faster in a low  $\beta^*$  system. In addition, if  $\beta^*$  is small, the plasma can be Joule heated through dissipation of only a small fraction of the available magnetic free energy. These arguments suggest that the most theoretically useful plasma-field configuration for energy dissipation and storage (cf. §10.2.1.1) is characterized by a low  $\beta^*$  such as force free configurations.

### 10.3.2 Double Layers

In recent years, numerous experimental and theoretical studies have investigated the properties of "double layers," with particular emphasis on their application to the Birkeland currents ( $J_{\parallel}$  currents) which couple electrodynamically the ionosphere and the magnetosphere. Because several excellent reviews on double layers already exist (Block 1975, 1978; Goetz, 1979; Carlqvist, 1979a; Torvén, 1979), we present here only a synopsis of the important aspects of double layers, with particular focus on applications to solar flares. In addition, since  $J_{\parallel}$ -driven double layers and anomalous resistivity models are related, to a certain extent (cf. §10.3.4), the discussion of excitation mechanisms for  $J_{\parallel}$ -driven double layers or anomalous resistivity is postponed to §10.4.

The first application of double layers to solar flares was due to Alfvén and Carlqvist, (Alfvén and Carlqvist, 1967; Carlqvist, 1969, 1979b). In their model, numerous double layers, driven by a high inductance current system, are formed in numerous current filaments, each with very high current densities, traversing the solar atmosphere. Alfvén and Carlqvist argued that inductively stored magnetic energy is released rapidly as non-thermal particles, plasma heating, and bulk plasma motion, as a consequence of the formation of double layers. The Alfvén-Carlqvist model was dismissed by Smith and Priest (1972), who maintained that the Buneman instability (Buneman, 1959) or the ion-acoustic instability would lead to plasma turbulence, and thus, to the occurrence of anomalous resistivity rather than double layers. Of course Smith and Priest's assertion, at that time, was well taken. Unfortunately Smith and Priest went beyond this reasonable assertion, and proposed erroneous critical conclusions (cf. §10.3.3) which further dampened theoretical interest in the Alfvén-Carlqvist model. There is considerable evidence at present, that local plasma evacuation, required for the formation of a double layer, can be caused by the Buneman instability or the ion-acoustic instability, under certain circumstances (Carlqvist, 1973; Smith (R.A.) and Goetz, 1978; Raadu and Carlqvist, 1979) thus contradicting the original assertion of Smith (D.F.) and Priest (1972). As a result the double layer or current interruption model of Alfvén and Carlqvist has recently invoked renewed interest.

A "double layer" consists of two, equal but oppositely charged, essentially parallel but not necessarily plane, laminar space-charge layers, which trap a large fraction of the current-carrying electron population and accelerates the remainder (Block, 1978). The potential, electric field, and space-charge density vary qualitatively within the layer, as shown in Figure (10.10). A

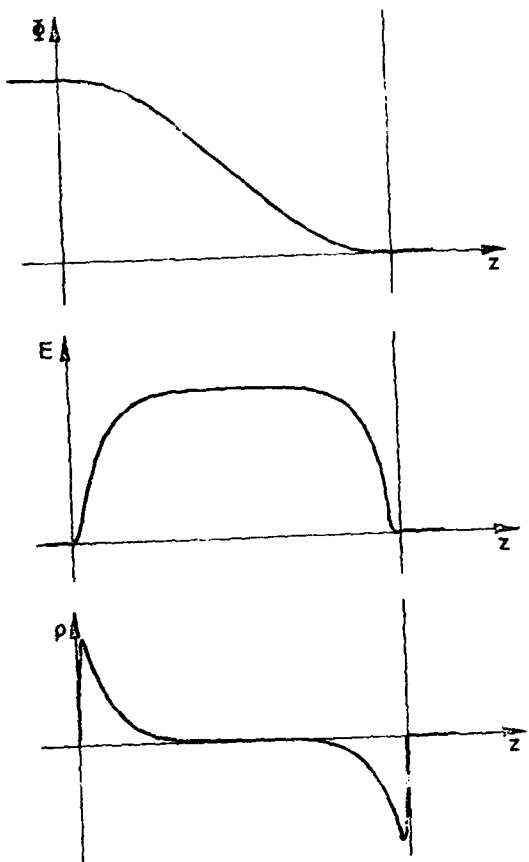


Figure 10.10 — Schematic of the potential ( $\Phi$ ), electric field ( $E$ ) and charge density of a double layer

double layer is believed to occur when a potential difference is applied to a finite length plasma in which the potential difference is concentrated in a shock-like localized region, rather than distributed over the entire length of the system. Such double layers are expected to produce mono-energetic particle distributions. Four conditions essentially must be fulfilled for double layers to occur (Block, 1978):

- (i) The potential difference  $\phi_0$  across the layer must satisfy  $|\phi_0| > k_b T_e / e$ .
- (ii) The electric field must be much stronger inside than outside the double layer, so that the integrated positive and negative charges nearly cancel;
- (iii) Quasi-neutrality is violated locally in both charge layers; and
- (iv) The collisional mean free path must be much greater than the double layer thickness, because the formation of a double layer is a collisionless phenomenon.

Note that for a double layer to be applicable to solar flares the potential difference  $\phi_0$  must be much greater than  $k_b T_e / e$ ; otherwise the energy gained by an electron traversing a double layer with  $\phi_0 \gtrsim k_b T_e / e$  is not appreciably greater than the thermal energy of the plasma. Hence, we require  $\phi_0 \gg k_b T_e / e$ , which indicates a strong double-layer. It was shown by Goertz and Joyce (1975) that a strong double layer requires for formation a current density given by  $|J| = nev_{T_e}$ , where  $v_{T_e}$  is the electron thermal speed, which is the current density required to excite the current driven Buneman instability (Buneman, 1959).

To utilize a current driven double layer for solar flare modelling we require that the system consisting of a current driver and a double layer be at marginal stability (i.e., in steady state) during some fraction of the flare duration. For this reason, the entire current system must be analyzed to understand the nature of the current generator, the inductive magnetic storage reservoir and the load as discussed in §10.2. Hence, double layers, as well as  $J_{\parallel}$ -driven anomalous resistivity systems, require large global time constants in order to keep the current roughly constant.

An important constraint on a double layer model is obtained by noting that double layers primarily lead to particle acceleration; intense Joule heating, if applicable occurs only in a very small volume  $\approx 10^{15} \text{ cm}^3$ . A double layer must be able to accelerate  $\approx 10^{36} - 10^{38}$  25-keV electrons during the course of a flare, to be consistent with a *non-thermal* hypothesis for typical hard X-ray bursts (Hooyng *et al.* 1976; Brown *et al.* 1979). Since acceleration essentially is collisionless through a double layer of thickness  $L_{DL}$ , the rate  $\gamma$  of electrons accelerated freely through  $L_{DL}$  by a potential  $e\phi_0$  is

$$\gamma^{-1} = \left( \frac{L_{DL} m_e}{e \phi_0} \right)^{1/2}, \quad (10.3.4)$$

where  $m_e$  is the electron mass.

The production rate of non-thermal electrons per unit volume is given approximately by

$$\frac{dn_b}{dt} = \gamma n_e - \frac{n_b}{\tau}, \quad (10.3.5)$$

where  $n_b$  represents the non-thermal number density, and  $\tau^{-1}$  the lost rate at which non-thermals are thermalized due to collisions in the acceleration volume. If we assume that  $\gamma$ ,  $n_e$  and  $\tau$  are roughly constant and  $t \gg \tau$ , then (10.3.5) yields  $n_b \approx n_e \gamma \tau$ .

Excitation of a double layer by the current drift speed requires  $v_D \geq v_{I_c}$ ; furthermore, it is necessary to maintain  $v_D \geq v_{I_c}$  to keep the double-layer at nearly steady state throughout a X-ray burst. Hence, using Ampere's equation, we find that the current density must exist in a channel with a thickness of roughly  $\delta r \approx \frac{c}{\omega_{pe}} \beta^{* - 1/2}$  (cf. §10.3.1). Taking a cylindrical shell for the current channel cross-section of area  $2\pi r \delta r$  and noting that the double-layer thickness is (Hubbard and Joyce, 1979)

$$L_{DL} \approx 6 \sqrt{\frac{e\phi_0}{k_b T_e}} \lambda_D \quad (10.3.6)$$

the total number of electrons accelerated by one double layer is

$$N_T \approx n_e \tau \sqrt{\frac{e\phi_0}{m_e}} 2\pi r \frac{c}{\omega_{pe}} \beta^{* - 1/2}, \quad (10.3.7)$$

where  $r$  is the radius of the current shell. Assuming  $n_e \approx 10^9 \text{ cm}^{-3}$ ,  $e\phi_0 \approx 25 \text{ keV}$ ,  $r \approx 5 \times 10^8 \text{ cm}$ ,  $\beta^* \approx 10^2$ , and an ambient plasma temperature of  $\approx 1 \text{ keV}$ , we find that  $N_T \approx 10^{32}$  electrons are accelerated in a volume of  $V \approx 2\pi r \delta r L_{DL} \approx 10^{15} \text{ cm}^3$ . Hence, approximately  $10^4$ – $10^6$  double layers, dispersed throughout a typical flare volume of  $\approx 10^{29} \text{ cm}^3$ , are required by the non-thermal hypothesis to explain a flare. Such a large number of double layers seems unlikely; however, one must remember that these estimates are based on double layer theory that is very much in its infancy and on the assumption of a non-thermal electron distribution. Note also that  $10^4$ – $10^6$  double layers constitute only  $10^{-8}$ – $10^{-10}$  of the entire volume flare!

A double layer in principle, can be modelled in an equivalent circuit model by a capacitance with an internal resistance *parallel* to the magnetic field lines. In this case, the properties of the capacitor and the resistor are *not* constant, but are highly non-linear functions of the electric field throughout the double layer (R. A. Smith, 1981); consequently Ohm's law, which is a local linear relationship between current and electric field, is not satisfied. In addition, an elongated turbulent region should exist on either side of the laminar double layer, with a length determined by the convective properties of the turbulence excited (Smith and Goetz, 1978).

### 10.3.3 Anomalous Joule Heating Due to D.C. Anomalous Resistivity

Anomalous Joule heating assumes a pivotal role in numerous flare and coronal heating theories, due to the rapid rates of heating and magnetic energy dissipation associated with this process (cf. Kuperus, 1976; Norman and Smith, 1978). Anomalous Joule heating occurs in plasmas in which collisionless transport, rather than collisional transport, dominates. In a collisionless plasma, the mechanisms by which the plasma state evolves are determined by the microturbulent (*i.e.*, processes with scale lengths much smaller than MHD scale lengths) electric and magnetic fields excited by various plasma instabilities. Energy and momentum are transferred from plasma currents to electric and magnetic field oscillations, and back again to the plasma particles as "thermal," or randomized energy. The reader is referred to the numerous reviews which have appeared within the last few years for depth (Mozer, 1976; Davidson and Krall, 1977; Papadopoulos, 1977; 1979), a detailed treatment being beyond the scope of this review. In the following section, however, we review the basic origins of both classical and anomalous resistivity. This allows us to distinguish between  $J_\perp$ -driven and  $J_\parallel$ -driven anomalous resistivity, problems associated with  $J_\perp$ -driven anomalous resistivity, and to discuss techniques for computing the magnitude of anomalous resistivity and resultant Joule heating under solar conditions.

## 10.3.3.1 Origins of Resistivity

To understand the physical origins of resistivity, consider the equation of motion of a test particle of charge  $-e$  and mass  $m_e$ , drifting with a velocity  $v_D$  with respect to a stationary ion background:

$$m_e \frac{d\mathbf{v}_D}{dt} = -e \mathbf{E} - m_e \mathbf{v}_D \nu(\mathbf{v}), \quad (10.3.8)$$

where  $\mathbf{E}$  is the macroscopic electric field, taken to be constant; and  $\nu(\mathbf{v})$ , the collision frequency is given by (Spitzer, 1962)

$$\nu(\mathbf{v}) = \frac{4\pi n_e e^4 \ln \Lambda}{m_e^2 v^3}, \quad (10.3.9)$$

where  $n_e$  is the background electron number density;  $v$ , the particle's net rms velocity; and  $\ln \Lambda = \ln(4\pi n_e \lambda_{De}^3)$ , with  $\lambda_{De}$  representing the electron Debye radius. In the absence of collisions, electrons are accelerated freely, relative to the ions, such that

$$\mathbf{v}_D = \frac{-e \mathbf{E} t}{m_e}. \quad (10.3.10)$$

Conversely when the electrons undergo collisions with the more massive ions or with slow-moving field electrons, a steady state can be achieved, characterized by

$$\mathbf{v}_D = \frac{-e \mathbf{E}}{m_e \nu(\mathbf{v})}. \quad (10.3.11)$$

The electron velocities are randomized during these collisions so that the energy associated with the drift velocity is converted to Joule heat. Using the following relationship between the current density and the electron drift velocity  $\mathbf{J} = -n_e e \mathbf{v}_D$ , and (10.3.11), we find a local relationship between  $\mathbf{J}$  and  $\mathbf{E}$ :

$$\mathbf{J} = \frac{n_e e \mathbf{E}}{m_e \nu(\mathbf{v})} = \frac{\mathbf{E}}{\eta}; \quad (10.3.12)$$

$\eta$ , the electrical resistivity, is given by

$$\eta = \frac{4\pi \nu(\mathbf{v})}{\omega_{pe}^2}, \quad (10.3.13)$$

where the plasma frequency  $\omega_{pe} = (4\pi n_e e^2 / m_e)^{1/2}$ .

If the drift velocity of the electrons is less than the electron thermal velocity,  $v_{Te} = (k_b T_e / m_e)^{1/2}$ , we have  $v = \sqrt{v_D^2 + v_{Te}^2} \approx v_{Te}$ , so that (10.3.9) reduces to

$$\nu = \frac{4\pi n_e e^4 \ln \Lambda}{m_e^{1/2} (k_b T_e)^{3/2}} \quad (10.3.14)$$

the classical result (Spitzer, 1962). Using the definition  $\lambda_{De} = v_{Te} / \omega_{pe}$ , (10.3.7) can be expressed as

$$\nu = \omega_{pe} \frac{\ln \Lambda}{\Lambda}. \quad (10.3.15)$$

Notice that the drag force on the electrons for which  $v_D < v_{Te}$ ,  $m_e \mathbf{v}_D \nu \sim v_D / v_{Te}^3$ , increases with  $v_D$ , so the steady-state condition given by (10.3.11) can be achieved; for electrons with drift velocities in the regime  $v_D > v_{Te}$ , the drag force decreases as  $v_D^{-2}$ , so a steady-state cannot be attained. The following physical picture thus emerges. In the low-velocity regime ( $v_D < v_{Te}$ ), where the drag force dominates the electric force, the electron motion is

essentially random and a steady-state can be achieved. However, as the dynamical friction becomes weaker at higher velocities, there is a critical velocity beyond which electrons are accelerated faster than collisions can decelerate them. As a result, these electrons continually gain more energy, because the friction they feel is reduced still further with increasing velocity. Eventually, the friction becomes sufficiently negligible that they are freely accelerated by the dominant electric force, until some other energy and momentum loss mechanism, such as radiation or an instability becomes dominant. The effect of these additional loss mechanisms invariably appears as a cutoff in the distribution function at higher energies. These freely accelerated electrons are called "runaway" electrons. The following expression for the critical velocity,  $v_c$ , at which electrons start to run away is obtained by balancing the two opposing forces on the RHS of (10.3.8) using (10.3.9):

$$v_c^2 = \frac{4\pi n_e e^3 \ln \Lambda}{m_e |E|}. \quad (10.3.16)$$

The *Dreicer* electric field,  $E_D$ , (Dreicer, 1959), is defined as the electric field at which a thermal electron will run away (*i.e.*, for which  $v_e = v_T$ ); hence,

$$E_D = \frac{e \ln \Lambda}{\lambda \bar{v}_n}. \quad (10.3.17)$$

Physically, this is the electric field at which the electron energy gained in one collision time is equal to the thermal energy. Using (10.3.16) and (10.3.17), we find that runaway occurs for any electron with a velocity

$$v \geq v_c = \left( \frac{E_D}{E} \right)^{1/2} v_{T_e}. \quad (10.3.18)$$

### 10.3.3.2 The Origins of Anomalous Resistivity

So far, we have treated *single particle motion* only. However the behavior of a *bulk electron distribution* changes remarkably in the presence of an external electric field, due to the reduction of  $v(v)$  with higher velocities. In the collision-dominated portion of the velocity distribution, we intuitively expect the electron distribution to be a slightly skewed Maxwellian, drifting relative to the ions with a velocity given by (10.3.11). At velocities much greater than  $v_c$ , however, electrons pick up more momentum from the electric field than is lost by momentum exchange with either the ions or field electrons through collisions. As a result, the electrons move in a direction anti-parallel to the electric field; the distribution therefore develops a long high energy "tail" which is concentrated parallel to the electric field. The entire electron distribution thus consists of a skewed and drifting Maxwellian, containing most of the population, with a very long and highly anisotropic tail anti-parallel to  $E$ . This anisotropic, drifting distribution is a source of excess free energy, capable of exciting various collective microinstabilities which may, in turn, inhibit the extent of the tail.

If the drift velocity of the skewed Maxwellian lies in the range  $(v_{T_e}, c_s) \leq v_D \leq v_{T_i}$ , where  $c_s = (kT_e/m_i)^{1/2}$  is the ion-sound velocity, and  $v_{T_i}$  the ion thermal velocity, various current-driven collective microinstabilities can be excited. Instabilities are driven by the bulk of the current carrying electrons as opposed to just the tail of the distribution—which may possess a bump. When this occurs the phenomenon of anomalous resistivity arises due to charge clumping caused by a microinstability. The plasma can be unstable to the generation of those types of waves, which are normal modes of the plasma; electrostatic waves, in particular, grow at the expense of the free energy associated with the drift energy of the electrons. Scattering of the drifting electrons by these turbulent wave electric fields causes an enhanced momentum and energy loss and so the term "anomalous resistivity."

To appreciate how these turbulent wave fields originate, we must consider the sources of collisions in a plasma, where the scale of charged-particle interactions is limited by Debye shielding. In the classical view of a plasma, a collision occurs when a series of small angle deflections becomes equivalent to a  $90^\circ$  deflection. These deflections are calculated assuming successive binary collisions between uncorrelated scattering centers within a Debye-shielded Coulomb field. Due to Debye shielding, only collisions with impact parameters less than a Debye radius,  $\lambda_{De}$ , need be considered. However, this classical approach to understanding collisions in a plasma is limited. A physically equivalent but more useful approach to understanding collisions in a plasma is to treat collisions as stochastic scatterings of particles in the stochastic electric fields of a thermal plasma. Stochastic electric field fluctuations with wavelengths  $\lambda < \lambda_{De}$  originate in the incoherent thermal motions of single particles, while stochastic fields with  $\lambda > \lambda_{De}$  result from the collective shielding effects of many particles. Fluctuations with  $\lambda > \lambda_{De}$  may be treated as coherent waves, which are neglected in the classical approximation. For a thermal plasma, the ratio of collective to classical collision frequency is  $\lambda^{-1}$ ; since  $\lambda$  usually is very large, collective effects are negligible. However, plasmas are rarely in thermal equilibrium. An available supply of free energy can interact with plasma wave modes, of negligible energy content in a quiescent thermal plasma, and drive them to non-negligible amplitudes. This interaction usually, *albeit not always*, constitutes a resonance plasma instability which causes a high level of plasma-wave turbulence. These collective stochastic fields for which  $\lambda > \lambda_{De}$ , result in stochastic particle scatterings and lead to *effective* binary collision frequencies, and thus transport coefficients, that can be orders of magnitudes greater than the classical Spitzer values.

To illustrate the relationship between classical collisions and enhanced scattering caused by collective effects, we refer to (10.3.15), which relates the classical collision frequency with the plasma frequency, and to the definition  $\Lambda = 4\pi n_e \lambda_{De}^3$ , the number of electrons in a Debye sphere. As noted above, the collective quantity  $\Lambda$  is a measure of the ratio of the electric-field energy density in thermal fluctuations,  $\langle \delta E^2 \rangle / 8\pi$ , to the thermal energy density,  $n_e k_b T_e$ , that is,

$$\frac{\langle \delta E^2 \rangle}{8\pi n_e k T_e} \approx \frac{1}{\Lambda} \quad (10.3.19)$$

(Krall and Trivelpiece, 1973). Hence (10.3.15) and (10.3.19) yield

$$\nu \approx \omega_{pe} \frac{\langle \delta E^2 \rangle}{8\pi n_e k_b T_e}. \quad (10.3.20)$$

Equation (10.3.20) suggests that, if it were possible to enhance the level of electric field fluctuations through which the drifting electrons are scattered, the collision frequency would be increased over that of a thermal plasma and, therefore, the transport coefficients and the resistivity would be modified. There are, in fact, a number of current driven microinstabilities that can result in enhanced electric-field fluctuations which exceed the thermal level by several orders of magnitude (Papadopoulos, 1977, 1979). However, not all high-frequency microinstabilities can cause an increased resistivity. For the bulk of the drift electrons to experience friction, the phase velocity of the waves produced by some microinstability must be small. That is,  $v_p = \frac{\omega}{|k|} \ll v_{T_i}, v_{D_i}$ , which implies that the frequency of the waves must be much less than the local plasma frequency. The physical explanation for this requirement is two fold: resistivity cannot be a resonance phenomenon between wave and particle \*; and, if  $v_p > v_{T_i}, v_{D_i}$  the electrons and clumps of charge due to collective effects would move together with little or no momentum exchange. Hence  $v_p \ll v_{T_i}, v_{D_i}$  implies that the electrons see a fixed scattering

\* If it were a resonance phenomenon, only a fraction of the electron distribution function would be affected.

center and, thus, the momentum exchange will be large. Also note that if the wave frequency is sufficiently small the electrons, with their small inertia, will not be affected by these waves. For example, Alfvén waves cannot directly cause anomalous resistivity. Furthermore a current with a drift velocity of order the ion sound speed or electron thermal speed requires very steep magnetic-field gradients, which are on the order of an electron or ion plasma skin depth ( $c/\omega_{pe}$  or  $c/\omega_{pi}$ ), where  $\omega_{pi}$  is the ion plasma frequency.

If a magnetic field is introduced into the problem of anomalous resistivity, we encounter new physical effects which alter some of the foregoing arguments. In particular, a current flowing perpendicular to the magnetic field will *not* give rise to runaway electrons, due to the adiabatic motion of charged particles in the presence of a magnetic field; hence, there is no difficulty in maintaining a stationary electron distribution. However, a current flowing parallel to the magnetic field presents theoretical problems, particularly when  $\Omega_{ce}/\omega_p \geq 1$ , which is true throughout a large fraction of the solar atmosphere, where  $\Omega_{ce}$  is the electron gyrofrequency, because the electron motion is essentially one-dimensional unless the effective collision frequency of the turbulence,  $\nu_{eff}$ , satisfies  $\Omega_{ce}/\nu_{eff} \ll 1$ ; otherwise the electrons will behave adiabatically. Thus, if a magnetized electron moves through a turbulent region where  $\Omega_{ce}/\nu_{eff} \geq 1$ , it enters and leaves the region of turbulence with the same magnetic moment so that its perpendicular energy remains unchanged. Consequently the electron velocities parallel to the magnetic field simply increase in the presence of the electric field driving the current, instead of being randomized in all directions as is required by the standard definition of a resistivity mechanism. Under these circumstances, we should expect the entire electron distribution to run away and not be restrained by any resistivity process. If this occurs, the concept of a local Ohm's law is no longer appropriate, because the drift velocity of the current is determined by the *global* electric field at each point along the current path rather than by *local* properties of the plasma. Thus, to regain a local Ohm's law, the bulk of the electron population that carries the current must be trapped while at the same time the parallel electron velocities must be thermalized; that is, the electrons velocities perpendicular to the magnetic field are increased at the expense of their parallel velocities.

Palmaresso *et al.* (1981) have recently developed and provided an elegant and *self-consistent* theory for DC anomalous resistivity parallel to a magnetic field, through numerical simulation techniques, which are in agreement with the experimental results of Kiwamoto *et al.* (1979), that a magnetized plasma contains two anomalous collision regimes: one characterized by a collision frequency  $\nu \sim E^{1/2}$ , and the other by  $\nu \approx E$ . They show that DC anomalous resistivity in a magnetized plasma results from a sequence of self-consistent plasma effects. Initially, a large-amplitude electrostatic ion density wave forms that traps, via the self-consistent electrostatic potential well associated with the wave, a large fraction of the lowest energy current-carrying electrons. To illustrate, they found that  $\delta n_e/n_i \approx 0.3$  traps  $\approx 60\%$  of the electron population with the remainder running away up to a maximum cut off energy, where  $\delta n_e/n_i$  is the ion density fluctuation level. As the untrapped population forms a "bump" on the tail of the velocity distribution due to the runaway process, two-stream instabilities initiate filling in of the region in velocity space between the bump and the trapped portion of the distribution, leading to a flatter distribution in this region. These processes continue until non-linear beam stabilization mechanisms stabilize the beam (Papadopoulos, 1975). When the tail of the runaway distribution reaches a critical velocity, however, it excites the anomalous Doppler cyclotron resonance instability, which generates obliquely propagating electron waves (Kadomtsev and Pogutse, 1968; Parail and Pogutse, 1976; Haber *et al.*, 1978). Since this mechanism pitch-angle scatters electrons with high  $v$  into  $v_{\parallel}$ , it results in a sharp deacceleration of the resonant runaway electrons and imposes a cut off velocity for the runaway tail, thereby forming a bump on the tail (Haber *et al.*, 1978). Hence, a number of competing mechanisms occur simultaneously: one process attempts to flatten the bump, while the others attempt to maintain the bump. The combination of these mechanisms thereby provides a continuous transfer of large parallel momentum into perpendicular momentum at high phase

velocities, which then cascades to lower phase velocities; the perpendicular energy of the trapped electrons thus is increased as is required of a resistivity mechanism. It is evident that  $J_{\parallel}$ -driven anomalous resistivity is far more complex in its origins than the simpler picture we presented earlier.

Anomalous resistivity resulting from a perpendicular current is conceptionally easier to understand.  $J_{\parallel}$ -driven instabilities which cause anomalous resistivity can be divided into two categories: those that are important when  $\Omega_{ce}/\omega_{pe} \ll 1$ , *i.e.*, the Buneman and ion acoustic instabilities; and those which predominate when  $\Omega_{ce}/\omega_{pe} \gg 1$ , *i.e.*, the beam-cyclotron, lower hybrid-drift, modified two-stream and ion-cyclotron drift instabilities (*cf.* Davidson and Krall, 1977; Papadopoulos, 1979). In the unmagnetized  $J_{\parallel}$ -driven instabilities, the excited turbulent waves *excited* can easily randomize the perpendicular electron and ion velocities, thus leading to heating in all directions. For the magnetized cases, heating occurs in directions normal to the magnetic field. The resultant distribution may be fully isotropized, however, by the concurrent excitation of secondary instabilities, such as whistler and electromagnetic ion-cyclotron, by the high-temperature isotropy that results from the  $J_{\parallel}$ -driven anomalous heating (Spicer, 1976).

#### 10.3.3.3 Techniques for Computing Plasma Turbulence Levels in Solar Physics

Various approaches to computing the level of plasma turbulence, and thus resistivity, from a given plasma instability have been applied to solar physics problems. For examples, the mode independent approach of Galeev and Sagdeev (1979), which is based on the conservation of energy and momentum between wave and particle at marginal stability. The assumption of marginal stability in solar problems is a particularly powerful technique for computing turbulence levels, because the growth times and saturation times of instabilities which produce anomalous resistivity are  $\sim 10^6$  times shorter than any macroscopic time, such as a tearing mode growth time or the life time of a flare. Thus, if anomalous resistivity is to be important in solar problems, the instability causing the anomalous resistivity must be at or near marginal stability and driven continually during the course of a flare by a source of free energy external to the instability. The marginal stability approach, whose principal proponent is W. Manheimer (Manheimer and Boris, 1972, 1977; Manheimer and Flynn, 1974; Manheimer *et al.* 1977; Manheimer, 1979a; Manheimer and Antonson, 1979), has yielded theoretical predictions which are very consistent with actual laboratory results.

In general a micro-unstable plasma is assumed to exist in a *linearly unstable state*. The transport coefficients are determined by the fluctuation level, which is limited by a local non-linear effect such as resonance broadening (Dupree, 1967) or mode coupling (Manheimer *et al.* 1976; Cohen *et al.* 1976). Thus, to obtain transport coefficients, it is essential to utilize a non-linear theoretical treatment of all relevant mechanisms. In the Manheimer approach, it is assumed that the relaxation of the plasma to the *linearly stable state* is the most effective stabilization mechanism, so that the plasma presumably is at or near marginal stability even if some mechanism continually drives it toward instability. Thus, non-linear theory of the relevant mechanism plays a far less important role in the analysis of a marginally stable plasma than for a plasma that is linearly unstable. This is not to say that non-linear effects play no role at all, because saturation levels must be used to limit the turbulence level; nevertheless, the marginal stability approach does not depend on the detailed non-linear evolution of the instability. In principle, the marginal stability approach is similar to the quasi-linear theory of turbulent transport (*cf.* Galeev and Sagdeev, 1979) but with the additional assumption that the characteristic time over which the instability can develop and field amplitudes vary is short compared to the time scale of the macroscopic fluid quantities.

To illustrate the marginal stability approach, we consider a magnetic loop in which a parallel current flows such that the net current is roughly constant for a time  $\tau \approx L/R$  and that  $J_{||}$  exceeds the threshold of the ion-acoustic instability (cf., e.g. Krall and Trivelpiece, 1973) along some fraction,  $\Delta s$ , of the loop length,  $L_0$ ; hence, unstable and growing ion-acoustic waves are present. We expect the level of turbulence to lie in the range between the classical value and the saturated value *as determined by the marginal stability condition*. Physically, three time scales are of interest: the anomalous Joule heating time,  $t_j$ ; the cooling time,  $t_c$ , due to radiation or diffusive transport, whichever process yields the smallest  $t_c$ ; and the hydrodynamic expansion time,  $t_H$ , due to expansion either parallel or perpendicular to the magnetic field, *whichever is shorter*. For solar flare plasmas,  $t_j < t_c < t_H$ . With these time scales in mind, we expect the following sequence of events (Spicer and Manheimer, 1982):

- (1) Rapid anomalous Joule heating, due to the existence of unstable ion-acoustic waves, induces modifications of the threshold condition for the ion-acoustic instability so that the instability is shut off and the transport coefficients resume to their classical values. This occurs within a few  $t_j$ .
- (2) Conductive cooling, *both* parallel and perpendicular to the magnetic field, and radiation eventually allow the threshold conditions to be again satisfied so that the instability is switched on again.
- (3) Sequence (1) and (2) will occur many times (subcycle) before hydrodynamic expansion occurs.
- (4) Finally, hydrodynamic expansion causes cooling and reduces the density in the heated volume. As a result,  $J_{||}$  increases to keep the net current constant. This increases the drift velocity,  $v_D$ , so that higher temperatures are achieved.

Hence, temperature will vary with subcycle (1) - (2) but continues to increase stepwise, according to (4), with progressively more energy being deposited *per unit volume*. This heating continues until the net current has decayed sufficiently that  $J_{||}$  cannot be maintained at the ion-acoustic instability threshold. In terms of lumped circuit parameters, this occurs in a time

$$t \approx \frac{L_0}{c^2 (R_T + \eta_{AN} \frac{\Delta s}{A})}, \quad (10.3.21)$$

where  $R_T$  represents the total load resistance as determined by the power generator in one foot of the loop and the load in the other foot;  $\eta_{AN}$ , the anomalous resistivity at marginal stability; and  $A$ , the cross-sectional area in which  $J_{||}$  exceeds threshold. In a cylindrical loop,  $A \approx 2\pi r \delta r$ , where  $\delta r \geq \left( \frac{m_i}{m_e} \right)^{1/2} \frac{c}{\omega_{pe}} \beta^{-1/2}$  for the ion-acoustic instability and  $r$  is the radius of the current channel (Spicer, 1981b). If we assume  $R_T \ll \eta_{AN} \Delta s / A$  then

$$t \approx \frac{L_0}{\Delta s} \tau_L, \quad (10.3.22)$$

where  $\tau_L$  is the local anomalous current-dissipation time (10.3.2).

Thus a dynamic balance is struck between anomalous heating and cooling, with the current-plasma system sitting at, or perhaps oscillating about, the marginal stability point. Since these oscillations about the marginal stability point occur many times in a hydro-time,  $t_H$ , the combination of heating and cooling can be treated as a steady-state process *within* a hydro-time scale. The fundamental quantity to determine, then, is not the level of turbulence but the temperature and density profiles during a hydro-time scale. Once  $J_{||}$  and these profiles are known,

we can calculate the amount of energy transported within a hydro-time. Once given the amount of energy transported we can compute the turbulent fluctuation level in a hydro-time, using simple quasi-linear theory. This logical sequence is just the reverse of conventional approach used in non-linear theory.

The marginal stability analysis proceeds as follows (Spicer and Manheimer, 1982). The steady-state electron heat-balance equation for anomalous Joule heating is

$$-\nabla \cdot \mathbf{Q}_e (\nu_{\text{eff}}) + n_e m_e v_D^2 \nu_{\text{eff}} - P_{\text{rad}} + \frac{3m_e}{m_i} \nu_{\text{ee}} n_e (T_e - T_i) = 0, \quad (10.3.23)$$

while the marginal stability condition for the ion-acoustic instability is

$$v_D = C_s (T_e, T_i) f (T_e, T_i) \quad (10.3.24)$$

where  $\mathbf{Q}_e$  is the thermal and *frictional* heat flux,  $P_{\text{rad}}$  the radiation loss;  $\nu_{\text{ee}}$ , the electron-ion collision frequency,  $v_D$ , the current drift velocity,  $f$  the ion Landau damping factor,  $\nu_{\text{eff}} = \nu_{\text{ee}} + \nu_{\text{AN}}$ ; and for simplicity, we have here assumed that  $T_i$ ,  $n_e$  and  $v_D$  are known. The marginal stability approach adopts (10.3.24) instead of (10.3.23) as the equation for temperature, while (10.3.23) is used to determine  $\nu_{\text{eff}}$ , the effective collision frequency.

Earlier attempts at applying the concept of marginal stability to flare theory (Spicer, 1981b; Duijveman *et al.* 1981) do not utilize the Manheimer approach outlined above, contrary to the claims of Duijveman *et al.* (1981). In addition, these attempts were not internally self-consistent. For example, the Duijvemenn *et al.* (1981) analysis assumes a *given* electric field which drives the current unstable, while feed back is not permitted to account for the alteration of the electric field with changing transport coefficients. Spicer's approach was even less self-consistent: global and local energy balance arguments are used to estimate flare temperature at marginal stability, but with *saturated* levels of turbulence.

#### 10.3.3.4 Applications of Anomalous Joule Heating to Flares

As noted in §10.2.2, Spicer and Brown (1980, 1981) have proposed a classification scheme whereby flare mechanisms, are separated into mechanisms driven by currents flowing either perpendicular or parallel to the magnetic field. This division according to the source of driving current is useful for reasons which will not be discussed here, (*cf.* Spicer and Brown, 1980, 1981), however we note that this approach enables us to recognize which instabilities might be important in a force-free loop, *i.e.*, those driven by  $\mathbf{J}_{\parallel}$ , and which might be important in a neutral sheet, *i.e.*, those driven by  $\mathbf{J}_{\perp}$ . In the past, two classes of flare models have been developed which utilize anomalous Joule heating: those driven by  $\mathbf{J}_{\perp}$ , and those driven by  $\mathbf{J}_{\parallel}$ . In §10.3.2 for example, we considered a  $\mathbf{J}_{\parallel}$ -driven model, denoted the modified Alfvén-Carlqvist model (Spicer, 1981b) to differentiate it from the original double-layer or current-interruption model of Alfvén and Carlqvist (Alfvén and Carlqvist, 1967; Carlqvist, 1969, 1979b). An alternate set of flare models that utilizes  $\mathbf{J}_{\perp}$  — driven anomalous resistivity to enhance the reconnection rate (*cf.* §10.3.5.2) and/or to cause anomalous Joule heating (Sturrock, 1966, 1967, 1972, 1974; Friedman and Hamberger, 1968; Priest and Heyvaerts, 1974; Kuperus, 1976; Heyvaerts *et al.* 1977; Tur and Priest, 1978; Heyvaerts and Kuperus, 1978). These models, to date, have utilized only the ion acoustic or Buneman instabilities as sources of anomalous resistivity; in this respect, these models are archaic. In particular, work by Huba and colleagues (Huba *et al.* 1977, 1978, 1980; Drake *et al.* 1981) has demonstrated that the most appropriate  $\mathbf{J}_{\perp}$ -driven mechanism for anomalous resistivity in neutral sheets is the lower-hybrid drift instability (LHDI) (for a review of anomalous resistivity in neutral sheets *cf.* Papadopoulos, 1979). The LHDI has a number of advantages over those of the ion-acoustic and Buneman instabilities because it can be excited by currents far weaker than those required of the ion-acoustic or Buneman and occurs even when  $T_e / T_i < 1$ . The level of

turbulent resistivity is also substantial. In addition, the lower-hybrid drift instability, which is characterized by wave numbers that satisfy  $\mathbf{k} \cdot \mathbf{B} = 0$ , is closely related to the modified two-stream instability (MTSI) ( $\mathbf{k} \cdot \mathbf{B} \approx 0$ ) (Gladd, 1976) and is capable of accelerating electrons stochastically to very high energies (Lampe and Papadopoulos, 1977). Application of the LHDI or the MTSI to neutral sheet flare models has yet to take place although Spicer *et al.* (1982) utilize both instabilities in a model of Type I metric bursts, and Kahler and Spicer (1982) invoke both instabilities to explain certain classes of impulsive electromagnetic bursts associated with flares.

The  $J_{\parallel}$ -driven anomalous Joule heated flare model discussed previously is an alternative to the double layer model of Alfvén and Carlqvist (*cf.* §10.3.2). It was formulated initially by Smith and Priest (1972), who objected to the Alfvén and Carlqvist double layer model for a number of invalid reasons as discussed in §10.3.2 (Carlqvist, 1973, 1979b, Spicer 1974; 1981b). Smith and Priest found that the  $L/R$  decay time of the relevant circuit is a factor  $\sim 10^6$  too large to explain a flare. However, this estimate is based on a decay time of the circuit due to anomalous resistivity alone, which is an incorrect assumption: the full cross-sectional area of a loop (the basic geometry of the Alfvén-Carlqvist model),  $\approx 10^{18} \text{ cm}^2$ , was used instead of the cross-sectional area of the current channel in which the unstable  $J_{\parallel}$  current flows,  $\approx 2\pi r \delta r \approx 10^{12} \text{ cm}^2$ . The ratio of these two areas is  $\approx 10^6$ , yielding an effective  $L/R$  time of  $\approx 10^2 \text{ s}$  (Spicer, 1981b).

The two primary advantages of an anomalous Joule heating flare mechanism are: the large heating rate associated with this process and the fact that anomalous Joule heating gives rise to a very hot *thermal* plasma ( $\approx 10 \text{ keV}$ ), which thus can provide a thermal explanation for a specific class of impulsive X-ray bursts (Spicer, 1981b). A distinct disadvantage of such models is the large current densities required; this disadvantage is more severe for  $J_{\parallel}$ -driven anomalous Joule heating and double layer models than for  $J_{\perp}$  neutral sheet models.

#### 10.3.4 Double Layers and Anomalous Resistivity

If a purist's definition of double layers and anomalous resistivity were required, we would state that a double layer is a collisionless laminar structure, much like a collisionless laminar electrostatic shock (*cf.* Tidman and Krall, 1971), and that anomalous resistivity results from highly turbulent structure. An examination of the aforementioned literature (§10.3.2 and §10.3.3) concerning the application and theoretical studies of these two  $J_{\parallel}$ -driven mechanisms, however, suggests a more confusing picture: *in which* double-layers consist of a turbulent structure superimposed on a gross laminar structure, while anomalous resistivity may require approximately laminar, large-amplitude ion density waves with similar turbulent structure. In addition, both mechanisms lead to trapping of large numbers of current carrying electrons, while simultaneously requiring similar magnitudes for the current drift speeds for excitation. This latter point implies that double layers, which are highly localized along the current path, may be embedded in a larger region characterized by anomalous resistivity, as discussed by Smith and Goetz (1978).

We also note that it is not at all clear how a double layer dissipates the stored magnetic energy since it appears to lead to primarily mono-energetic beams without any local irreversible dissipation of the current, except possibly through beam driven instabilities or where the beam is stopped, *e.g.*, in the footprints of a loop. In addition, the sequence of events found by Palmadesso *et al.* (1980) may well occur for a double-layer in a magnetized plasma. That is, the beam formed by the double layer should become two-stream unstable, leading to the formation of a quasi-linear plateau, while at the same time this beam should excite the anomalous Dopper cyclotron-resonance instability; the resultant transfer of high-velocity parallel momentum into perpendicular momentum thereby isotropizes the particles trapped in the double layer. For

these reasons, we would like to caution the reader against advocating either mechanism for applications to solar phenomena until both mechanisms are subjected to more thorough theoretical and experimental investigation; at present it appears, to the author at least, that these mechanisms may well represent two aspects of a more general  $J_{\parallel}$ -driven mechanism in magnetized plasmas.

### 10.3.5 Ideal Magnetohydrodynamics (MHD) and Reconnection Mechanisms in Flares

In this section, we review two macroscopic processes commonly invoked to explain flares: ideal MHD and dissipative MHD mechanisms. These processes are very closely related, although they usually are treated as separate phenomena. Reconnection is a particular dissipative MHD mechanism which is distinguished from the ideal MHD process by the existence of a dissipative boundary layer. By definition, a dissipative boundary layer is a narrow region in which the solution of the relevant differential equation changes rapidly and which must vanish in the limit of zero dissipation. Hence, many of the effects associated with an ideal MHD mechanism also are associated with dissipative MHD mechanisms; for example, an ideal MHD kink of mode  $m = 1$  is identical in many respects, to the  $m = 1$  resistive MHD kink (a cylindrical or toroidal tearing mode), except within the resistive boundary layer (Drake, 1978). In the absence of boundary layers, however, dissipative effects still are important in the context of understanding flares; for example, ideal MHD motions often yield large convective flows perpendicular to a magnetic field which, in turn, can provide significant heating and particle acceleration if the relevant dissipative mechanisms are included properly. Hence, we consider two types of MHD mechanisms those in which boundary layers play an important role for both macroscopic stability and the thermalization of free magnetic energy, and those in which boundary layers play no role, e.g., when magnetic flux expands freely into an exponential atmosphere. In this section, therefore, we develop and review the general significance of ideal MHD, as opposed to dissipative MHD, and illustrate how a simple ideal MHD phenomenon may explain a flare. Then the concept of ideal MHD stability is discussed briefly. In this regard, we distinguish between those MHD instabilities which lead to a lowering of magnetic free energy and those which do not. In addition, we discuss the significance of  $\mathbf{k} \cdot \mathbf{B} = 0$  resonant surfaces in ideal-MHD and dissipative MHD stability theory. We complete this section with an introduction to reconnection and the theory of fast and slow tearing modes, and a review of recent developments in tearing mode and reconnection theory, in the context of the potential role of these processes in solar flares.

#### 10.3.5.1 Ideal MHD Theory

The fundamental distinction between ideal MHD and dissipative MHD theory is that magnetic flux is a conserved quantity in the ideal MHD case. The conservation of flux in ideal MHD is a consequence of Faraday's law,

$$\frac{1}{c} \frac{\partial \mathbf{B}}{\partial t} = -\nabla \times \mathbf{E}, \quad (10.3.25)$$

which derives from the fact that the electric field,  $\mathbf{E}$ , around any closed contour, is the negative rate of change of the magnetic flux though that contour,  $\Phi$ , defined by

$$\Phi = \frac{1}{c} \int \mathbf{B} \cdot d\mathbf{S}. \quad (10.3.26)$$

In the non-relativistic limit, Faraday's law is consistent with the following transformation of the electric fields  $\mathbf{E}$ , and  $\mathbf{E}_m$  (Jackson, 1962):

$$\mathbf{E}_f = -\frac{\mathbf{v} \times \mathbf{B}}{c} + \mathbf{E}_m , \quad (10.3.27)$$

where  $\mathbf{E}_f$  and  $\mathbf{E}_m$  are measured in fixed and moving frames of reference, respectively, and  $\mathbf{v}$  is the velocity of the moving frame relative to the fixed frame. Using (10.3.25), (10.3.26) and (10.3.27), the rate of change of flux through any moving contour is

$$\frac{d\Phi}{dt} = -\oint d\mathbf{l} \cdot \left( \mathbf{E}_f + \frac{\mathbf{v} \times \mathbf{B}}{c} \right) , \quad (10.3.28)$$

where  $\frac{d}{dt} = \frac{\partial}{\partial t} + \mathbf{v} \cdot \nabla$ . For a perfectly conducting plasma, Ohm's law requires

$$\mathbf{E}_f = -\frac{\mathbf{v} \times \mathbf{B}}{c} ; \quad (10.3.29)$$

that is, the electric field in the frame moving with the plasma,  $\mathbf{E}_m$ , is zero and cannot have a component parallel to  $\mathbf{B}$ . Hence, (10.3.28) reduces to  $\frac{d\Phi}{dt} = 0$ , which means that the magnetic flux,  $\Phi$ , is convected along with the perfectly conducting plasma and is a constant of the motion.

If toroidal flux surfaces are imbedded in the perfectly conducting fluid, the *local* quantity

$$q(\Phi) = \frac{d\Phi_t}{d\Phi_p} , \quad (10.3.30)$$

where  $\Phi_t$  and  $\Phi_p$  are the toroidal and poloidal fluxes, is convected along with the plasma; hence,  $\frac{dq}{dt} = 0$ . In a cylindrically symmetric (homogeneous in  $\theta$  and  $z$ ) cylinder of length  $L_0$ , the toroidal and poloidal fluxes are

$$\Phi_t = \int_0^{2\pi} \int_0^r B_z(r, t) r dr d\theta = 2\pi \int_0^r B_z(r, t) r dr \quad (10.3.31)$$

and

$$\Phi_p = \int_0^{L_0} \int_0^r B_\theta(r, t) dr dz = L_0 \int_0^r B_\theta(r, t) dr \quad (10.3.32)$$

so that

$$q(r, t) = \frac{2\pi r B_z(r, t)}{L_0 B_\theta(r, t)} . \quad (10.3.33)$$

The geometrical significance of the parameter  $q$  is indicated in Figure (10.11), which represents an unfolded cylinder. In this projection, the magnetic field lines appear locally as straight lines so that  $q$  is a local measure of the pitch of the field lines, as follows:

$$q = \frac{2\pi}{L_0} \frac{dz}{dr} . \quad (10.3.34)$$

The quantity  $q$  is most commonly called the safety factor because of its relation to laboratory MHD stability. We return to the application of this parameter later in this section.

The ideal-MHD property of flux conservation immediately suggests a new and very simple model of a flare, using magnetic flux emerging from the photosphere as the flare driver. Assume that the magnetic flux emerging from the photosphere,  $\Phi_0$ , is associated with a field pressure that greatly exceeds the ambient atmospheric pressure. If no barrier exists above the emerging flux, the configuration lowers its energy by expanding at roughly the Alfvén velocity,  $V_A$ , and with an acceleration  $V_A^2/R$ , where  $R$  is the radius of curvature of the field lines (Book, 1981; Spicer *et al.* 1982). The work thus performed on the surroundings is of order  $\Delta W \approx$

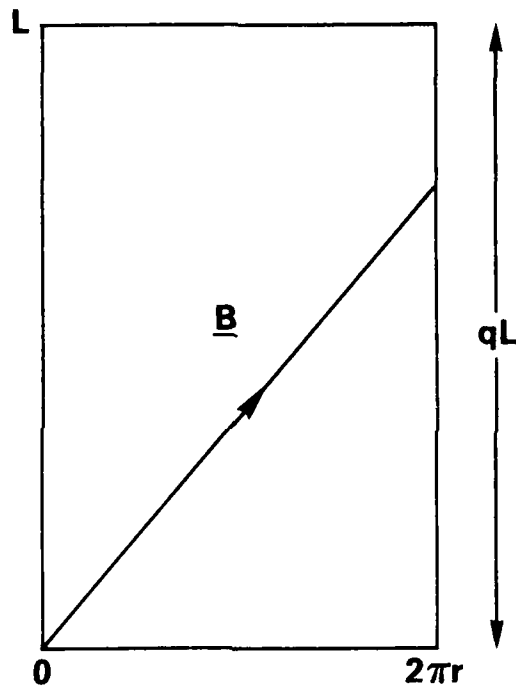


Figure 10.11 — Schematic representation of the local quantity  $q$

$\Delta V B^2 8\pi \sim L_i \Phi_0^2 / 4.8\pi$ , where  $\Delta V$  is the initial volume of the emerging flux;  $B$ , the initial magnetic field;  $L_i$ , the initial length of the emerging flux; and  $\Phi_0$ , the initial area. Taking  $A_i \approx 10^{16} \text{ cm}^2$ ,  $L_i \approx 10^7 \text{ cm}$  and  $B \approx 10^3 \text{ G}$ , we find  $\Delta W \approx 4 \times 10^{29} \text{ erg}$ , enough to power a small flare. In addition, the emerging flux ejects a mass  $\Delta m = \rho \Delta V$  (Book, 1981); for  $\Delta V \approx 10^{15} \text{ cm}^3$  and  $\rho \approx 10^{-10} \text{ g cm}^{-3}$ ,  $\Delta m \approx 10^{15} \text{ g}$ . The total power involved in expansion initially is  $P_i \sim \rho V \Delta V / R$  (Spicer *et al.*, 1982), which yields  $P_i \approx 10^{26} \text{ ergs s}^{-1}$  for  $R \approx \pi L_i$ . This power output increases rapidly at first, then drops back to zero when the flux system reaches pressure equilibrium with the ambient atmosphere. Since the emerging flux moves at velocities greater than the local Alfvén or sound speeds, the flux drives collisionless shocks in front of it. These shocks may represent the irreversible heating mechanism needed to explain the observed flare heating and particle acceleration. The temperature changes due to the collisionless shock are estimated to be  $\Delta T \sim \frac{9T_i}{8} (V_i/C_s)^2$  for large Alfvénic Mach numbers, where  $C_s$  is the local sound speed and  $T_i$  is the initial temperature (Kahler and Spicer, 1982). Since  $V_i \gtrsim 10 C_s$  was assumed changes of  $\Delta T \approx 100 T_i$  can result.

The simple results obtained above illustrate three important points: no macroscopic instability is necessary to explain a flare with this model; remote, photospherically stored magnetic energy can explain a flare; and ideal MHD motions can indirectly drive perpendicular currents that are sufficient to excite crossfield anomalous resistivity effects in the form of collisionless shocks.

Next, consider how the motion of a perfectly conducting plasma induces currents, which then produce heating. Assume that a sudden pressure increase occurs at the center of a cylindrical plasma, in which is imbedded only an axial magnetic field,  $B_z$ . As the central plasma pressure is increased, the resultant radial force imbalance drives an outward radial flow, with velocity  $v_r$ . This flow velocity produces an azimuthal electric magnetic field,  $-v_r B_z / c$ , which reduces the axial field according to Faraday's law. This reduction in the  $B_z$  profile induces azimuthal currents, thus providing an inward  $J_\theta B_z$  force which restores force balance at the higher plasma pressure. In the absence of dissipation, the plasma overexpands and then oscillates spatially about the new equilibrium. If dissipation is permitted, these oscillations are damped by Ohmic (collisional or collisionless) and/or viscous dissipation so that the oscillation energy reappears as heat. In this manner a MHD process can transport energy, from a small volume, into a larger volume without invoking diffusive transport mechanisms, and, if dissipation is permitted, can deposit the energy in a larger volume.

We now review the ideal MHD instabilities relevant to solar flare theory. Our goal is to introduce the appropriate concepts that allow us to differentiate ideal MHD instabilities and resistive MHD instabilities. There are basically two *equilibrium* sources of driving energy for both ideal and resistive MHD instabilities: currents perpendicular and parallel to the magnetic field. Currents perpendicular to  $\mathbf{B}$ , due to pressure gradients, are responsible for driving the so-called interchange instabilities. These instabilities cause one portion of a plasma to exchange places with another portion, and depend only on the local conditions near the line of force; therefore, they constitute local instabilities or modes, as opposed to global modes. In general, the interchange instabilities, which are local do not necessarily imply global instability; some level of local instability is tolerable and usually appears as convective turbulence. This turbulence may be manifested in various solar features such as prominences (Spicer, 1979b). The second source of driving energy currents parallel to  $\mathbf{B}$ , drives macroscopic instabilities which spread themselves out over the plasma volume. These "kinks," or helical instabilities, can be subdivided further into free-boundary kinks (external kinks) and internal kinks. The external kink involves motions of the *entire* plasma-magnetic field configuration; in the solar context, a classical example appears to be the erupting prominences (Sakurai, 1976; Spicer, 1976, 1979b). On the other hand, internal kinks involve distortions and motions *within* the plasma-magnetic field configuration (PMFC), and are not necessarily visible to an external observer.

As a general rule, ideal MHD instabilities occur when a perturbation to a PMFC does not bend or stretch the magnetic field lines. Such perturbations do not provide magnetic restoring forces, which are necessary for restoration of equilibrium, so that the perturbation continues to grow. To identify, in a more definitive manner, those effects which are capable of causing instability and those which are capable of stabilizing, we utilize the energy principle (Bernstein *et al.*, 1958). By dividing the potential energy  $\delta W$  into positive and negative parts, we can identify the stabilizing and destabilizing terms.\* We write  $\delta W$  in the form (Furth *et al.*, 1966)

$$\delta W = \delta W_f + \delta W_v + \delta W_s, \quad (10.3.35)$$

where  $\delta W_f$ , the change in potential energy resulting from the perturbation of the *plasma*, is given by

$$\delta W_f = \frac{1}{2} \int d^3x \left\{ \begin{array}{l} \frac{\delta B_\perp^2}{4\pi} + 4\pi \left| \frac{\delta B_{||}}{4\pi} - \frac{\mathbf{B}_0 \cdot \nabla P_0}{B_0^2} \right|^2 \\ \text{(Alfven)} \quad \text{(Magneto sonic)} \\ + \gamma_0 P_0 (\nabla \cdot \boldsymbol{\xi})^2 \\ - \frac{\mathbf{J}_0 \cdot \mathbf{B}_0}{B_0^2} (\mathbf{B}_0 \times \boldsymbol{\xi}) \cdot \delta \mathbf{B} \\ \text{(kink)} \quad - \frac{2\boldsymbol{\xi} \cdot \nabla P_0 \boldsymbol{\xi} \cdot \boldsymbol{\kappa}}{\text{(interchange)}} \\ \text{(Ballooning)} \end{array} \right\}; \quad (10.3.36)$$

$\delta W_v$ , the change in potential energy resulting from the perturbation of any *vacuum* magnetic field, is given by

$$\delta W_v = \frac{1}{2} \int d^3x \frac{|\delta \mathbf{B}|^2}{4\pi}; \quad (10.3.37)$$

and  $\delta W_s$ , the change in potential energy associated with any surface currents present, is given by

$$\delta W_s = \frac{1}{2} \int d\mathbf{S} \cdot \left[ \left[ \nabla \left( P_0 + \frac{B_0^2}{8\pi} \right) \right] \right] (\hat{\mathbf{n}} \cdot \boldsymbol{\xi})^2, \quad (10.3.38)$$

where  $\boldsymbol{\xi}$  is the fluid displacement,  $\gamma_v$ , is the ratio of the specific heats;  $\hat{\mathbf{n}}$ , is a unit vector normal to the equilibrium magnetic surface;  $\delta \mathbf{B}$ , the perturbed magnetic field; and

$$\boldsymbol{\kappa} = \frac{1}{2B_0^4} [\mathbf{B}_0 \times \nabla (8\pi P_0 + B_0^2)] \times \mathbf{B}_0 \quad (10.3.39)$$

is the curvature of the magnetic field.  $\delta W_f$  always provides stabilization, and  $\delta W_s$  vanishes if no surface currents exist.

The first three terms in  $\delta W_f$  are stabilizing while the last two are destabilizing. The first of the two potentially destabilizing terms results from currents flowing parallel to  $\mathbf{B}_{||}$ , and the second destabilizing term is due to the interaction of the pressure gradient with the field curvature. Notice that these terms arise from  $\mathbf{J}_{||}$  and  $\mathbf{J}_\perp$ , respectively. In solar PMFC's  $\beta$  can vary by orders of magnitude, so that  $\mathbf{J}_\perp$  may play an important role in part of a PMFC while  $\mathbf{J}_{||}$  predominates in other parts (Spicer, 1979b). However, just the opposite is true inside neutral sheets, where  $\beta \rightarrow \infty$  since  $\mathbf{B} \rightarrow 0$  so that  $\mathbf{J}_\perp$  becomes very important. Interchanges are expected in neutral sheets where finite curvature effects exist, according to Uchida and Sakurai

\*The reader should note that the following arguments are geometry independent; e.g., kinks can occur in any geometry, although with differing growth rates and manifestations. For example, the  $m = 1$  kink requires curvature effects which are a natural consequence of cylindrical and toroidal geometry, but not of slab geometry; hence, a  $m = 1$  kink cannot exist in slab geometry.

(1977), and might play an important role in the energetics of neutral sheet reconnection during a flare.

The first and second stabilizing terms in  $\delta W_f$  arise because energy is required to stretch and shift lines of force wherever the direction of the magnetic field is changed by the perturbation. Contained within this term is the global magnetic shear, the average shear over the entire magnetic surface, and the local shear, the amount a field line must be stretched if it is to exactly replace a neighboring field line in the course of the perturbation (Ware, 1965). Magnetic shear provides stabilization because the direction of the magnetic field changes its direction with position in a sheared magnetic field. It is very difficult to interchange two neighboring field lines which are oriented at an angle to one another, unless a line is bent and/or stretched. Since bending and stretching require that work be done on the field,  $\delta W_f$  increases rather than decreases; hence shear is stabilizing. We emphasize, at this point, that shear is stabilizing in the *ideal* MHD limit because flux is conserved, *i.e.*, field lines cannot be broken. However, dissipation effects, such as resistivity, allow the lines of force to break and reconnect. Thus, shear in the presence of dissipation is less effective as a stabilizing influence than in the ideal MHD approximation.

Two compression terms exist in (10.3.36), both of which are stabilizing:  $\gamma_0 p_0 (\nabla \cdot \xi)^2$  and  $\frac{(\mathbf{B}_0 \cdot \nabla p_0)^2}{B_0^2}$ . This follows because they are a measure of the net energy absorbed by the PMFC in compressing the magnetic field and the plasma. As with stretching, a finite amount of compression is necessary if one field line is to replace another exactly. Notice also that both terms become ineffective in the limit of  $\beta \rightarrow 0$ .

The destabilizing term  $\mathbf{J}_0 \cdot \mathbf{B}_0 (\mathbf{B}_0 \times \xi) \cdot \delta \mathbf{B}$  is responsible for driving kink instabilities in force-free fields, by means of forces resulting from the interaction of the currents parallel to  $\mathbf{B}_0$  and  $\delta \mathbf{B}$  (Voslamber and Callebaut, 1962; Green and Johnson, 1962; Anzer, 1968; Raadu, 1972; Spicer, 1976; 1977; Van Hoven *et al.*, 1977; Van Hoven, 1981). Energy is released by lowering the net current along the magnetic field. The constraint that the magnetic flux within a given flux surface be conserved is satisfied by bending and stretching the field lines into a helical or screw shape (Kruskal and Kulsrud, 1958). The decrease in the magnitude of  $\mathbf{B}_0$  inside the flux surface is balanced by an increase in the cross section of the bounding surface; this accounts for the expansion of prominences (Sakurai, 1976; Spicer, 1979b).

The term  $2\xi \cdot \nabla p_0 \xi \cdot \kappa$  is related to the curvature and, thus, the tension of the lines of forces, and is responsible for driving the interchange instability.\* This tension results in a force which is proportional to  $\mathbf{B}^2$ , so that work must be done to move lines of force against this tension. One additional stabilizing effect, line tying, is not obvious from the discussions (*cf.* §10.2.2).

Although the  $m = 1$  kink will be discussed in more detail under reconnection it is pertinent to briefly comment on the nature of the kink instability. As has been shown, kinks are effectively incompressible perturbations since  $p_0$  does not appear in the driving term  $(\mathbf{J}_0 \cdot \mathbf{B}_0 (\mathbf{B}_0 \times \xi) \cdot \delta \mathbf{B})$ ; that is, they would exist with or without a finite  $\beta$ . As a result of their incompressibility the kink driving force must provide a torque,  $T_z$ , in the axial direction; *i.e.*,

$$T_z = \nabla \times \left[ - \frac{\nabla p + \mathbf{J} \times \mathbf{B}}{c} \right]_z. \quad (10.3.40)$$

\*The Rayleigh-Taylor instability is essentially an interchange instability but with gravitational acceleration  $g$  as the driving term not  $\kappa$ . It arises as a result of a coupling between the pressure gradient and  $g$ .

Linearization of (10.3.40) for perturbations of the form  $\xi = \xi(r) \exp[i(m\theta + kz)]$  yields

$$\delta T_z = \delta B_r \frac{dJ_{z0}}{dr} + ik_{||} |B_0| \delta J_z, \quad (10.3.41)$$

where  $dJ_{z0}/dr$  provides the driving force. In general, the second term is negative and provides a stabilizing force except where the perturbation is constant along the equilibrium field, where  $\mathbf{k}_{||} \cdot \mathbf{B}_0/B_0^2 = 0$ . Thus, depending on the sign and magnitude of  $dJ_{z0}/dr$  at the point where  $\mathbf{k} \cdot \mathbf{B}_0 = 0$  instability may or may not result. Therefore, knowledge of the equilibrium current density profile is of crucial importance in comprehending the MHD stability of solar features in which parallel currents are believed to flow, such as loops and prominences.

If no component of  $\mathbf{B}$  exists other than that produced by  $J_z$ , the system is considered shearless because the induced field component  $B_\theta$  has lines of force which are all in the same direction. However, if more than one component of  $\mathbf{B}$  exists,  $\mathbf{B}$  has shear because the direction of  $\mathbf{B}$  varies from point to point. For a cylindrically symmetric field, the pitch of the magnetic field,  $\mu$ , is given by

$$\mu = \frac{rB_z}{B_\theta} \propto q \quad (10.3.42)$$

hence, shear represents the change of field line pitch with radius and is just the derivative  $dq/dr$ . Shear also can be related to  $dJ_z/dr$  by the integral expression (Wesson, 1978)

$$\frac{d\mu}{dr} = \frac{2\pi L_0}{r^3 B_z} \int_0^r r'^2 \frac{dJ_{z0}}{dr'} dr'. \quad (10.3.43)$$

The main point, then, is that steep current density profiles, *i.e.*, profiles with large  $dJ_z/dr$ , produce large degrees of shear so that a solar PMFC with a steep current gradient should be relatively stable to ideal MHD kink modes and interchange modes, as discussed in §10.2.2.2. However, the introduction of finite resistivity, which relaxes the ideal MHD constraint of flux conservation, changes the above argument.

We now consider the parameter  $q$ , as defined by (10.3.30), and its relationship to the mode rational surface. Denoting an unperturbed equilibrium quantity by the subscript "0" and perturbed quantities with the prefix " $\delta$ ," the linearized equations of motion for a current free magnetized plasma are

$$\rho_0 \frac{\partial \delta \mathbf{v}}{\partial t} = -\gamma_0 \frac{P_0}{\rho_0} \nabla \delta p + \frac{1}{4\pi} (\nabla \times \delta \mathbf{B}) \times \mathbf{B}_0. \quad (10.3.44)$$

$$\frac{\partial \delta p}{\partial t} + \rho_0 \nabla \cdot \delta \mathbf{v} = 0. \quad (10.3.45)$$

and

$$\frac{\partial \delta \mathbf{B}}{\partial t} = \nabla \times (\delta \mathbf{v} \times \mathbf{B}_0), \quad (10.3.46)$$

where the adiabatic relation  $\rho = \gamma_0 p/c_s^2$  has been used. Assuming  $\mathbf{B}_0 = B_0 \hat{e}_z$ ,  $\nabla = ik$  and  $\frac{\partial}{\partial t} = -i\omega$ , and solving for  $\delta \mathbf{v}$ , we find (Jackson, 1962)

$$-\omega^2 \delta \mathbf{v} = -c_s^2 \mathbf{k} \cdot (\delta \mathbf{v}) + V_A^2 \hat{e}_z \times [\mathbf{k} \times \{\mathbf{k} \times (\delta \mathbf{v} \times \hat{e}_z)\}], \quad (10.3.47)$$

where  $V_A = B_0/\sqrt{4\pi\rho_0}$ . Taking  $\mathbf{k}$  to be in the  $y - z$  plane, then due to isotropy in the  $y - z$  plane, (10.3.47) yields the following expressions for the components of  $\omega^2 \delta \mathbf{v}$ .

$$\omega^2 \delta v_x = k_z^2 V_A^2 \delta v_x, \quad (10.3.48)$$

$$\omega^2 \delta v_z = k_x c_s^2 (k_x \delta v_y + k_z \delta v_z) + (k_x^2 + k_y^2) V_A^2 \delta v_y, \quad (10.3.49)$$

and

$$\omega^2 \delta v_z = k_z c_s (k_z \delta v_z + k_z \delta V_z). \quad (10.3.50)$$

Equation (10.3.48) yields the dispersion solution

$$\omega^2 = k_z^2 V_i^2 = k^2 V_i^2 \cos^2 \theta = \frac{(\mathbf{k} \cdot \mathbf{B}_0)^2}{4\pi\rho_0}, \quad (10.3.51)$$

where  $\theta$  is the angle between  $\mathbf{k}$  and  $\mathbf{B}_0$ , while (10.3.48) and (10.3.49) together yield

$$\omega^2 = \frac{k^2}{2} \{ (V_i^2 + c_s^2) \pm ((V_i^2 + c_s^2)^2 + 4c_s^2 V_i^2 \sin^2 \theta)^{1/2} \}. \quad (10.3.52)$$

Equation (10.3.51) is the dispersion relation for shear Alfvén waves. For  $\theta = 0$ , (10.3.51) yields two solutions  $\omega^2 = k^2 c_s^2$  and  $\omega^2 = k^2 V_i^2$ ; for  $\theta \approx \pi/2$ , the two roots are  $\omega^2 = k^2(c_s^2 + V_i^2)$  and  $\omega^2/k^2 \approx 0$ . We emphasize that shear Alfvén waves are non-compressional, since  $\delta v_x = \delta v_z = 0$ ; at  $\theta = 0$  only the sound wave,  $\omega^2 = k^2 c_s^2$ , compresses; while at  $\theta \approx \pi/2$  the magnetosonic wave  $\omega^2 = k^2(c_s^2 + V_i^2)$ , compresses.

If the plasma is characterized by  $\beta \ll 1$  we can assume that the plasma is incompressible perpendicular to the lines of force ( $\gamma_0 \rightarrow \infty$ ). In this situation, compressibility provides no stabilization, so that only shear Alfvén waves are available to stabilize against perturbations. Shear Alfvén waves have frequencies  $\omega^2 = (\mathbf{k} \cdot \mathbf{B}_0)^2/4\pi\rho_0$  and equal zero when  $\mathbf{k} \cdot \mathbf{B}_0 = 0$ . Suppose, then, that some perturbation drives the magnetized plasma toward instability, which requires  $\omega^2 < 0$ , but that initially  $\omega^2 > 0$ . If  $\omega^2 \gg 0$  initially, the perturbation lowers  $\omega^2$  at most, while if initially  $\omega^2 \geq 0$ , the perturbation may lead to  $\omega^2 < 0$  and instability. Clearly the most likely condition for instability to occur is if  $\omega^2 = 0$  initially; that is, if the perturbation wave number vector satisfies  $\mathbf{k} \cdot \mathbf{B}_0 = 0$ . Thus, if the perturbation results in  $\mathbf{k} \cdot \mathbf{B}_0 \neq 0$ , the perturbing flow couples to shear Alfvén waves, which tend to stabilize the system. However, we must emphasize that instability can occur even if  $\mathbf{k} \cdot \mathbf{B}_0 \neq 0$ , as long as the unstable flow is sufficient to overwhelm the stabilization effect of Alfvén waves. If an instability exists and  $\mathbf{k} \cdot \mathbf{B}_0 \neq 0$ , the instability is localized along the field lines since the perturbation is forced to vary along the field line exciting stabilizing shear Alfvén waves. If  $\mathbf{k} \cdot \mathbf{B}_0 = 0$ , the perturbation is resonant, because the pitch of the perturbation exactly matches the pitch of the magnetic field.

The definition of  $q$ , given by (10.3.33) for a cylindrically symmetric diffuse pinch, we derive by expanding  $\mathbf{k} \cdot \mathbf{B}_0 = k_z B_z + \frac{m B_\theta}{r}$  and rewriting it in the form  $\mathbf{k} \cdot \mathbf{B}_0 = (q + m/n)n B_\theta/r$ , where  $m$  is the azimuthal mode number; a finite cylinder of length  $L_0$  also is assumed so that only axial wave numbers which satisfy  $k_z = 2\pi n/L_0$  fit the system. Hence,  $\mathbf{k} \cdot \mathbf{B} = 0$  when  $q = -m/n$ . These surfaces are called mode rational surfaces. However, the existence of such surfaces in a solar magnetic configuration is unlikely, because they are an artifact of the periodic boundary conditions imposed on the axial coordinate; thus, if the cylinder were bent into a torus, the pitches of the field lines at each end of the cylinder would match identically. However, in a solar loop, the pitches of the field lines will differ at the ends of the loop, in general, because of inhomogeneity of the field along the field line, something that is not accounted for in the cylindrically symmetric loop. Consequently, a loop can not be treated as if it were topologically equivalent to a torus. The fact that  $q$  is a *local* quantity, in general, except in cases of high symmetry, justifies our previous contention that the use of local stability criteria reveals us nothing about global stability (cf. §10.2.2.2).

Shear and line-tying stabilization can now be easily understood in the MHD picture. If a finite, homogeneous axial magnetic field is placed between two perfectly conducting end plates, the parallel (axial) wave numbers are limited to  $k_{\parallel 0} = 2\pi n/L_0$ . Hence, the available wave frequencies, defined by  $\omega^2 = (\mathbf{k} \cdot \mathbf{V}_i)^2 = (2\pi n V_i/L_0)^2$ , always are positive and thus exert a stabilizing influence. If the end plates are removed the plasma is free to chose a parallel

wavelength equal to zero. However, if a variation is induced in the direction of  $\mathbf{B}$  this freedom is removed and shear stabilization is obtained. If the two stabilization mechanisms, shear and line-tying, are combined the stabilization is further enhanced.

As noted in §10.2, several mechanism can cause polarization currents to exist perpendicular to magnetic field lines; these currents tend to discharge along magnetic field lines by means of shear Alfvén waves. When charges of opposite polarities on differing field lines are neutralized, a parallel current system is established. This can be better understood, together with how shear Alfvén waves stabilize against instabilities in the electrodynamic coupling picture, by utilizing a linearized form of (10.2.2) with the pressure gradient neglected,  $\nabla \cdot \delta \mathbf{J} = 0$  and (10.3.50) to obtain the first order parallel current associated with an Alfvén wave given by

$$\delta \mathbf{J}_\parallel = \frac{\mu B_0}{4\pi\omega} \mathbf{k}_\parallel \cdot (\mathbf{k}_\parallel \times \delta \mathbf{v}). \quad (10.3.53)$$

Equation (10.3.53) demonstrates that magnetosonic waves ( $\mathbf{k}_\parallel \rightarrow 0$ ) do not produce parallel currents, while shear Alfvén waves do. Hence, perturbations with  $\mathbf{k} \cdot \mathbf{B}_0 = 0$  cannot generate charge neutralizing parallel currents to short circuit the polarization currents associated with  $\delta \mathbf{J}_\parallel$ , while perturbations with  $\mathbf{k}_\parallel \neq 0$  can produce parallel currents. Thus, because  $\nabla \cdot \delta \mathbf{J} = 0$  is required for equilibrium (*cf.* §10.2.2.2), instability results from perturbations that satisfy  $\mathbf{k}_\parallel = 0$ . Furthermore, since  $\mathbf{k}_\parallel$  cannot vanish in finite systems, line-tying results from the fact that a finite  $\delta \mathbf{J}$  always is produced with a magnitude that depends on  $\mathbf{k}_\parallel$ . Hence, the larger the system the smaller the stabilizing effect of line-tying.

Returning to the  $m = 1$  kink mode, we note from (10.3.14), that the driving term,  $dJ_{z0}/dr$ , still can become sufficiently large to exceed the stabilizing term associated with the shear Alfvén waves, if  $\mathbf{k}_\parallel$  is not allowed to vanish. Thus, a kink will develop, localized along the field lines. The presence of any inhomogeneity in both  $\theta$  and  $z$  will further localize the mode along the field lines, thus requiring even larger current densities and gradients to drive the kink instability, as suggested in §10.2.2.2. This implies that larger currents can exist in loops than present stability analyses permit. It further implies that more magnetic energy can be stored in such configurations.

### 10.3.5.2 Reconnection

Reconnection is, without doubt, the most popular flare mechanism ever proposed. This process is attractive for two fundamental reasons: it allows magnetic energy stored globally to be locally converted into thermal energy and convective flows, while simultaneous giving rise to large induced electric fields, and thus particle acceleration, parallel to the magnetic field. Because most of the recent developments in reconnection theory that are pertinent to solar flares are associated with the tearing instability, the bulk of our review is focussed on that instability. In addition, because flares appear to be closely involved with curvilinear plasma-magnetic field configurations, we compare tearing in a slab geometry with that in a cylindrical or toroidal geometry. The following review assumes that reconnection is collisionally dominated, at least in the linear growth phase.

A "bare bones" explanation of reconnection is as follows: a resistive boundary layer mechanism that violates the conservation of magnetic flux, the fundamental constraint of ideal MHD theory, and thus leads to topological changes in the magnetic flux surfaces that change the path for current closure. These topological changes are manifested by what are called neutral points and magnetic islands. A neutral point is denoted as either an  $X$  point or an  $0$  point (Figure (10.12)); a magnetic island consists of at least one  $X$  point and one  $0$  point. Neutral points represent sites where large current densities can be produced without being opposed by

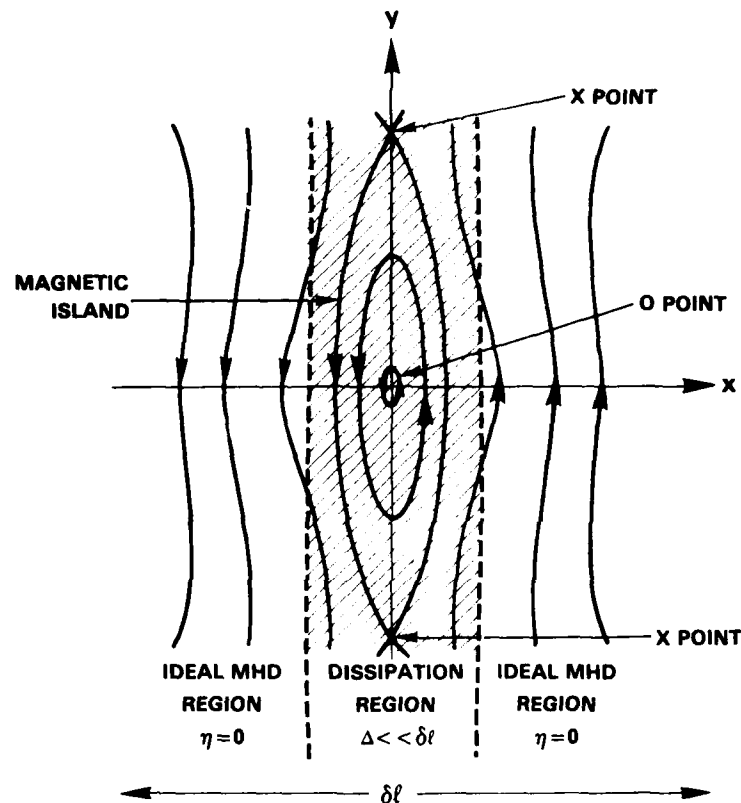


Figure 10.12 — Schematic of a single magnetic island with one O point and two x points; ideal and resistive MHD regions are delineated

$\mathbf{J} \times \mathbf{B}$  forces, as first demonstrated by Dungey (1953), and therefore provide ideal sites for producing large  $\mathbf{J}$  currents, which may be manifested as accelerated particle streams. However, topological changes in magnetic flux surfaces only can occur under rather special conditions. In particular, the flow field which drives reconnection, must be an odd function of position with respect to the mode rational surface, where  $\mathbf{k} \cdot \mathbf{B}_0 = 0$ , so that the two fluid elements on opposite sides of the mode rational surface are flowing toward each other. In this respect, two basic types of treatments of reconnection are found in the literature: those in which steady-state flow fields on opposite sides of the mode rational surface always face each other in the presence of one  $X$ -point; and those which assume a dynamic flow field that includes flow elements on opposite sides of the mode rational surface flowing either towards or away from each other in the presence of one or more  $X$ -points. The latter type of flow characterizes reconnection by the tearing mode instability (Furth *et al.*, 1963, Drake and Lee, 1977, Mahajan *et al.* 1979, Hassam, 1980), while the former type of flow characterizes steady-state reconnection theories (see Vasylunas, 1975 for a review). Presently a clear relationship does not exist between the dynamic and steady-state theories of reconnection, although presumably a steady-state reconnection model describes the saturated state of one magnetic island consisting of one  $X$  point and 0 point.

The role of the mode rational surface in reconnection is illustrated by the following example. After Manheimer (1979b), consider a two-dimensional incompressible flow field of a perfectly conducting fluid in the  $x-y$  plane, defined by

$$V_x = \begin{cases} -V_0 \cos ky & \Delta < x \\ -V_0 \frac{x}{\Delta} \cos ky & 0 < x < \Delta \end{cases} \quad (10.3.54a)$$

$$V_x = \begin{cases} -V_0 \frac{x}{\Delta} \cos ky & 0 < x < \Delta \end{cases} \quad (10.3.54b)$$

with  $V_x(-x) = -V_x(x)$ , and

$$V_y = \begin{cases} 0 & \Delta < x \\ \frac{V_0}{\Delta k} \sin ky & 0 < x < \Delta \end{cases} \quad (10.3.55a)$$

$$V_y = \begin{cases} \frac{V_0}{\Delta k} \sin ky & 0 < x < \Delta \end{cases} \quad (10.3.55b)$$

with  $V_y(-x) = V_y(x)$  such that  $\nabla \cdot V = 0$ ;  $\Delta$  represents the thickness of the resistive boundary layer and is assumed here to be arbitrarily small, and  $k$  is a wave number in the  $y$  direction. This type of flow field is called *tearing flow*. An examination of (10.3.54) and (10.3.55) shows that a very rapid flow exists in the  $y$  direction where  $|x| < \Delta$ . The flow streamlines shown in Figure (10.13), illustrate that, as the fluid elements with  $y > 0$  approach the  $x = 0$  plane from the positive and negative directions, they continuously turn away from the  $x = 0$  plane into the  $y$  direction and then continuously back into the negative and positive  $y$ -directions, respectively. Those fluid elements with  $y < 0$  flow in a similar manner, but move away from the  $x = 0$  plane in the  $-y$  direction and then back into the negative and positive  $x$  direction, respectively. The fluid element initiated located at  $y = 0$  does not develop a velocity component in the  $y$  direction, but piles up at the stagnation point at  $x = y = 0$ .

If the perfectly conducting flow field is now imbedded in an equilibrium magnetic field of the form

$$\mathbf{B}_0 = B_0 \frac{x}{\delta l} \hat{e}_y \quad (10.3.56a)$$

which results from a current sheet of the form

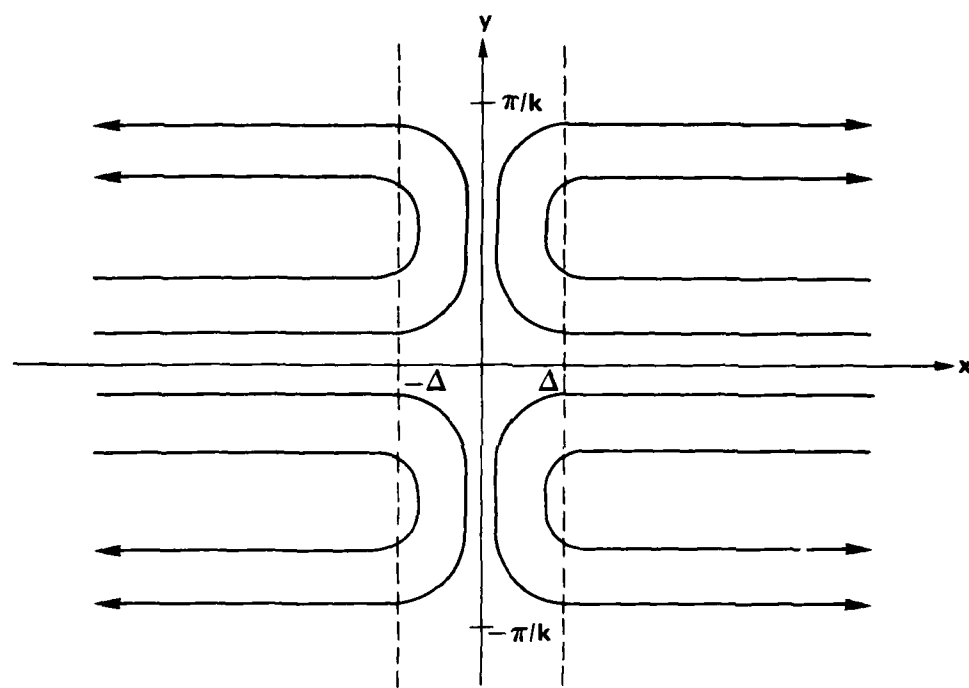


Figure 10.13 — The velocity field stream lines for tearing flow (after Manheimer, 1979b)

$$J_z = \frac{c}{4\pi} \frac{B_0}{\delta l}, \quad (10.3.56b)$$

where  $\delta l$  is the magnetic field shear length such that  $\Delta \ll \delta l$  (Figure 10.12), the magnetic field will begin to be contorted by the flow field because the magnetic field is frozen into the flow. The time history of the magnetic field is shown in Figure (10.14): the magnetic field becomes more and more contorted on either side of the  $x = 0$  plane, as time increases, and the bending of the magnetic field lines causes larger and larger forces which attempt to restore the magnetic field lines to their original form. Notice that no magnetic restoring forces are generated where  $\mathbf{k} \cdot \mathbf{B}_0 = 0$  (i.e., at  $x = 0$ ), and that the magnetic field is straight and anti-parallel within  $|x| < \Delta$  on opposite sides of the  $x = 0$  plane. Eventually, the magnetic restoring forces equal the forces exerted by the flow field and a steady-state is achieved. These arguments qualitatively demonstrate that tearing flow is stable in the ideal MHD approximation at least in slab geometry. An analytical proof can be found in Furth *et al.* (1963), who first treated the theoretical aspects of the tearing mode for slab geometry.

If the perfectly conducting constraint is relaxed and finite dissipation (non-zero resistivity) is permitted, the foregoing picture changes. In both cases, the gradients in the magnetic field, and thus the  $J_z$  currents, increase as the magnetic field is distorted. In the ideal MHD case, the resultant large currents can not be dissipated, but simply build up in magnitude. With finite dissipation, however, these currents can be dissipated, or "annihilated" in the form of Joule heating and particle acceleration. The magnetic restoring forces thus are reduced, and thus lead to the collapse of the steep current profile developing across the  $x = 0$  plane that was built up by the flow field.\* In addition, long anti-parallel magnetic field lines exist on opposite sides of the  $x = 0$  plane within the resistive boundary layer  $\Delta$ , due to the tearing flow (see Figure 10.14). In the presence of finite dissipation these anti-parallel magnetic field lines can diffuse together, and merge to form neutral points of the  $X$  and  $0$  type (Figure (10.12)). Since the addition of dissipation permitted the *lowering* of magnetic energy *tearing flow* leads to an instability, called the *tearing mode*, in the presence of finite dissipation.

The role of the mode rational surface is illustrated quantitatively as follows. Consider a magnetic field of the form

$$B_z = B_0 F(x)/\delta l, \quad B_z \gg B_0, \quad B_x = 0, \quad (10.3.57)$$

where  $B_z$  is spatially constant; and  $F(x) = \mathbf{k} \cdot \mathbf{B}_0 / |\mathbf{k} \cdot \mathbf{B}_0| \approx x$  for  $x \ll \delta l$ , and  $F(|x| \gg \delta l) \rightarrow 1$ ,  $\delta l$  representing the shear length or, equivalently, the thickness of the current layer peaked at  $F(x) \approx 0$ . Following Adler *et al.*, (1980), we introduce a flux function,  $\psi(x, y)$ , such that,

$$\mathbf{B} = \nabla \psi \times \hat{e}_z + B_z \hat{e}_z; \quad (10.3.58)$$

Ampere's equation thus yields

$$\nabla^2 \psi = - \frac{4\pi}{c} J_z. \quad (10.3.59)$$

Using Ohm's law (10.2.5) with a constant scalar resistivity, Faraday's equation, and assuming incompressible flow, we find the following equation for  $\psi$ :

$$\frac{\partial \psi}{\partial t} + \nabla(\psi \mathbf{v}) = \frac{\eta c^2}{4\pi} \nabla^2 \psi. \quad (10.3.60)$$

Operating on the momentum equation with  $\hat{e}_z x \nabla x$ , and introducing a stream function,  $\phi$ , for the incompressible flow, such that  $\mathbf{v} = \nabla \phi \times \hat{e}_z$ , yields

\*From this point of view reconnection can be viewed as a mechanism by which flow energy is converted to magnetic energy and then into particle kinetic energy.

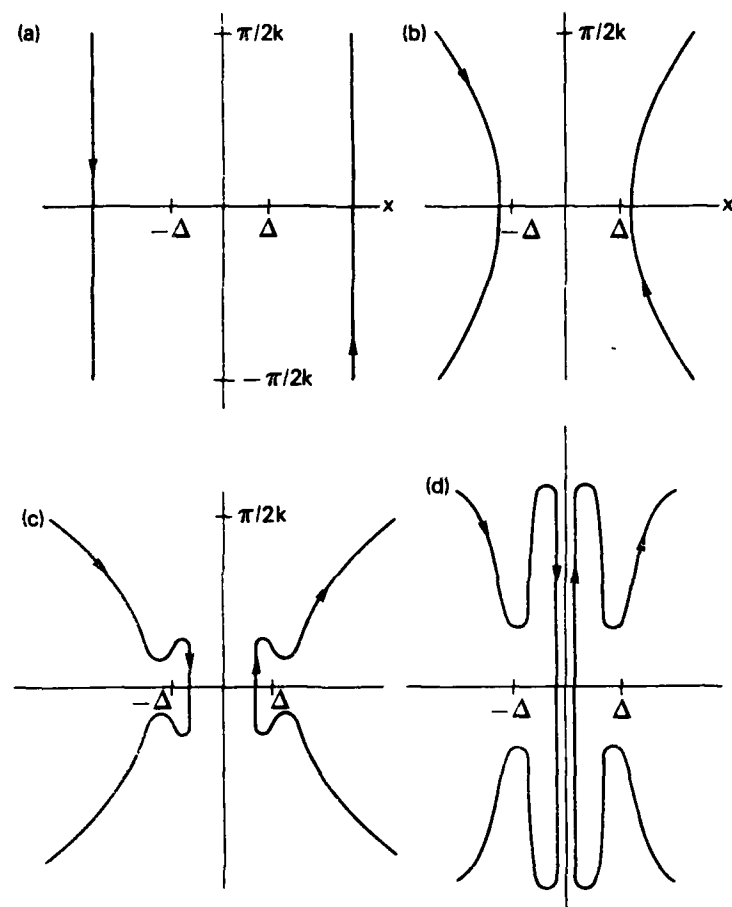


Figure 10.14 — The evolution of the magnetic field lines at different times in the presence of tearing flow

$$\rho_0 \frac{d\nabla^2\phi}{dt} = -\hat{e}_z \cdot [\nabla\psi x \nabla (\nabla^2\psi)]. \quad (10.3.61)$$

The set of coupled equations (10.3.60) and (10.3.61) must now be solved subject to the appropriate boundary and initial conditions. These equations are linearized in terms of  $\delta\phi$  and  $\delta\psi$ , where

$$\psi(x,y) = \psi_0(x,y) + \delta\psi(x)\cos ky, \quad (10.3.62)$$

and

$$\phi(x,y) = (\gamma/kB_0) \delta\phi(x) \sin ky, \quad (10.3.63)$$

and both quantities are assumed to vary exponentially with time as  $\exp(\gamma t)$ . Hence, we obtain

$$\delta\psi = (\gamma\tau_L)^{-1} \left[ \frac{d^2\delta\psi}{dx^2} - k^2\delta\psi \right] + \delta\phi F(x) \quad (10.3.64)$$

and

$$-\gamma^2\tau_A^2 \left[ \frac{d^2\delta\phi}{dx^2} - k^2\delta\phi \right] = F(x) \left[ \frac{d^2\delta\psi}{dx^2} - k^2\delta\psi \right] - \frac{d^2F(x)}{dx^2} \delta\psi, \quad (10.3.65)$$

where  $\tau_A = (kV_A)^{-1}$  and  $\tau_L = 4\pi(\delta l)^2/\eta c^2$  are the characteristic hydromagnetic and resistive diffusion times for the problem. The magnetic Reynolds number,  $S = \tau_L/\tau_A$  is  $> 10^{10}$  for solar plasmas.

If  $\eta$  is very small but finite and  $F(x)$  never vanishes, then (10.3.64) demonstrates that  $\delta\psi$  and thus  $\psi$  are reasonably well conserved and resistivity is unimportant. However, if  $\eta \neq 0$  but  $F(x)$  vanishes at some  $x$ , then the resistive term is dominant in (10.3.64), within the layer of thickness  $\Delta$  about the mode rational surface at  $F(x) = 0$ . Outside the mode rational surface, the resistive term is no longer important and ideal MHD analysis is valid. Figure (10.12) illustrates the splitting between resistive-dominated and ideal MHD-dominated regions.

The aforementioned division into resistive and ideal-MHD regions suggests that (10.3.64)-(10.3.65) can be solved using a boundary layer analysis (Furth *et al.*, 1963), where the resistivity is assumed to be negligible everywhere except within the resistive region  $|x| < \Delta$ . For "constant  $\psi$ " tearing modes (*cf.* below),  $\Delta$  is given by (Furth *et al.*, 1963; Drake and Lee, 1977)

$$\Delta = 2 \left[ \frac{\gamma\tau_A^2}{\tau_L} \right]^{1/4} \delta l \quad (10.3.66)$$

In the ideal MHD region,  $\delta\psi$  and  $\delta\phi$  satisfy

$$\left[ \frac{d^2}{dx^2} - k^2 - \frac{1}{F} \frac{d^2F}{dx^2} \right] \delta\psi = 0 \quad (10.3.67)$$

and

$$\delta\phi = \delta\psi/F. \quad (10.3.68)$$

The solution to (10.3.67) has a discontinuous derivative at the mode rational surface; therefore, the quantity

$$\frac{d\Delta}{dx} = \Delta' = \frac{d}{dx} (\ln \delta\psi) \Big|_{-\Delta}^{\Delta} \quad (10.3.69)$$

is used to characterize the current profile in linear tearing mode theory and is a measure of the available magnetic free energy which can be dissipated (Adler *et al.*, 1980).

In the resistive region,  $F(x) \approx x$  and  $\Delta'/\Delta \ll 1$ , if we assume the so called "constant  $\psi$ " approximation; then  $\delta\psi$  is roughly constant in magnitude across the resistive layer, although  $d\delta\psi/dx$  may change considerably. With this assumption, the following versions of (10.3.64) and (10.3.65), are applicable within the resistive layer;

$$\frac{\delta l \gamma^2 \tau_L^2}{x} \frac{d^2 \delta\phi}{dx^2} = - \frac{d^2 \delta\psi}{dx^2}, \quad (10.3.70)$$

and

$$\delta\psi(0) - \frac{x}{\delta l} \delta\phi = (\gamma \tau_L) + \frac{d^2 \delta\psi}{dx^2}. \quad (10.3.71)$$

Integrating (10.3.70) across the resistive layer from  $-\Delta$  to  $\Delta$ , we obtain

$$\frac{\delta l \gamma^2 \tau_L^2}{\delta\psi(0)} \int_{-\Delta}^{\Delta} \frac{d^2 \delta\phi}{dx^2} \frac{dx}{x} = - \Delta', \quad (10.3.72)$$

which must be matched at  $x = \pm\Delta$  to the ideal MHD solution of (10.3.67). Equation (10.3.72), together with the solutions to (10.3.70)-(10.3.71), yield the growth rate for "constant  $\psi$ " tearing modes in slab geometry:

$$\gamma = \left( \frac{\Gamma(1/4) \Delta' \delta l}{\pi \Gamma(4/5)} \right)^{4/5} \frac{S^{2/5}}{\tau_L}. \quad (10.3.73)$$

From (10.3.73), we see that instability occurs when  $\Delta' > 0$ , marginal stability when  $\Delta' = 0$ , and stability when  $\Delta' < 0$ . Hence, the tearing mode grows in such a way as to cause  $\Delta'$  to vanish. In physical terms, this instability causes the current density profile to be flattened as the width of magnetic island,  $W$ , increases, so that saturation occurs when  $W$  equals the thickness of the current channel,  $\delta l$ , as illustrated in Figure (10.15).

To illustrate how tearing modes lead to parallel electric induction fields, we express the perturbed electric field parallel to the magnetic field as

$$\delta E_{\parallel} = - \frac{\gamma \delta A_{\parallel}}{c} - ik_{\parallel} \delta\Phi, \quad (10.3.74)$$

where  $\delta A_{\parallel}$  is the perturbed component of the vector potential parallel to the equilibrium magnetic field and  $\delta\Phi$  is the perturbed electrostatic potential. Since  $\delta A_{\parallel} = \delta\psi \hat{e}_z$ , (10.3.74) becomes

$$\delta E_{\parallel} = -\gamma \frac{\delta\psi}{c} - ik_{\parallel} \delta\Phi. \quad (10.3.75)$$

The parallel induction field  $-\gamma \delta\psi/c$  causes the electrons to flow with a velocity  $\delta v_{\text{eff}}$ . However, because the induction field leads to charge separation between ions and electrons, a parallel electrostatic field  $-ik_{\parallel} \delta\Phi$  also is produced, which shorts out the induction field for sufficiently large  $k_{\parallel}$ , thus,  $\delta E_{\parallel} = 0$  except where  $k_{\parallel} \rightarrow 0$ , where  $\delta E_{\parallel} = -\gamma \delta\psi/c$ . Within the resistive layer, therefore large parallel electric fields are produced and particle acceleration can occur (Drake and Lee, 1977), only in the vicinity of  $k_{\parallel} = 0$ .

From both the qualitative and quantitative arguments presented, it is clear that the occurrence of either steady-state or dynamic reconnection, is determined by the nature of the flow field required in the presence of a dissipative boundary layer located at the mode rational surface. Thus, to evaluate the importance of reconnection, in solar phenomena the source of the flow field, or equivalently the free energy supply that produces the requisite flow field, must be identified. There are two possible sources of magnetic free energy: perpendicular and parallel currents. As is indicated by (10.2.2) reconnection can be driven by a perpendicular current,

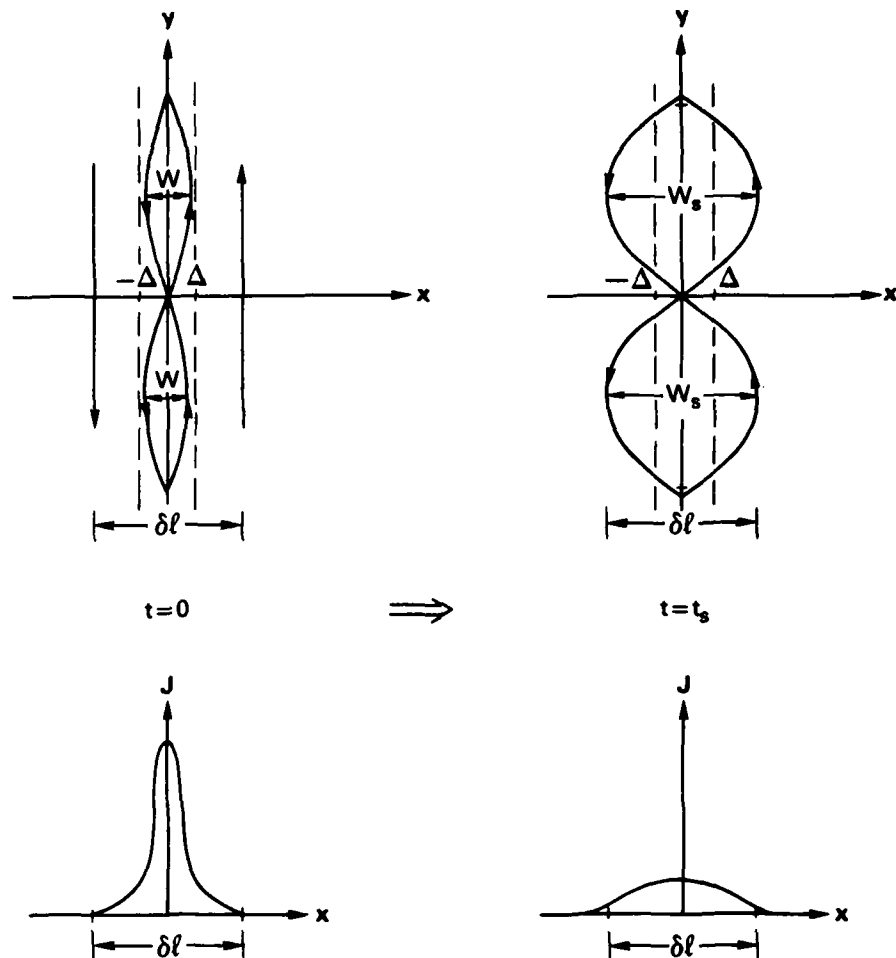


Figure 10.15 — Schematic of the evolution of the magnetic island width,  $W$ , relative to the resistance layer  $2\Delta$  thick. The evolution of the current profile is also schematically shown.

by means of either a pressure gradient or a flow field perpendicular to the magnetic field. With regard to flare energy requirements and magnetic energy storage it is impossible to explain a flare with energy stored in the form of an equilibrium pressure gradient, as can be proven by a simple estimate of the pressure required and how it would manifest itself observationally. Thus, for a flare to be initiated by  $J_{\parallel}$  driven reconnection, a tearing flow field must exist outside the reconnection region; if a flare were attributed to  $J_{\parallel}$ -driven reconnection in the corona, a tearing flow must exist in the corona just prior to and during the flare process. Various ways of achieving these flow fields have been proposed. The two sources of flow fields that are most common in flare theory are solar wind-driven, inverted- $Y$  neutral sheet theories (Carmichael, 1964; Sturrock, 1966b, 1967, 1972, 1974, 1980; Kopp and Pneumann, 1976) and the emerging-flux-driven flow field (Priest and Heyvaerts, 1974; Canfield *et al.* 1974; Heyvaerts *et al.* 1977; Tur and Priest, 1978; Krivsky, 1968).

A tearing flow field can be driven *indirectly* by a parallel current in several ways, and is the basis of the loop flare model of Spicer and Colgate (Spicer, 1975, 1976, 1977a, b, 1980, 1981a; Colgate, 1978; Sturrock, 1980). To illustrate  $J_{\parallel}$  driven reconnection recall that in §10.3.5 we noted that kink modes are driven by a parallel current. In particular consider the  $m = 1$  kink, which is uniquely a curvilinear effect that cannot occur in slab geometry. Assume as an *example* a diffuse pinch in cylindrical geometry, that all perturbed quantities vary as  $\exp i(m\theta + kz)$  and for simplicity that  $B_z \gg B_{\theta}(r)$ , with  $B_z$  independent of  $r$ . The perturbations are perpendicular to  $\mathbf{B}$  when  $\mathbf{k} \cdot \mathbf{B}_0 = kB_z + \frac{m}{r}B_{\theta}(r_s) = 0$ , so that the unstable  $m = 1$  kink is localized about the mode rational surface at  $r = r_s$ . Since  $B_z$  is independent of  $r$  and  $B_z \gg B_{\theta}$ , the wave number  $k \approx \frac{m}{r} \frac{B_{\theta}}{B_z} \ll \frac{m}{r}$ . This implies that the perturbation varies rapidly in  $\theta$  but slowly axially, so that the plasma motion is essentially two dimensional in the  $\theta - r$  plane. Consequently, perturbations in the axial magnetic field and velocity are negligible. Using the axial component of the curl of the perturbed momentum equation,

$$\gamma \left[ \frac{1}{r} \frac{\partial}{\partial r} (r\rho_0 \delta v_{\theta}) - \rho_0 i m \delta v_r \right] = \frac{1}{c} \left[ (\delta \mathbf{B} \cdot \nabla) \mathbf{J}_0 + (\mathbf{B}_0 \cdot \nabla) \delta \mathbf{J} - (\delta \mathbf{J} \cdot \nabla) \mathbf{B}_0 - (\mathbf{J}_0 \cdot \nabla) \delta \mathbf{B} \right], \quad (10.3.76)$$

where  $\gamma$  is the growth rate, and using the incompressibility condition  $\nabla \cdot \delta \mathbf{v} = 0$ , we find

$$\begin{aligned} & -\gamma \left[ -\frac{i}{r} \frac{\partial}{\partial r} \frac{r\rho_0}{m} \frac{\partial}{\partial r} (r \delta v_r) + i \rho_0 \frac{m}{r} \delta v_r \right] \\ & = \frac{1}{c} \left[ \delta B_r \frac{\partial J_{\theta z}}{\partial r} + \frac{i}{4\pi} c (\mathbf{k} \cdot \mathbf{B}_0) \left( \frac{i}{mr} \frac{\partial}{\partial r} \left[ r \frac{\partial}{\partial r} (r \delta B_r) \right] - i \frac{m}{r} \delta B_r \right) \right]. \end{aligned} \quad (10.3.77)$$

The dependence on  $\delta B_r$  is eliminated by using the relation

$$\nabla \times \delta \mathbf{E} = -\frac{1}{c} \frac{\partial \delta \mathbf{B}}{\partial t}, \quad (10.3.78)$$

together with Ohm's Law, in the ideal MHD approximation,

$$\delta \mathbf{E} + \frac{\delta \mathbf{v} \times \mathbf{B}_0}{c} = 0, \quad (10.3.79)$$

to find

$$\gamma \delta B_r = i \mathbf{k} \cdot \mathbf{B}_0 \delta v_r. \quad (10.3.80)$$

On insertion into (10.3.77), this yields

$$\frac{1}{r} \frac{\partial}{\partial r} \left( r^3 F \frac{\partial}{\partial r} (\delta v_r) \right) = (m^2 - 1) F \delta v_r + \gamma^2 r \frac{\partial \rho_0}{\partial r} \delta v_r, \quad (10.3.81)$$

where  $F = (\mathbf{k} \cdot \mathbf{B}_0)^2 + \rho \gamma^2$ . Equation (10.3.81) must be solved subject to the following boundary conditions:  $\delta v_r$  is well-behaved at  $r = 0$ , and  $\delta v_r$  is continuous across the external boundary (in a laboratory device,  $\delta v_r$  must vanish at the walls).

Near  $r = 0$ , (10.3.81) can be approximated by

$$\frac{\partial}{\partial r} \left( r^3 \frac{\partial \delta v_r}{\partial r} \right) = -r(1 - m^2) \delta v_r, \quad (10.3.82)$$

which has solutions of the form  $\delta v_r \sim r^n$  for  $n = -1 \pm m$ . For  $|m| \geq 2$ , one root yields a well-behaved solution,  $\delta v_r = 0$  at  $r = 0$ , the other root does not provide a well-behaved solution. Hence, the center of the plasma does not move for  $|m| \geq 2$  modes.

For the  $m = \pm 1$  modes, the well-behaved solution for  $\delta v_r$  is  $\delta v_r = \text{constant}$  at  $r = 0$ , which implies that the center of the plasma is displaced. Near  $r = 0$ ,  $\delta v_r$  is proportional to  $\cos(\pm \theta + kz)$  (the real part of  $\exp[i(m\theta + kz)]$ ), so that  $\delta v_r$  changes direction as the perturbation is followed axially. Hence, the  $m = 1$  kink is a rigid helical displacement of the center of the plasma which does not bend the field lines. A helical displacement consists of a finite displacement  $\Delta r$  of the fluid from  $r = 0$  plus a rotation; the basic motion of a kink, therefore, consists of a rigid displacement in the  $r - \theta$  plane coupled to rapid flow about  $r_s$  in the  $\theta$  direction. Such a flow represents a radial flow that develops a  $\theta$  component as it bounces off a stationary fluid and that rotates as a function of  $z$  (Figure 10.16). A comparison of the kink flow field with the tearing flow field shows that both flows are essentially equivalent (see Figure 10.13). Thus, the magnetic energy stored in the parallel current can drive tearing flow in the form of a  $m = 1$  kink perpendicular to the magnetic flux surfaces, which appears as large perpendicular currents. In the ideal-MHD picture these large perpendicular currents could generate large restoring forces which could stabilize the system. If finite dissipation is permitted, however, the perpendicular currents can be dissipated and reconnection can occur via an  $m = 1$  tearing mode. The above discussion qualitatively demonstrates how a parallel current drives reconnection in a cylindrical diffuse pinch; analytical proofs can be found in Coppi *et al.*, (1976) and Drake (1978). In general, we can state that certain MHD motions can lead to reconnection.

As is noted earlier, the gradient in the current density provides the driving energy of the kink. To prove this, and also to prove that the same driving energy is the source of energy that drives the tearing mode (or the resistive kink as it is sometimes called), we multiply (10.3.77) by  $i \delta v_r^*, r/m$  and integrate over the plasma volume to obtain

$$2\pi\gamma \int_0^a r dr \left[ \rho_0 (\delta v_r^2 + \delta v_\theta^2) + \frac{1}{4\pi} (\delta B_r^2 + \delta B_\theta^2) \right] = -2\pi\gamma \int_0^a \frac{r dr}{mc(\mathbf{k} \cdot \mathbf{B})} \frac{d J_{z0}}{dr} \delta B_r^2, \quad (10.3.83)$$

where the second derivative is integrated by parts, the incompressibility condition is assumed, the end-point contributions are neglected, and  $a$  denotes the outer-boundary radius of the configuration. The LHS of (10.3.83) is positive definite and represents (through the multiplicative factor  $\gamma$ ) the rate of change of perturbed kinetic plus magnetic energy, while the RHS represents a possible driving term for instability if the product  $H = (\mathbf{k} \cdot \mathbf{B}_0)^{-1} \frac{d J_{z0}}{dr}$  is negative.

This result does not depend on the resistivity, thus demonstrating that the parameter  $H$  determines stability, and that the sign and the slope of the gradient of the parallel current density are crucial in determining kink stability. A more elegant proof of this statement can be found in Adler *et al.* (1980).

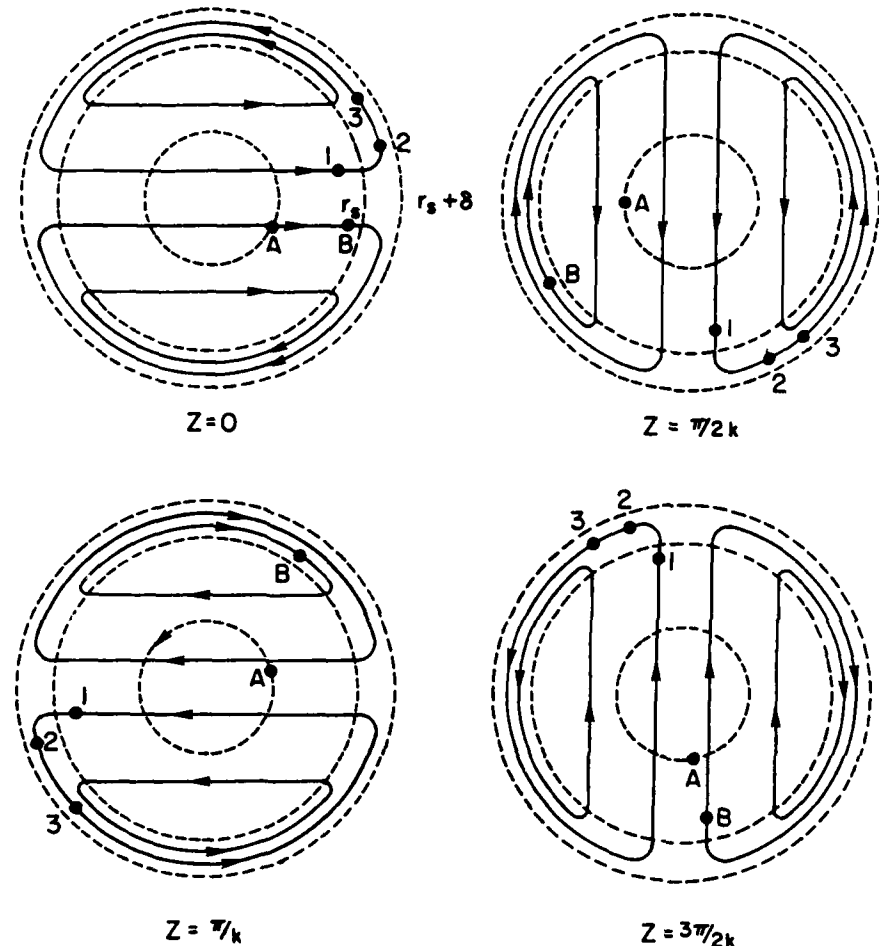


Figure 10.16 — A two dimensional schematic of the magnetic field produced in the  $r - \theta$  plane at different axial positions by an  $m = 1$  kink driven tearing flow (after Manheimer, 1979b)

From the above discussions it is clear that reconnection only occurs when a plasma-magnetic field configuration is stable to tearing flow in the ideal MHD approximation; if it is unstable to tearing flow, ideal MHD motions lower the magnetic energy by expansion. For example, a cylindrically symmetric diffuse pinch may be stable to  $m = 1$  tearing flow in the ideal MHD approximation, while a toroidal diffuse pinch may be unstable to the same flow. Hence,  $m = 1$  reconnection may occur in a cylindrical diffuse pinch but not in a toroidal diffuse pinch simply because the toroidal system is able to lower its energy by expansion.

A more subtle conclusion from our discussions, which is related to the problem of electrodynamic coupling of the solar atmosphere, is that tearing flow is a means by which a parallel current can drive a perpendicular current across field lines. In this way, tearing flow can cause neighboring anti-parallel currents to link via a perpendicular current and essentially short-circuit the current system and in the process lower the total inductance of the current system. In terms of an equivalent-circuit (*cf.* §10.2), reconnection causes a time rate of change of the inductance  $L$ ,  $\dot{L}$ , which then enters the equivalent-circuit equations as an effective impedance term that can be much larger than the initial impedance of the circuit. The time rate of change of  $L$  can be approximated in the linear growth regime by  $\gamma L$ , where  $\gamma$  is the growth rate of the tearing mode. If  $\gamma L \gg R$ , the time constant of the circuit is determined by  $\dot{L}$ , because the  $L/R$  time of the circuit can be radically reduced by an  $\dot{L}$  term. Hence, the rate at which reconnection occurs can greatly affect the response of the global current system to reconnection.

As is shown earlier the growth rate of a "constant  $\psi$ " tearing mode is characterized by the magnetic Reynolds number,  $S$ . The linear growth rate for any tearing mode can be written as

$$\gamma = \alpha_1 S^p / \tau_L, \quad (10.3.84)$$

where  $\alpha_1$  is proportional to the driving energy of the tearing mode evaluated at the mode rational surface, and  $p$  is always less than unity and is mode dependent. For example, we compare the growth rate of a typical tearing mode in slab geometry, given by (10.3.73), with that of an  $m = 1$  tearing mode (cylindrical geometry), given by the following expression (Coppi *et al.*, 1976; Drake, 1978):

$$\gamma = \left( r_s \frac{dq}{dr} \bigg|_{r_s} \right)^{2/3} \frac{S^{2/3}}{\tau_L}. \quad (10.3.85)$$

The  $m = 1$  tearing mode has a rate of growth  $\sim S^{4/15}$  greater than a slab tearing mode, that is,  $\approx 400$  times greater if  $S \sim 10^{10}$ . The difference in linear growth rates also is manifested in radically different non-linear evolution. These differences are attributable to the "constant  $\psi$ " approximation, which is typically assumed in linear analysis of the tearing mode. The "constant  $\psi$ " approximation originates in the neglect of the inertial contribution to (10.3.61), which is equivalent to assuming that the perturbed plasma is in MHD equilibrium away from the mode rational surface. The growth time of the tearing mode thus is required to be large compared to the time required to achieve pressure balance by shocks or magnetosonic waves. Hence, neglecting the inertia term implies that pressure balance must be assured at all times, in the region outside the mode rational surface. Conversely, inclusion of the inertial term implies that pressure balance is not achieved in the region outside the mode rational surface. Tearing modes for which the inertial term must be included are called "fast" or "non-constant  $\psi$ " tearing modes. Fast tearing modes include the  $m = 1$  and double tearing modes (e.g., Coppi *et al.*, 1976; Drake, 1978; Pritchett *et al.* 1980; Schnack and Killeen, 1977, 1979) and were first applied to loop models of flares by Spicer (1976, 1977, 1981a). Tearing modes for which the inertial term can be neglected are called "slow" or "constant  $\psi$ " tearing modes, and were first applied to flares by Jaggi (1964) and Sturrock (1966, 1967, 1972, 1974). The terminology "non-constant  $\psi$ " or "constant  $\psi$ " corresponds to the fact that  $\delta\psi$  may vary greatly or very little, respectively within the boundary layers.

Analysis (Pritchett *et al.*, 1980) shows that the growth time of the fast tearing mode,  $\gamma_f^{-1}$ , is equal to the diffusion time (sometimes called the skin time) associated with the boundary layer; that is,

$$\gamma_f^{-1} = \frac{4\pi\Delta^2}{\eta c^2}. \quad (10.3.87)$$

The growth time of the slow tearing mode,  $\gamma_s^{-1}$ , on the other hand, is much greater than the diffusion time of the layer. Consequently, the flux perturbations generated by slow tearing modes have time to communicate across the boundary layer during their growth so the  $\delta\psi$  remains roughly constant, while the flux perturbations generated by the fast tearing modes occur to rapidly to communicate across the layer so that  $\delta\psi$  varies radically throughout. This result has important implications for flares because the electric fields, parallel to the magnetic field at the  $X$  points,  $\delta E_{\parallel}$ , induced by the fast tearing process do not have time to penetrate into the magnetic islands produced by the tearing process (see below), so that the plasma volume accelerated by  $\delta E_{\parallel}$  remains the same as that produced by a slow tearing mode in the linear regime. On the other hand, the  $\delta E_{\parallel}$  produced by a slow mode has sufficient time to penetrate into the islands, causing  $\delta E_{\parallel}$  to weaken as the magnetic island widens.

The non-linear evolution of fast tearing modes also differs radically from that of slow modes. Rutherford (1973) showed that exponential growth of the slow tearing mode changes, in the non-linear regime, to algebraic growth; the width of the magnetic island generated by the slow tearing processes,  $W$ , remains constant in time after  $W$  exceeds the resistive boundary-layer width,  $\Delta$ . However, the widths of the magnetic islands generated by fast tearing modes grow exponentially until saturation (Waddell *et al.* 1976; Schnack and Killeen, 1977, 1979). This result was used by Spicer (1981a) to estimate the heating rates and electric induction fields generated by a fast tearing mode.

For both fast and slow tearing modes electric induction fields estimated using *solar parameters* always exceed the Dreicer electric field defined by (10.3.17). Estimates of parallel electric fields generated by slow tearing modes (Van Hoven, 1979) indicate that the predicted electric field is  $\sim 3$  times the Dreicer field, while estimates of the parallel electric field from a fast tearing mode (Spicer, 1981a) always exceeded the Dreicer field by orders of magnitude if the saturated value of the electric field is assumed. The physical basis for these results appears to be as follows: since solar current systems are inductively dominated, due to the large solar diffusion times, the current will attempt to remain constant; at the same time, the small resistive skin depth, characteristic of a solar plasma constrains the electric induction field to small channels about the  $X$ -points. These two effects together require the electric fields to be large. Collision dominated tearing modes thus may develop into semi-collisionless or collisionless tearing modes (Drake and Lee, 1977) and  $J_{\parallel}$ -driven anomalous resistivity may be produced, thereby altering the local non-linear evolution of the tearing mode even further (Spicer, 1981a).

Returning to the growth rate defined by (10.3.73) or (10.3.85) note that  $\gamma$  is defined entirely in terms of *local* quantities, which is not too surprising since the linear growth rate of a boundary-layer instability is not affected greatly by global conditions. However, the global configuration is expected to dominate the non-linear evolution of the instability, even through local effects may dictate local dissipation rates that influence the global evolution. Further, because reconnection is a boundary-layer phenomenon, the standard conservation jump relationships must apply and mass flux, magnetic flux, and energy flux are conserved through the layer (Parker, 1963). Thus, although the dissipation process is localized to a thin layer, the global conservation relations are preserved. The non-linear evolution of the reconnection process must be consistent with global conditions, therefore, and the entire global current system ultimately determines the evolution of the reconnection process. We further emphasize, that

because the inductive properties of a laboratory plasma-magnetic field configuration with a magnetic Reynolds number of  $10^4$  differ radially from those of a typical solar Reynolds number  $\sim 10^{10}\text{-}10^{12}$ , comparisons between solar plasma and laboratory experiments or numerical simulations with low  $S$  only represent useful guides.

Before proceeding to non-linear effects of potential importance in solar phenomena, we present a brief comparison between steady-state reconnection and the  $m = 1$  tearing mode, which is the only tearing mode that can be compared to the standard single  $X$  point, steady-state reconnection theories. Previous theoretical work in the area of steady-state reconnection has been aimed primarily at understanding reconnection in standard neutral sheets or in neutral sheets with a component of the magnetic field parallel to the current sheet (cf. Vasylunas, 1975, for a review). The fastest steady-state reconnection rate derived to date was found by Petschek (1964), from an analysis assuming steady-state tearing flow, one  $X$ -point and one 0 point split into two halves each placed at  $\pm L$ , where  $L$  is the length of the sheet. Petschek found that steady-state reconnection depends logarithmically on the resistivity, which differs from the Sweet-Parker form of reconnection (Sweet, 1958; Parker, 1963) because Petschek accounted for the role of hydrodynamic waves in removing energy downstream from the  $X$ -point. The curvilinear tearing flow that most closely approximates the Petschek flow is the  $m = 1$  tearing mode in cylindrical or toroidal geometry, as can be seen by topologically bending the neutral sheet at the  $X$  point and matching the two halves of the 0 point at  $\pm L$  together. The similarity between the  $m = 1$  tearing mode and the Petschek flow is also reflected in the growth rate of the  $m = 1$  tearing mode, given by (10.3.85); the physical origin of this relationship is that an  $m = 1$  tearing mode essentially is *driven* by the tearing flow caused by motion of an  $m = 1$  ideal MHD kink mode.

#### 10.3.5.3 Non-Linear Effects Associated with Reconnection

In the previous discussions, we have considered only one tearing layer. However, a number of non-linear effects can result from the interaction of tearing modes and in principle, can greatly enhance the rate at which reconnection occurs in solar flares (Spicer, 1976, 1977a,b; 1981b): multiple tearing modes, mode coupling, magnetic braiding, and island coalescence.

Multiple tearing modes occur when more than one unstable mode-rational surface, with the same mode wave number  $\mathbf{k}$ , are juxtaposed in a magnetized plasma. As each unstable tearing layer grows, the physical interaction with each unstable neighbor sets up a tearing flow pattern that drives new magnetic flux into the  $X$  points of the neighboring layers. In a similar manner, the adjacent unstable layer drives new flux into the  $X$ -points of its neighbors, and so on. These tearing flow patterns result in a violation of the "constant  $\psi$ " approximation and are characterized by a growth rate identical to (10.3.85) because the MHD region between the unstable layers is not in pressure balance. Multiple tearing modes most probably occur in magnetic configurations with anti-parallel currents, as occurs in force free magnetic fields. Non-linear simulations of double tearing modes have been performed by Cross and Van Hoven (1973), White *et al.* (1977) and Schnack and Killeen (1977, 1979), while linear analyses have been performed by Furth *et al.* (1973) and Pritchett *et al.* (1980).

The non-linear coupling of tearing modes with incommensurate  $\mathbf{k}$ 's is primarily a three-dimensional phenomenon and presently is amenable only to three-dimensional numerical simulation (Waddell *et al.* 1979; Carreras *et al.* 1979, 1980, 1981) or to analytical treatments with very simplifying assumptions (Satya and Schmidt, 1979); furthermore, the results are only valid for tokamak-like conditions and low Reynolds numbers. Nevertheless they do demonstrate the fundamental point: different tearing modes non-linearly destabilize other tearing modes on a rapid time scale (2-3 times faster than a single tearing mode) and greatly alter the transport

processes within the magnetic configuration. In this way, inductively-stored magnetic energy may be rapidly converted into flare-associated convection, Joule heating and accelerated particles, as proposed by Spicer (1976, 1977a).

Magnetic braiding, also due to the coupling of different tearing modes with incommensurate  $\mathbf{k}$ 's, induces large magnetic fluctuations, which, in the presence of large electron mobility parallel to  $\mathbf{B}$ , cause an anomalously large electron viscosity and thus anomalously large electron thermal conductivity perpendicular to  $\mathbf{B}$  (Rechester and Stix, 1976; Rechester and Rosenbluth, 1978). The effects of this anomalously large electron viscosity, which is due to high-harmonic secondary magnetic islands smearing the current-density profile around the neutral points of the primary islands, on the non-linear growth of the incommensurate tearing modes have been investigated by Kaw *et al.* (1979). For low magnetic Reynolds numbers they found that tearing mode growth can be increased dramatically. As noted by Spicer (1976, 1977a), these effects can be particularly important under solar conditions because the large solar scale sizes can produce close spacing of the incommensurate modes. In addition, small changes in the electron viscosity can lead to significant changes in the growth rates of the tearing modes, because of the high solar Reynolds numbers.

In the above discussions, we have outlined the evolution of a plasma-magnetic field configuration that is initially tearing unstable and then evolves until saturation, at which time a chain of magnetic islands is fully developed. Because each island represents a current filament, with current flowing in the same direction, they attract one another. Furthermore, an equilibrium is established because each island feels equal and opposite attractive forces from its counter parts on either side. However, if one of the islands is displaced towards the right for example, the islands to the right of the displaced island feel a greater attractive force to those on the left of the displaced one. As the displaced island begins to move towards its neighbor to the right, however, the magnetic flux between the two islands is compressed; the local magnetic pressure thus is increased, forcing the islands apart. If the compression force is dominant, the plasma is stable, whereas if the attraction force is dominant, the islands coalesce. Finn and Kaw (1977) first examined this phenomenon and found that the attractive force is dominant and the islands coalesce. Pritchett and Wu (1979) simulated this effect in the ideal-MHD approximation, and found that compression ultimately stops the island coalescence when the magnetic pressure becomes sufficiently large. However, when finite resistivity is permitted coalescence proceeds to completion. Spicer (1976, 1977a) has used island coalescence to explain a class of impulsive electromagnetic bursts associated with flares.

The above synopsis of non-linear effects in the reconnection process clearly illustrates that the reconnection process can be quite complex, unlike the simple reconnection theories sometimes applied to solar phenomena. The lack of high symmetry in solar magnetic-field configurations strongly suggests that these non-linear effects should occur whenever reconnection occurs in solar plasmas.

#### 10.3.6 Which Dissipation Mechanism Will Prevail?

As noted in the introduction to this section, the most controversial aspect of flare theory is choosing *one* of the mechanisms reviewed as the explanation for the sudden release of magnetic energy. This controversy is unwarranted, however. Studies of both laboratory and near-earth space plasmas have shown that the normal situation in an unstable magnetized plasma is for many instabilities to be operating simultaneously. For example, an MHD instability, such as a kinking prominence, may drive a shock in front of it. If this shock is associated with  $J_\parallel$ -driven anomalous transport mechanisms (Davidson and Krall, 1977), a highly anisotropic perpendicular and parallel temperature ratio can be produced, thus leading to excitation of various loss cone mechanisms (Spicer, 1976). As a second example, a constant net current

flowing in a loop may excite the superheating instability, which steepens the current density gradient (cf. §10.4), thus exciting a  $m = 1$  ideal or resistive kink; the resultant kink may drive large perpendicular and parallel currents, both of which can induce anomalous resistivity mechanisms, and so on (Spicer 1976). These examples illustrate that the flare process is quite complex, simultaneously involving many instabilities and requiring a careful examination of how each process can either excite or interact with another to produce a flare. While this view may appear self-evident, the reader is forewarned that the view that a single instability is the cause of the flare still exists (cf. Van Hoven, 1981).

Despite the aforementioned complexity of the flare problem, we can attempt to identify which of the three instabilities reviewed is most likely to occur first. In the case of  $J_1$ -driven reconnection and anomalous transport, this question can be answered, in part. If the flow field initially convects new magnetic flux towards the mode rational surface faster than it can be dissipated by a tearing mode, the current steepens until  $J_1$ -driven anomalous resistivity mechanisms are excited and dissipate the current buildup. However, if the new flux initially is convected at a rate less than the tearing mode dissipation rate, the current is dissipated by the reconnection process itself and anomalous resistivity is unlikely to occur, except possibly through the induced electric field associated with the reconnection.

In the case of  $J_{||}$ -driven mechanisms, the current density or the current-density profile is the important threshold criterion for excitation of double layers, anomalous resistivity, or MHD processes (ideal or resistive). To determine which MHD process occurs first, a full understanding of the *global three-dimensional* current system is required — not an easy task. It is generally believed that MHD processes precede double layers or anomalous resistivity mechanisms (Van Hoven, 1981). However, the universal applicability of this belief is questionable, because MHD processes are very geometry dependent. Furthermore, the Birkeland current system clearly contradicts the view that MHD processes precede the double-layer or anomalous resistivity mechanisms. The Birkeland current is MHD stable and is made up of parallel currents, flowing along the potential magnetic field of the earth, that are capable of driving anomalous resistivity mechanisms or double layers (Wolf, 1975). Hence, it is not at all obvious which  $J_{||}$ -driven mechanism occurs first. The reader should be particularly cautious therefore in accepting arguments for or against a specific  $J_{||}$ -driven mechanism, until our understanding of the *three-dimensional* MHD stability of solar configurations has been greatly improved (cf. §10.2.2.2).

#### 10.4 THE PREFLARE STATE AND FLARE TRIGGERS

Flare models have assumed, historically, that a flare instability must be excited by some external perturbation or "trigger" (cf. Sturrock, 1966; Sweet 1969, Van Hoven *et al.*, 1980; Spicer and Brown, 1981), as opposed to directly driving the flare, *e.g.*, by externally applied flow fields (Heyvaerts *et al.*, 1977). Sturrock (1966) has noted that there are two basic types of instability onsets: "explosive" or "non-explosive." The explosive onset occurs when a system is near marginal stability, and is linearly stable to infinitesimal perturbations but non-linearly unstable to finite perturbations. Conversely, non-explosive onsets occur when a system is linearly unstable to infinitesimal perturbations. Sturrock also contended that only instabilities with explosive onsets are viable as flare mechanisms. This point of view is justified as follows: for preflare storage of energy to occur, energy must accumulate in the plasma-magnetic field configuration without being dissipated continuously through instabilities excited by infinitesimal perturbations; rather, the energy must accumulate up to some level beyond which a finite perturbation can drive the configuration to instability, thus releasing the accumulated energy.

We reviewed three mechanisms, in §10.3, two of which can be driven directly by both  $J_1$  or  $J_{||}$ : reconnection and anomalous Joule heating. We also argued that  $J_1$  driven mechanisms

require externally imposed flow fields. Hence,  $J_{\parallel}$ -driven mechanisms do not require triggers and are excited directly once the flow field exceeds the necessary speeds. However,  $J_{\perp}$ -driven mechanisms can be either driven directly or triggered. A directly-driven  $J_{\perp}$  mechanism can result from the natural evolution of the current profile that accompanies the time-dependent, preflare magnetic-energy storage process. Conversely, a  $J_{\perp}$ -driven mechanism may be initiated by a trigger that leads to an alteration of the current profile even after the maximum amount of magnetic energy has been stored. Nevertheless, because the preflare magnetic energy storage processes apparently occur in times much greater than a MHD transit time (cf. §10.2.2.1 and §10.2.2.2), the preflare state can be examined under the assumption of a quasi-equilibrium. As discussed in §10.2.2.2, various authors have utilized this approach. Others have assumed the preflare magnetic configuration slowly stores energy during its evolution, until the configuration is on the verge of losing its quasi-equilibrium (Jockers, 1976; Low, 1977; Anzer, 1978; Birn *et al.* 1978; Heyvaerts *et al.* 1979; Priest and Milne, 1979; Hood and Priest, 1980). This approach is related to bifurcation theory: as the relevant parameters are varied, there is a point of bifurcation at which the equilibrium either can go unstable or can enter a more stable regime. This approach is more realistic than the stability approach reviewed in §10.2.2.2, primarily because the treatments usually involve more than one dimension and allow for global electrodynamic coupling, to a certain degree, through more reasonable boundary conditions. However, the approach is limited, at present, because all analyses have utilized some symmetry condition to reduce the extreme mathematical complexity of the problem, which has the unfortunate consequence of removing the degrees of freedom available to the magnetic configuration for lowering its energy state. In addition, these analyses do not account for transport phenomena which, in real magnetized plasmas, help control the evolution of the existing current profiles. For example, preflare magnetic energy storage involves induction currents and, as noted in §10.2, these induction currents may flow in very narrow channels. Thus, the current profile is dictated, in part, by the resistivity profile in the magnetized plasma, as well as the resistivity profile at the boundaries.

Accounting for the aforementioned transport effects naturally leads to examination of the role of thermal instabilities in altering the current profile, and thus in triggering a flare. Thermal instabilities were studied first by Parker (1953) and Field (1965), while Sweet (1969) and Kahler and Kreplin (1970) first pointed out the importance of thermal instabilities in flares. Thermal instabilities ensue when thermal conduction is reduced, or is prevented from removing any input of energy or replacing any decrease of energy in the presence of a strongly temperature dependent radiation function such as occurs in plasmas with solar abundances. In a magnetized plasma, this process corresponds to preventing thermal conduction parallel to the magnetic field and can be accomplished by a long-wavelength perturbation parallel to the magnetic field.

The electromagnetic superheating (overheating) instability (Kadomtsev, 1966), which is a thermal instability applicable to both neutral sheets and *sheared* magnetic fields, may be particularly important for triggering flares, and has been utilized in several flare models (Coppi and Friedland, 1971; Heyvaerts, 1974a; Coppi, 1975; Spicer, 1976, 1977a). The superheating instability requires a current flowing parallel to a magnetic field, driven by a parallel, roughly equipotential, electric field that may differ in strength on different field lines. Thus, because  $J_{\parallel} = E_{\parallel}/\eta$  and  $E \cdot J = E^2/\eta$  any perturbation that yields an increase in temperature will reduce  $\eta$ , increase  $J_{\parallel}$ , then the temperature again and so on. This process then results in an increase of both the current density and the temperature. For a cylindrically symmetric diffuse pinch with an equilibrium magnetic field  $\mathbf{B}_0 = (0, B_a(r), B_z(r))$ , the superheating instability is localized about mode rational surfaces, for which  $\mathbf{k} \cdot \mathbf{B}_0 = 0$ , because the first-order perturbation to the divergence of the heat flux, vanishes there. The superheating instability will occur if

$$\frac{J_0 \eta_0}{n_0 k_b T_0} > - \frac{3}{2 n_0 k_b} \frac{dQ_R}{dT_0}, \quad (10.4.1)$$

where the subscript "0" specifies the equilibrium quantities, and  $Q_K$ , the radiation loss function. Hence, if  $dQ_R/dT_0 < 0$  and (10.4.1) is satisfied, this instability occurs. The superheating instability is physically manifested in the form of plasma striations, composed of long wavelength filaments parallel to the magnetic field with high current density and temperature, alternating with filaments of low current density and temperature.

In the context of flare theory, the superheating instability is important because it promotes buildup of the current-density in locations where  $\mathbf{k} \cdot \mathbf{B}_0 = 0$ , while a tearing mode attempts to flatten the localized current-density profile. In other words, these mechanisms work in opposition to one another and, possibly, a non-linear balance may be achieved between the two competing instabilities. Thus steady-state reconnection may occur in sheared fields, but only if cross-field transport does not limit the further growth of the superheating instability before a tearing instability occurs. The current density rises with a characteristic e-folding time,  $t_{SH}$ , and then becomes unstable to a tearing mode with growth time  $t_T$ . If  $t_{SH} < t_T$ , the tearing mode does not have time to develop, and the current-density profile continues to steepen until the current density is sufficiently large to excite a tearing mode of growth time  $t_T < t_{SH}$ . At this time, either the tearing mode completely flattens the current profile before the superheating instability can raise the current density again, or the two instabilities evolve towards a state of marginal stability so that steady-state reconnection can occur. At present, the superheating instability only has been treated in the local approximation, analogous to the manner in which the stability analysis of loops has been treated locally (cf. §10.2.2.2), and no accounting for the role of global electrodynamic coupling has been given.

Chiuderi and Van Hoven (1979) have treated thermal cooling instabilities in sheared magnetic configurations, using the local approximation as described in §10.2.2.2. They allow for a generalized heating function and only treat the stability of the energy equation. Because their treatment does not include electromagnetic effects and Joule heating, the superheating instability does not appear. Nevertheless, they contend that thermal cooling instabilities at the mode rational surface induces triggering of tearing modes because the temperature drop increases the resistivity precipitously. However, this argument is questionable, because their analysis is incapable of comparing the growth rate of the cooling instability with that of the superheating instability. Such a comparison shows that, for current densities typically required to explain a flare by tearing modes, the growth rate of the superheating instability is largest. In addition, an examination of tearing mode growth rates shows that the tearing mode growth rate is more sensitive to higher current densities, as would be generated by the superheating instability, than to a higher resistivity which tends to smooth out the current profile thereby reducing the tearing mode growth rate.

Various triggers for  $J_{||}$ -driven double layers, and also for anomalous Joule heating mechanisms, are discussed by Carlqvist (1979b). Since a double layer is driven by a high-inductance current system and requires a current drift speed of  $\geq v_{Te}$  (cf. §10.3.2), local reduction in the density provides the basic trigger of a double layer. The triggering results from the requirement of a temporally-constant net current; the current drift speed must increase, in the presence of a density decrease, sufficiently to keep the current constant. According to Carlqvist (1979b), this density reduction may occur in several ways. The most promising method for reducing the density in the quasi-equilibrium loop is by localizing heating, which causes both *hydromagnetic* expansion perpendicular to the magnetic field and *hydrodynamic* expansion parallel to the magnetic field. The requisite heating could be generated by the superheating instability, the tearing mode, or anomalous Joule heating resulting from a  $J_{||}$ -driven anomalous resistivity mechanism with a much lower threshold than a double layer, e.g., the electrostatic ion-cyclotron instability (cf. Kindel and Kennel, 1970). Since hydrodynamic expansion parallel to the magnetic field results in a constant pressure along the field lines (neglecting gravity), an increase in temperature of 10-100 causes the density to be reduced by a corresponding amount. Hence, an

initial current drift speed of  $\sim 5 \times 10^5$  cm/s results in an increase in the drift speed to  $5 \times 10^6$  –  $5 \times 10^7$  cm/s, sufficient to trigger a double layer.

An alternate trigger for a double layer can occur in a high inductance parallel current system, as in an emerging flux loop. As the flux loop expands, the density drops until the drift speed of the current exceeds threshold for either an anomalous Joule heating mechanism or a double layer. For this triggering mechanism to apply, the net current cannot change appreciably during the expansion process.

Other effects which may be important as trigger mechanisms, and which have not been examined in the context of solar flares, as yet, are:

(1) Investigations by Dobrott *et al.* (1977) and Pollard and Taylor (1979) have shown that equilibrium diffusion flows have an important effect on the stability of a magnetic configuration to tearing modes.

(2) Lau and Liu (1980) have examined the stability of shear flow in a magnetized plasma slab. They found that velocity shear alone cannot produce a MHD instability that qualitatively alters the initial laminar state of the plasma. However, they suggest that a small amount of magnetic field curvature, such as occurs in solar configurations, may reverse this conclusion.

## 10.5 MAGNETIC ENERGY STORAGE AND CONVERSION: FUTURE RESEARCH

In the previous sections, we reviewed various problems associated with magnetic energy storage and conversion. How should we proceed, in the future, if we intend to solve these problems? The most serious problem which must be addressed forthwith, is to identify the site where magnetic energy, believed to be the free energy supply of the flare, is stored; this task is of particular importance, because the storage location strongly controls the initial conditions imposed on any given conversion mechanism. In accord with the arguments presented in §10.2.2.4 and §10.3, we contend that the flare energy must be stored in the *low* atmosphere, either in the photosphere or in the low chromosphere; that the flare originates *low* in the atmosphere; and that either the PMFC associated with the energy storage rises to higher altitudes as the energy conversion proceeds, thus appearing as a coronal event, or the current within the PMFC is somehow shunted from a photospheric path into a coronal path, e.g., by the topological changes in the current path attributable to reconnection. These conclusions are based, in part, on the extreme constraints imposed by flare energy requirements on the net current necessary to explain a flare ( $\geq 10^{22}$  stat amps), and on the extreme limitations imposed by conversion mechanisms on the current densities and/or current density gradients necessarily associated with the net currents (*cf.* §10.2.2). It is difficult to believe that *non-potential* magnetic fields associated with net currents of  $\geq 10^{22}$  stat-amps, as well as the strong magnetic-field gradients associated with the high current densities and/or current-density gradients required by the relevant conversion mechanisms, can exist anywhere in the corona in any semblance of a steady state; pressure balance is extremely difficult to achieve under these circumstances and the Virial theorem requires external stresses even if the currents are force free. Hence, storage of sufficient magnetic energy to power a solar flare *must* occur in the low atmosphere, where the substantial fluid pressures can support the large non-potential magnetic fields required by flare theory. If this conclusion is correct then the traditional view (*cf.* §10.2.2 and Van Hoven *et al.*, 1980), which assumes coronal flare-energy storage, is incorrect, and a thorough re-examination of pre-flare magnetic energy storage must begin. Furthermore, the assumption that energy is stored *in situ* must be abandoned in favor of a *remote* storage site.

A second fundamental problem is the lack of a fully self-consistent treatment of the global electrodynamic coupling characterizing a current system in the presence of an actual conversion mechanism under solar conditions. Even the studies of  $J_{\parallel}$ -driven anomalous Joule heating

by Spicer and Manheimer (1982), which utilize a 1-D hydrodynamic code coupled to an equivalent circuit representing the inductive properties of a co-axial current carrying solar loop, do not account for the local changes in the current circuit resulting from a sudden, localized onset of anomalous resistivity within the global circuit. Furthermore, existing analyses of reconnection and the subsequent partitioning of annihilated magnetic free energy into kinetic and thermal energies have utilized boundary conditions which are quite unrealistic for the solar phenomena under consideration, such as the periodic boundary conditions with low Reynolds numbers ( $S \geq 10^2$ ) used by Van Hoven and Cross (1973), or the "hard wall" boundary conditions applied to Tokamaks by Schnack and Killeen (1978). In addition, no studies, as yet, have accounted for the feedback between the global circuit and the reconnection process. Thus, the results reported to date should be considered with caution.

A third problem of pertinent interest involves the efficiency and location of current generators (or MHD dynamos) which convert flow energy into the electrodynamic energy eventually manifested as a flare. Future investigations also should attempt to ascertain what observable manifestations might be produced by these current generators, in order to develop a preflare predictive capability.

In summary, a wealth of complex and critical difficulties remain in theoretical treatments of magnetic energy storage and conversion in the context of solar physics, which must be carefully examined without pre-existing prejudices. Most theoretical and experimental efforts in the area of magnetic energy storage and conversion have been tainted, heretofore by strong subjective biases, thus producing investigations aimed more at confirming pet ideas than at seeking the truth. If the puzzling phenomena of magnetic energy storage and conversion in the solar atmosphere are ever to be understood, then both theoreticians (including the author) and experimentalists must avoid the overly simplified, highly qualitative, and over-intuitive "cartoon pictures" that presently infest the solar physics literature, and confront these challenging problems in a physically realistic manner.

#### ACKNOWLEDGMENTS

The author appreciates useful comments, criticisms, and discussions, concerning various topics reviewed in the manuscript, with Drs. D. Book, J.F. Drake, J. Feddars, J. Guillory, W. Manheimer, P. Palmadesso and R.A. Smith. The author also would like to make special thanks to Dr. J. Karpen for comments, criticisms, and excellent editing of the manuscript. Special thanks also goes to Joyce Brown and Lori Sizemore who typed the many drafts of the manuscript.

The author is supported, in part, by a grant from the National Aeronautics and Space Administration (Office of University Affairs).

#### REFERENCES

- Adler, E.A., Kulsrud, R.M. and White, R.B.: 1980, *Phys. Fluids* 23, 1375.
- Alfvén, H. and Carlqvist, P.: 1967, *Solar Phys.* 1, 220.
- Alfvén, H.: 1977, *Rev. of Geophysics and Space Physics* 15, 271.
- Anzer, U.: 1968, *Solar Phys.* 3, 298.
- Anzer, U.: 1978, *Solar Phys.* 57, 111.
- Barbosa, D.D.: 1978, *Solar Phys.* 56, 55.
- Barnes, C.W. and Sturrock, P.A.: 1972, *Astrophys. J.* 174, 659.
- Bernstein, I.B., Freeman, E.K., Kruskal, M.D. and Kulsrud, R.M.: 1958, *Proc. Roy. Soc. A244*, 17.
- Birn, J., Goldstein, H. and Schindler, K.: 1978, *Solar Phys.* 57, 81.
- Block, L.P.: 1975, in Hultqvist, B. and Stenflo, L. (eds.) *Physics of Hot Plasmas in the Magnetosphere*, Plenum, N.Y.

Block, L.P.: 1978, *Astrophys. Space Sci.* 55, 59.

Bodin, H.A.B. and Newton, A.A.: 1980, *Nucl. Fusion* 20, 1255.

Book, D.L., Turchi, P. and Stein, D.L.: 1979, *J. Computational Phys.* 33, 271.

Book, D.L.: 1981, NRL Memo Rept. 4408.

Boström, R.: 1974, B.M. McCormac (ed.) *Magnetospheric Physics*, p. 45, D. Reidel, Dordrecht-Holland.

Brown J.C., Melrose, D. and Spicer, D.S.: 1979, *Astrophys. J.* 228, 592.

Brown J.C. and Smith, D.F.: 1979, *Rep. Prog. Phys.* 43, 125.

Buneman, O.: 1959, *Phys. Rev.* 115, 503.

Canfield, R.C., Priest, E.R. and Rust, D.M.: 1974, *Flare Related Magnetic Field Dynamics* HAO, p. 361.

Carlqvist, P.: 1969, *Solar Phys.* 7, 503.

Carlqvist, P.: 1973, Tech. Rept. TRITA-EPP-73-05, Dept. of Plasma Phys., Royal Inst. of Tech., Stockholm, Sweden.

Carlqvist, P.: 1979a, P.J. Palmadesso and K. Papadopoulos (eds.) *Wave Instabilities in Space Plasmas*, p. 83, D. Reidel, Dordrecht-Holland.

Carlqvist, P.: 1979b, *Solar Phys.* 63, 353.

Carmichael, H.: 1964, in Hess, W.N. (ed.) *AAS-NASA Symp. on Physics of Solar Flares*, NASA SP-50, p. 451.

Carreras, B., Waddell, B.V. and Hicks, H.R.: 1979, *Nucl. Fusion* 19, 1423.

Carreras, B., Hicks, H.R., Holmes, J.A., and Waddell, B.V.: 1980, *Phys. Fluids* 23, 1811.

Carreras, B., Hicks, H.R. and Lee, D.K.: 1981, *Phys. Fluids* 24, 66.

Chiuderi, C., Giachetti, R. and Van Hoven, G.: 1977, *Solar Phys.* 54, 107.

Chiuderi, C. and Van Hoven, G.: 1979, *Astrophys. J. Letters* 232, L69.

Cohen, B.I., Krommes, J., Tang, W.M. and Rosenbluth, M.N.: 1976, *Nucl. Fusion* 16, 971.

Colgate, S.A.: 1978, *Astrophys. J.* 221, 1068.

Coppi, B. and Friedland, A.B.: 1971, *Astrophys. J.* 169, 379.

Coppi, B.: 1975, *Astrophys. J.* 195, 545.

Coppi, B., Galvao, R., Pellat, R., Rosenbluth, M.N. and Rutherford, P.H.: 1976, *Sov. J. Plasma Phys.* 2, 533.

Cross, M.A. and Van Hoven, G.: 1971, *Phys. Rev. A4*, 2347.

Cross, M.A. and Van Hoven, G.: 1976, *Phys. Fluids* 19, 1591.

Davidson, R.C. and Krall, N.A.: 1977, *Nucl. Fusion* 17, 1313.

Dobrott, D.R., Prager, S.C. and Taylor, J.B.: 1977, *Phys. Fluids* 20, 1850.

Drake, J.F. and Lee, Y.C.: 1977, *Phys. Fluids* 20, 1341.

Drake, J.F.: 1978, *Phys. Fluids* 21, 1777.

Drake, J.F., Gladd, N.T. and Huba, J.D.: 1981, *Phys. Fluids* 24, 78.

Dreicer, H.: 1959, *Phys. Rev.* 115, 238.

Duijverman, A., Hoyng, P. and Ionson, J.A.: 1981, *Astrophys. J.* in press.

Dungey, J.W.: 1953, *Phil. Mag.* 44, 725.

Dupree, T.H.: 1967, *Phys. Fluids* 10, 1049.

Ellison, M.A.: 1963, *Quart. J. Roy. Astron. Soc.* 4, 62.

Ferraro, V.C.A. and Plumpton, C.: 1966, *An Introduction to Magneto-Fluid Mechanics*, Clarendon Press, Oxford.

Field, G.B.: 1965, *Astrophys. J.* 142, 531.

Finn, J.M. and Kaw, P.K.: *Phys. Fluids* 20, 72.

Finn, J.M., Manheimer, W.M., and Ott, E.: 1980, NRL Memo Rept. 4316, submitted *Phys. Fluids*.

Furth, H.P., Killeen, J. and Rosenbluth, M.N.: 1963, *Phys. Fluids* 6, 459.

Furth, H.P., Killeen, J., Rosenbluth, M.N. and Coppi, B.: 1966, *Plasma Physics and Controlled Nuclear Fusion Research*, Vol. 1, 617, IAEA.

Furth, H.P., Rutherford, P.A. and Selberg, H.: 1973, *Phys. Fluids* 16, 1054.

Galeev, A.A. and Saydeev, R.Z.: 1979, in M.A. Leontovich (ed.) *Reviews of Plasma Physics*, Vol. 7, Consultants Bureau, N.Y.

Giachetti, R., Van Hoven, G. and Chiuderi, C.: *Solar Phys.* 55, 371.

Gibbon, M. and Spicer, D.S.: 1981, *Solar Phys.*, in press.

Gladd, N.T.: 1976, *Plasmas Phys.* 18, 27.

Goedbloed, J.P. and Sakanaka, P.H.: 1974, *Phys. Fluids* 17, 908.

Goetz, C.K. and Joyce, G.: 1975, *Astrophys. Space Sci.* 32, 165.

Goetz, C.K.: 1979, *Rev. Geophys. and Space Phys.* 17, 418.

Green, J.M. and Johnson, J.L.: 1962, *Phys. Fluids* 5, 510.

Haber, I., Huba, J.D., Palmadesso, P. and Papadopoulos, K.: 1978, *Phys. Fluids* 21, 1013.

Hamada, S.: 1962, *Nuclear Fusion* 2, 23.

Hasan, S.S.: 1980, *Solar Phys.* 67, 267.

Hassam, A.B.: 1980, *Phys. Fluids* 23, 2493.

Heyvaerts, J.: 1974a, *Astron. Astrophys.* 37, 65.

Heyvaerts, J.: 1974b, *Solar Phys.* 38, 419.

Heyvaerts, J., Priest, E.R. and Rust, D.M.: 1977, *Astrophys. J.* 216, 123.

Heyvaerts, J. and Kuperus, M.: 1978, *Astronomy and Astrophys.* 64, 219.

Heyvaerts, J., Lasry, J.M., Schatzman, M. and Witomsky, G.: 1979, in E. Jensen (ed.) *Physics of Solar Prominences*, IAU Colloquium No. 44, p. 174.

Hicks, H.R., Carresas, B. and Lynch, S.J.: 1979, Oak Ridge Memo Rept. 79/22.

Hood, A. and Priest, E.R.: 1979, *Solar Phys.* 64, 303.

Hood, A. and Priest, E.R.: 1980, *Solar Phys.* 66, 113.

Hooyng, P., Brown, J.C. and Van Beek, H.F.: 1976, *Solar Phys.* 48, 197.

Huba, J.D., Gladd, N.T. and Papadopoulos, K.: 1977, *Geophys. Res. Letts.* 4, 125.

Huba, J.D., Gladd, N.T. and Papadopoulos, K.: 1978, *J. Geophys. Res.* 83, 5217.

Huba, J.D., Drake, J.F. and Gladd, N.T.: 1980, *Phys. Fluids* 23, 552.

Hubbard, R. and Joyce, G.: 1979, *J. Geophys. Res.* 84 (A8), 4297.

Jackson, J.D.: 1962, *Classical Electrodynamics*, John Wiley and Sons, Inc., N.Y.

Jaggi, R.K.: 1964, in W. Hess (ed.) *AAS-NASA Symp. on Physics of Solar Flares*, NASA SP-50, p. 419.

Jockers, V.: 1976, *Solar Phys.* 50, 405.

Kadomtsev, B.B.: 1966, in M.A. Leontovich, (ed.) *Reviews of Plasma Physics* 2 (New York, Consultants Bureau), p. 153.

Kadomtsev, B.B. and Pogutse, O.P.: 1968, *Soviet Phys. JETP*, 26, 963.

Kahler, S.W. and Kreplin, R.W.: 1970, *Solar Phys.* 14, 372.

Kahler, S.W. and Spicer, D.S.: 1982,

Kaw, P., Valeo, E.J. and Rutherford, P.H.: 1979, *Phys. Rev. Lett.* 43, 1398.

Kindel, J.M. and Kennel, C.F.: 1971, *J. Geophysical Res.* 76, 3055.

Kiwamoto, Y., Kuwahara, H. and Tanaka, H.: 1979, *J. Plasma Phys.* 21, 475.

Kopp, R.A. and Pneuman, G.W.: 1976, *Solar Phys.* 50, 85.

Krall, N.A. and Trivelpiece, A.W.: 1973, *Principles of Plasma Physics*, McGraw Hill, N.Y.

Kravsky, L.: 1968, *Structure and Development of Solar Active Regions*, IAU Symp. 35 (D. Reidel Publishing Co., Dordrecht-Holland), p. 465.

Kruskal, M.D. and Kulsrud, R.M.: 1958, *Phys. Fluids* 1, 265.

Kulsrud, R.M.: 1967, P.A. Sturrock (ed.), *Plasma Astrophysics*, p. 46, Academic Press, N.Y.

Kuperus, M. and Athay, R.G.: 1967, *Solar Phys.* 1, 361.

Kuperus, M. and Raadu, M.A.: 1974, *Astron. and Astrophys.* 31, 189.

Kuperus, M.: 1976, *Solar Phys.* 47, 79.

Kuperus, M. and Van Tend, W.: 1979, Proceedings of the CECAM Workshop on Solar Flare Physics, submitted *Solar Phys.*

Kuperus, M., Ionson, J. and Spicer, D.S.: 1981, *Annual Rev. of Astron. and Astrophys.*, Vol. 19.

Lampe, M. and Papadopoulos, K.: 1977, *Astrophys. J.* 212, 886.

Lau, Y.Y. and Liu, C.S.: 1980, *Phys. Fluids* 19, 1644.

Lerche, I. and Low, B.C.: 1980a, *Solar Phys.* 67, 229.

Lerche, I. and Low, B.C.: 1980b, *Solar Phys.* 66, 285.

Lerche, I. and Low, B.C.: 1980c, *Monthly Notices Roy. Astron. Soc.* 192, 611.

Levine, R.H.: 1975, *Solar Phys.* 44, 365.

Levine, R.H.: 1976, *Solar Phys.* 46, 159.

Longmire, C.L.: 1963, *Elementary Plasma Physics*, Interscience.

Low, B.C. and Nakagawa, Y.: 1975, *Astrophys. J.* 199, 237.

Low, B.C.: 1975, *Astrophys. J.* 197, 251.

Low, B.C.: 1977a, *Astrophys. J.* 212, 234.

Low, B.C.: 1977b, *Astrophys. J.* 217, 288.

Lundquist, S.: 1951, *Phys. Rev.* 83, 307.

Machado, M.E. and Emslie, A.G.: 1979, *Astrophys. J.* 232, 903.

Mahajan, S.M., Hazeltine, R.D., Strauss, H.R. and Ross, D.W.: 1979, *Phys. Fluids* 22, 2147.

Manheimer, W. and Boris, J.P.: 1977, *Comm. Plasma Physics Cont. Fusion* 3, 15.

Manheimer, W. and Flynn, R.W.: 1974, *Phys. Fluids* 17, 409.

Manheimer, W.M., Colombant, D. and Flynn, R.W.: 1976, *Phys. Fluids* 19, 1354.

Manheimer, W.M.: 1979a, *Journal De Physique* 40, C7-269.

Manheimer, W.M.: 1979b, unpublished notes.

Manheimer, W. and Antonson, T.M.: 1979, *Phys. Fluids* 22, 957.

Mozer, F.S.: 1976, in B.M. McCormac (ed.) *Magnetospheric Particles and Fields*, p. 125, D. Reidel, Dordrecht-Holland.

Nakagawa, Y. and Raadu, M.A.: 1972, *Solar Phys.* 25, 127.

Nakagawa, Y.: 1973, *Astron. Astrophys.* 27, 95.

Nakagawa, Y.: 1974, in Y. Nakagawa and D.M. Rust (eds.) *Flare Related Magnetic Field Dynamics*, HAO Boulder, p. 53.

Nakagawa, Y.: 1978, *Astrophys. J.* 219, 314.

Nakagawa, Y., Steinolfson, R.S., and Wu, S.T.: 1978, *Solar Phys.* 47, 193.

Nakagawa, Y. and Stenflo, J.O.: 1979, *Astron. and Astrophys.* 72, 67.

Newcomb, W.A.: 1959, *Phys. Fluids* 2, 362.

Norman, C.A. and Smith, R.A.: 1978, *Astron. Astrophys.* 68, 145.

Norman, C.A.: 1979, Proceedings of the CECAM Workshop on Solar Flare Physics,

Palmaresso, P., Rowlands, H. and Papadopoulos, K.: 1982, *Phys. Rev. Letts.*

Papadopoulos, K.: 1975, *Phys. Fluids* 18, 1769.

Papadopoulos, K.: 1977, *Rev. Geophys. Space Phys.* 15, 113.

Papadopoulos, K.: 1979, S.-I. Akasofu (ed.) *Dynamics of the Magnetosphere*, p. 289, D. Reidel, Dordrecht-Holland.

Parail, V.V. and Pogutse, O.P.: 1976, *Sov. J. Plasma Phys.* 2, 125.

Parker, E.N.: 1953, *Astrophys. J.* 117, 431.

Parker, E.N.: 1957, *Phys. Rev.* 107, 830.

Parker, E.N.: 1963, *Astrophys. J. Suppl.* 8, 177.

Pereversev, G.V., Shafranov, V.D. and Zakharov, I.E.: 1978, *Theoretical and Computational Physics*, p. 469, IAEA.

Petscheck, H.L.: 1964, in Hess, M.N. (ed.) *AAS-NASA Symp. on Phys. of Solar Flares*, NASA SP-50.

Pneuman, G.: 1978, *Phys. of Solar Prominences*, IAU Colloquium No. 44, Oslo, p. 281.

Pneuman, G.: 1979, *Solar and Interplanetary Dynamics*, IAU Symposium No. 91, Cambridge, Mass.

Pneuman, G.: 1980, *Solar Phys.* 65, 369.

Pneuman, G.: 1981, submitted *Solar Phys.*

Pollard, R.K. and Taylor, J.B.: 1979, *Phys. Fluids* 22, 126.

Priest, E.R. and Heyvaerts, J.: 1974, *Solar Phys.* 36, 433.

Pritchett, P.C., Wu, C.C. and Dawson, J.M.: 1978, *Phys. Fluids* 21, 1543.

Pritchett, P.C. and Wu, C.C.: 1979, *Phys. Fluids* 22, 2140.

Pritchett, P.C., Lee, Y.C. and Drake, D.F.: 1980, *Phys. Fluids* 23, 1368.

Raadu, M.A. and Nakagawa, Y.: 1971, *Solar Phys.* 20, 64.

Raadu, M.A.: 1972, *Solar Phys.* 22, 425.

Raadu, M.A. and Carlqvist, P.: 1979, TRITA-EPP-79-21, Dept. of Plasma Phys., Royal Inst. of Tech., Stockholm, Sweden.

Rechester, A.B. and Stix, T.H.: 1976, *Phys. Rev. Letts.* 35, 587.

Rechester, A.B. and Rosenbluth, M.N.: 1978, *Phys. Rev. Letts.* 40, 38.

Roederer, J.G.: 1979, C.F. Kennedy, L. Lanzerotti and E.N. Parker (eds.) *Solar System Plasma Physics*, Vol. 2, p. 1.

Rutherford, P.H.: 1973, *Phys. Fluids* 16, 1903.

Sakurai, K.: 1976, *Publ. Astron. Soc. Japan* 28, 177.

Sakurai, K. and Uchida, Y.: 1979, *Solar Phys.*

Sakurai, K.: 1980,

Sato, T. and Iijima, T.: 1979, *Space Sci. Rev.* 24, 347.

Schmidt, G.: 1979, *The Physics of High Temperature Plasmas*, 2nd Ed., Academic Press, New York.

Schnack, D.D. and Killeen, J.: 1978, in *Theoretical and Computational Plasma Physics*, IAEA, Vienna.

Schnack, D.D. and Killeen, J.: 1979, *Nucl. Fusion* 19, 877.

Shafranov, V.D.: 1966, *Reviews of Plasma Physics* 2, 103.

Silleen, R.M.J. and Kattenberg, A.: 1980, *Solar Phys.* 67, 47.

Smith, D.F. and Priest, E.R.: 1972, *Astrophys. J.* 176, 487.

Smith, R.A. and Goetz, C.K.: 1978, *J. Geophys. Res.* 83, 2617.

Smith, R.A.: 1981, *Physical Rev. Letts.*, submitted.

Solov'ev, L.S.: 1975, *Reviews of Plasma Physics* 6, 239.

Spicer, D.S.: 1975, *Bull. Am. Astron. Soc.* 7, 398.

Spicer, D.S.: 1976, *An Unstable Arch Model of a Solar Flare*, NRL Formal Rept. 8036.

Spicer, D.S.: 1977a, *Solar Phys.* 53, 305.

Spicer, D.S.: 1977b, *Solar Phys.* 51, 431.

Spicer, D.S.: 1977c, *Solar Phys.* 54, 379.

Spicer, D.S. and Brown, J.C.: 1980, *Solar Phys.* 67, 385.

Spicer, D.S.: 1981a, *Solar Phys.* in press.

Spicer, D.S.: 1981b, *Solar Phys.* in press.

Spicer, D.S. and Brown, J.C.: 1981, C. Jordan (ed.) *The Sun as a Star*, NASA/CNRS.

Spicer, D.S. and Manheimer, W.: 1982, in preparation.

Spicer, D.S., Benz, A.O. and Huba, J.D.: 1982, *Astron. and Astrophys.*

Stenflo, J.O.: 1969, *Solar Phys.* 8, 115.

Sturrock, P.A.: 1966a, *Phys. Rev. Letts.* 16, 270.

Sturrock, P.A.: 1966b, *Nature* 211, 695.

Sturrock, P.A.: 1967, IAU Symp. No. 35, p. 471.

Sturrock, P.A.: 1972, in P.A. McIntosh and M. Dryer (eds.) *Solar Activity Observations and Predictions*, MIT Press, Cambridge, p. 173.

Sturrock, P.A.: 1974, IAU Symp. 57, p. 437.

Sturrock, P.A.: 1980, P.A. Sturrock (ed.) *Solar Flares*, Colorado Associated University Press, p. 411.

Svestka, Z.: 1976, *Solar Flares*, Reidel, Dordrecht-Holland.

Syrovatskii, S.I.: 1966, *Astron. Zh.* 43, 340.

Tanka, K. and Nakagawa, Y.: 1973, *Solar Phys.* 33, 187.

Taylor, J.B.: 1963, *Phys. Fluids* 6, 1529.

Taylor, J.B.: 1974, *Phys. Rev. Letts.* 33, 1139.

Tidman, D.A. and Krall, N.A.: 1971, *Collisionless Shock Waves*, J. Wiley and Sons.

Torven, S.: 1979, P.J. Palmadesso and K. Papadopoulos (eds.) *Wave Instabilities in Space Plasmas*, p. 109, D. Reidel, Dordrecht-Holland.

Tur, T.J. and Priest, E.R.: 1978, *Solar Phys.* 58, 181.

Uchida, Y. and Sakurai, T.: 1977, *Solar Phys.* 51, 413.

Van Hoven, G. and Cross, M.A.: 1973, *Phys. Rev. A7*, 1347.  
Van Hoven, G., Chiuderi, C. and Giachetti, R.: 1977, *Astrophys. J.* **213**, 869.  
Van Hoven, G. et al.: 1980, P.A. Sturrock (ed.) *Solar Flares*, Colorado Associated Press, p. 177.  
Van Hoven, G.: 1980, E.R. Priest (ed.) *Solar Flare Magnetohydrodynamics*, Gordon and Breach, New York and London, p. 217.  
Van Tend, P. and Kuperus, M.: 1978, *Solar Phys.* **59**, 115.  
Vasyliunas, V.M.: 1975, *Rev. Geophys. Space Phys.* **13**, 303.  
Vasyliunas, V.M.: 1976, B.M. McCormac (ed.) *Magnetospheric Particles and Fields*, p. 99, D. Reidel, Dordrecht-Holland.  
Voslamber, D. and Callebant, D.K.: 1962, *Phys. Rev.* **128**, 2016.  
Waddell, B.V., Carreaus, B., Hicks, H.R. and Holmes, J.A.: 1979, *Phys. Fluids* **22**, 896.  
Ware, A.A.: 1965, Culham Lab Rept. CLM-M53.  
Wesson, J.A.: 1966, *Nucl. Fusion* **6**, 130.  
Wesson, J.A.: 1978, *Nucl. Fusion* **18**, 87.  
White, R.B., Monticello, D.A., Rosenbluth, M.N. and Waddell, B.V.: 1977, *Phys. Fluids* **20**, 800.  
Widing, K.G. and Spicer, D.S.: 1980, *Astrophys. J.* **142**, 1243.  
Wolf, R.A.: 1975, *Space Science Rev.* **17**, 537.  
Woltzer, L.: 1958, *Proc. Nat. Acad. Sci.* **44**, 489.

